

An Elementary Integral Equation Method Applied
To Boundary Value Problems in Geomechanics

Mohammad Osama Al-Hunaidi

A Thesis

in

The Department

of

Civil Engineering.

Presented in Partial Fulfillment of the Requirements
for the degree of Master of Engineering
Concordia University
Montréal, Québec, Canada

April 1984

© Mohammad Osama Al-Hunaidi 1984

ABSTRACT

An Elementary Integral Equation Method Applied To Boundary Value Problems in Geomechanics

Mohammad Osama Al-Hunaidi

Contact stresses in soil-structure interaction problems are important in two respects, first: evaluating the deflection, flexural moments and shearing forces in the structural unit, and secondly, establishing the stress and displacement fields in the supporting soil medium.

In this thesis, a numerical method of solution is presented for the prediction of contact stresses, as well as, the displacement of simple rigid structural units embedded in elastic, isotropic and semi-infinite soil medium.

The analysis is based on a displacement integral equation. The integral equation describes the displacement field in the half-space (due to a traction function at some boundary within the half-space) using Melan's fundamental solution and the principle of superposition.

The technique is applied to circular pipes (embedded horizontally), and to strip footings of various cross-sectional configurations.

ACKNOWLEDGEMENT

The author gratefully acknowledges the invaluable guidance and cooperation of Dr. H.B. Poorooshassab and Dr. M. M. Douglass, under whose supervision this work was carried out.

Thanks are due to Dr. A.M. Hanna who was always available for consultation.

Thanks are also due to Mr. R. Lombardo for his help and cooperation, and to Mrs. Madeleine Klein for her judicious typing of the entire thesis.

The author is grateful to the National Science and Engineering Council of Canada for the financial assistance.

TABLE OF CONTENTS

	<u>Page</u>
ABSTRACT	i
ACKNOWLEDGEMENT	ii
LIST OF SYMBOLS	iv
LIST OF FIGURES	vi
LIST OF TABLES	viii
<u>CHAPTER 1:</u> INTRODUCTION	1
1.1 Fundamental definitions and Relationships	2
1.2 Melan's Fundamental Solution	15
1.3 Ideal Soil Systems	20
1.4 Soil Structure Interaction	25
<u>CHAPTER 2:</u> FORMULATION OF SOLUTION THEORY	27
<u>CHAPTER 3:</u> APPLICATIONS	36
3.1 Contact Stresses on Horizontally Embedded Rigid Pipes	38
3.2 Contact Stresses on Strip Footings of Various Shapes	43
<u>CHAPTER 4:</u> NUMERICAL RESULTS	47
4.1 Horizontal Pipe	48
4.2 Strip Footings	54
<u>CHAPTER 5:</u> DISCUSSION AND CONCLUSION	69
REFERENCES	73
APPENDIX	75

LIST OF SYMBOLS

ANG	Angular size of footing
BR	Breadth of footing
C	Contour in half-space
C^k	Segment arc length
D	Depth of pipe centre
E	Modulus of elasticity
g	Acceleration due to gravity
G	Modulus of rigidity
H	Depth of bedrock
I_i	Invariants of a tensor
K_o	Coefficient of earth pressure at rest
n	Number of segments
R	Radius of pipe
\bar{R}	Body force in radial direction
S	Arc distance
\bar{s}	Body force in tangential direction
t_i	Traction function
\underline{t}	Traction component function
\bar{t}	Traction component function
[T]	Rotation matrix
u	Displacement in x-direction
u_j	Displacement tensor
\bar{u}	Vertical displacement of structural unit
U	Displacement influence function
v	Vector quantity, displacement in y-direction
V	Displacement influence factor

w	Displacement in z-direction
w	Load on footing
\bar{x}	Body force in x-direction
\bar{y}	Body force in y-direction
γ	Density, engineering shear strain
ϵ_{ij}	Strain tensor
η	stress ratio
ν	Poisson's ratio
ξ	Line load position
Ω	Region within a half-space
σ_{ij}	Stress tensor
ϕ	Stress function
θ	Angle between normal to a contour and positive x-direction

LIST OF FIGURES

FIGURE

- 1.1 Sign Convention in Geomechanics
- 1.2 Rotation of Coordinates and Definition of Direction Cosines
- 1.3 Tensorial and Engineering Shear Strains
- 1.4 Sign Convention for Stress in Polar Coordinates
- 1.5 Free Body Diagram of Infinitesimal Element at the Boundary
- 1.6 Line Load within the half-space
- 1.7 General axes system for line load within half-space
- 1.8 The yield locus is a function of the stress ratio
- 1.9 Results of a special test studying the yield criterion
- 2.1 Discretisation of boundary for numerical analysis
- 2.2 Vertical and horizontal components of boundary traction
- 3.1 Idealization of the structural units treated
- 3.2 Discretization of the pipe boundary
- 3.3 Resolving Traction for Pipe Problem
- 3.4 Resolving Traction for Strip Footings Problem
- 4.1 Horizontal Pipe Stress Distribution (N=20)
- 4.2 Horizontal Pipe Stress Distribution (N=40)
- 4.3 Semi-circular strip footing stress distribution (N=20)
- 4.4 Triangular Strip footing stress distribution (N=20)

- 4.5 Flat Strip footing stress distribution (N=20)
- 4.6 Semi-circular strip footing stress distribution (N=40)
- 4.7 Triangular strip footing stress distribution (N=40)
- 4.8 Flat Strip footing stress distribution (N=40)

LIST OF TABLES

TABLE

- 4.1 Results of "PIPE" (N=20)
- 4.2 Results of "PIPE" (N=40)
- 4.3 Results of "CIRFDN" (N=20)
- 4.4 Results of "TRIFDN" (N=20)
- 4.5 Results of "FLAFDN" (N=20)
- 4.6 Results of "CIRFDN" (N=40)
- 4.7 Results of "TRIFDN" (N=40)
- 4.8 Results of "FLAFDN" (N=40)

Just a mere piece of sand in the
Eastern Ocean.....

(An old Vietnamese saying)

CHAPTER 1

INTRODUCTION

This study applies an elementary integral technique to obtain the solution of a certain class of boundary value problems in soil mechanics. This technique is applicable when:

- (i) The boundaries of the region are small compared to the solution region. Boundaries in this sense include internal boundaries such as holes, joint planes, or locations where material properties might change.
- (ii) A fundamental solution exists and,
- (iii) The principle of superposition can be applied.

The one fundamental solution used for problems treated in this study is attributed to Melan (1932). It describes the state of stress (and hence deformation) for a line load extending from $-\infty$ to $+\infty$ and acting at a certain level within the elastic half-space. Since the half space is assumed elastic, those classes of problems in geotechnical analysis to which Melan's fundamental solution can be applied must be recognized. In addition, the appropriate boundary conditions must be correctly stated.

In view of the above brief remarks, this introductory chapter is written in four sections.

- In section one, the fundamental definitions and relationships in elasticity are reviewed.

- In section two, the nature of Melan's fundamental solution is explained.
- In section three, a brief account of deformation properties of ideal soil systems (cohesionless as well as cohesive) is given to justify the use of the fundamental solution.
- In section four, the nature of the problems treated is discussed together with their appropriate boundary conditions under the heading "Soil-Structure Interaction".

1.1 Fundamental Definitions and Relationships

Review of Stress

Fig.(1.1) shows an element of a large continuous body. The forces are transmitted across each of the six faces, and they can be described in terms of the stress tensor

$$[\sigma_{ij}] = \begin{bmatrix} \sigma_{xx} & \sigma_{xy} & \sigma_{xz} \\ \sigma_{yx} & \sigma_{yy} & \sigma_{yz} \\ \sigma_{zx} & \sigma_{zy} & \sigma_{zz} \end{bmatrix} \quad (1.1)$$

Each component of the stress represents a force acting in a specific coordinate direction on a unit area oriented in a particular way. Thus σ_{yx} is the force acting in the positive x-direction on a unit area whose outward normal is the negative y-direction. That is, in accordance with geotechnical convention, compression components are positive and the tensile components are negative. This sign convention is at

variance with the one used in continuum mechanics.

Fig. (1.2) shows two coordinate systems x, y, z and x', y', z' . The direction cosines are the cosines of the angles between pairs of coordinate directions. These are denoted by the coordinate labels enclosed in parenthesis, thus (y, x') is the cosine of the angle between direction y and x' .

A point with coordinates (x, y, z) in one system will have coordinates (x', y', z') in the other system, defined by

$$\begin{Bmatrix} x' \\ y' \\ z' \end{Bmatrix} = \begin{bmatrix} (x, x') & (y, x') & (z, x') \\ (x, y') & (y, y') & (x, y') \\ (x, z') & (y, z') & (z, z') \end{bmatrix} \begin{Bmatrix} x \\ y \\ z \end{Bmatrix} \quad (1.2)$$

The 3×3 matrix is called the rotation matrix $[T]$. Any vector $\{v\}$ written in the x, y, z system can be transformed into $\{v^*\}$ in the x', y', z' system by

$$\{v^*\} = [T] \{v\} \quad (1.3)$$

The stress $[\sigma]$ in the x, y, z system can be transformed into $[\sigma^*]$ in the x', y', z' system by

$$[\sigma^*] = [T] [\sigma] [T]^T \quad (1.4)$$

From the theory of matrices, one can find a set of rotations of coordinates in Eq. (1.4) which will give a stress $[\sigma^*]$ that has only diagonal or normal terms

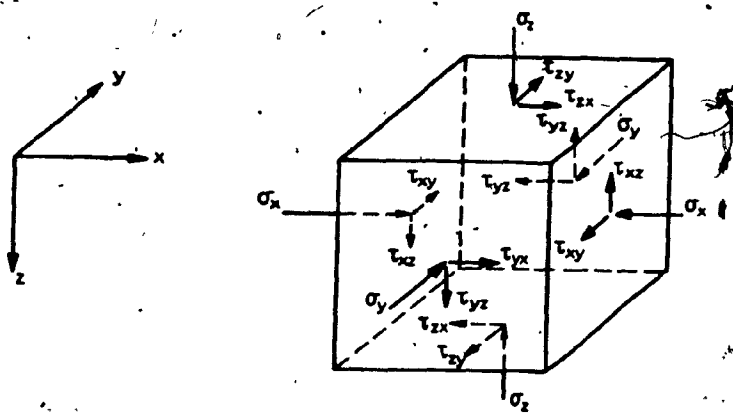


FIG. 1.1: Sign Convention for Stress in Geomechanics

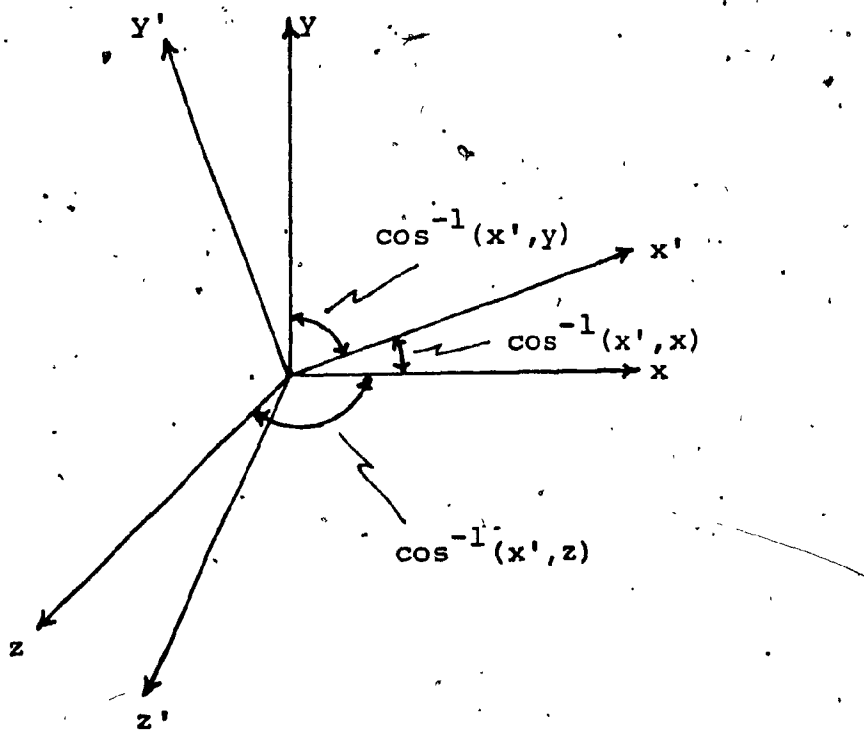


FIG. 1.2: Rotation of coordinates and definition of direction cosines

$$[\sigma^*] = \begin{bmatrix} \sigma_x & 0 & 0 \\ 0 & \sigma_y & 0 \\ 0 & 0 & \sigma_z \end{bmatrix} \quad (1.5)$$

The diagonal terms are called the principal stresses. They are the solutions of the equation

$$\sigma^3 - I_1\sigma^2 + I_2\sigma - I_3 = 0 \quad (1.6)$$

where,

$$I_1 = \sigma_{xx} + \sigma_{yy} + \sigma_{zz}$$

$$I_2 = \sigma_{xx}\sigma_{yy} + \sigma_{yy}\sigma_{zz} + \sigma_{zz}\sigma_{xx} - \sigma_{xy}^2 - \sigma_{yz}^2 - \sigma_{xz}^2$$

$$I_3 = \sigma_{xx}\sigma_{yy}\sigma_{zz} - \sigma_{xx}\sigma_{yz}^2 - \sigma_{yy}\sigma_{zx}^2 - \sigma_{zz}\sigma_{xy}^2 + 2\sigma_{xy}\sigma_{yz}\sigma_{zx}$$

These are called the first, second and third invariants of the stress tensor, respectively. Since the principal stresses are physical quantities independent of the choice of coordinate axes, the invariants must also be independent of the choice of axes, hence the name invariant.

Review of Strain

The deformation of a body is described by the strain. If the displacements are u , v , w in the x , y , z directions, respectively, the components of strain will be

$$\epsilon_{xx} = \frac{\partial u}{\partial x} \quad \epsilon_{yy} = -\frac{\partial v}{\partial y} \quad \epsilon_{zz} = -\frac{\partial w}{\partial z}$$

$$\gamma_{xy} = -\left(\frac{\partial u}{\partial y} + \frac{\partial v}{\partial x}\right)$$

$$\gamma_{xz} = - \left(\frac{du}{dz} + \frac{dw}{dx} \right)$$

$$\gamma_{yz} = - \left(\frac{dv}{dz} + \frac{dw}{dy} \right) \quad (1.7)$$

A positive normal strain corresponds to a decrease in length and a positive shear strain represents an increase in the right angle between the axes' positive directions. The same equations can be expressed more compactly by using a subscript notation in which u_1, u_2, u_3 are the displacements in the x_1, x_2, x_3 directions respectively. The strain is then shown as,

$$\epsilon_{ij} = - \frac{1}{2} \left(\frac{du_i}{dx_j} + \frac{du_j}{dx_i} \right), \quad \gamma_{ij} = 2 \cdot \epsilon_{ij} \quad (1.8)$$

It is noted that there are two definitions of shearing strain, the γ 's and the ϵ 's. The former are called the "engineering strains". They are useful for experimental work. The latter are called the "tensorial shear strains", and they are more useful for theoretical derivations in which it is important to keep components clearly distinguished (Timoshenko and Goodier, 1970).

Fig. (1:3) illustrates the physical meaning of the components of shearing strain. It is noted that the tensorial definition of shear strain describes a pure deformation, but the engineering definition includes some rotation.

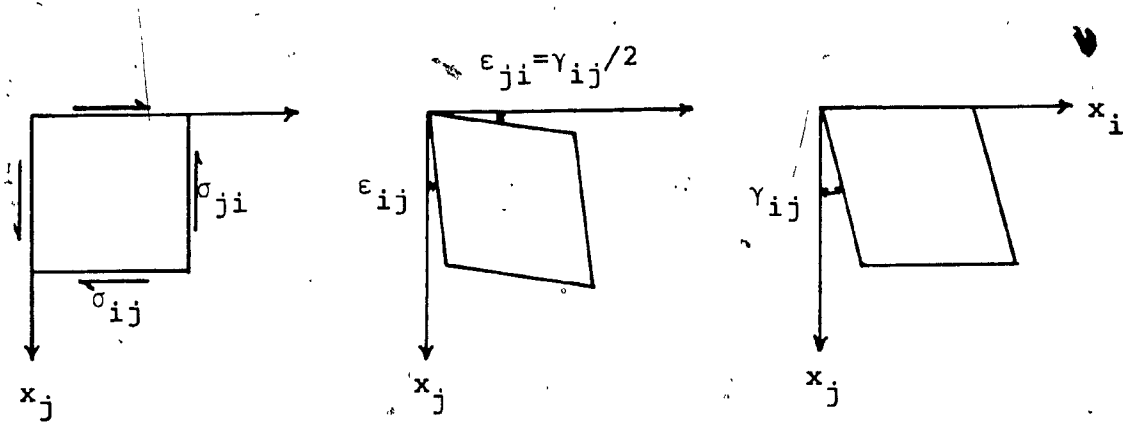


Fig. 1.3: Tensorial and Engineering Shear Strains

As for the stress tensor, the strain tensor can be expressed in the following form,

$$[\epsilon_{ij}] = \begin{bmatrix} \epsilon_{xx} & \epsilon_{xy} & \epsilon_{xz} \\ \epsilon_{yx} & \epsilon_{yy} & \epsilon_{yz} \\ \epsilon_{zx} & \epsilon_{zy} & \epsilon_{zz} \end{bmatrix}$$

As any other tensor, the strain tensor follows all rules of transformation. It has invariants and principal values.

Hooke's Law

A material is said to be perfectly elastic if it resumes its initial form completely after removal of all external forces. If the relations between the components of stress and the components of strain are linear, the material is said to be linear elastic. Linear relations between the components of stress and the components of strain are known generally as Hooke's Law. The unit elongation of an element submitted to the action of normal stress

σ_x uniformly distributed over two opposite sides is given as,

$$\epsilon_x = \frac{\sigma_x}{E} \quad (1.9)$$

in which E is the modulus of elasticity in tension or compression depending whether σ_x is tension or compression. This deformation in the direction x is, of course, accompanied by lateral strain components in the y and z directions given by

$$\epsilon_y = -\nu \frac{\sigma_x}{E} \quad \epsilon_z = -\nu \frac{\sigma_x}{E} \quad (1.10)$$

in which ν is a constant called Poisson's ratio. Using the principle of superposition, axial strains in terms of axial stresses are given as,

$$\begin{aligned} \epsilon_x &= \frac{1}{E} [\sigma_x - \nu(\sigma_y + \sigma_z)] \\ \epsilon_y &= \frac{1}{E} [\sigma_y - \nu(\sigma_x + \sigma_z)] \\ \epsilon_z &= \frac{1}{E} [\sigma_z - \nu(\sigma_x + \sigma_y)] \end{aligned} \quad (1.11)$$

It should be noted at this stage that the principle of superposition is legitimate so long as the deformation are small and the corresponding small displacements do not substantially affect the action of external forces. In such cases small changes in the dimensions of deformed bodies are neglected and also small displacements of external forces. Calculations are based on initial dimensions and shape of the body. The resultant displacement will then be obtained by superposition in the form of linear functions of external forces.

The shearing strains in terms of shearing stresses are given by,

$$\begin{aligned}\gamma_{xy} &= \frac{1}{G} \sigma_{xy} \\ \gamma_{yz} &= \frac{1}{G} \sigma_{yz} \\ \gamma_{zx} &= \frac{1}{G} \sigma_{zx}\end{aligned}\tag{1.12}$$

in which G is the shear modulus and it is equal to $\frac{E}{2(1+\nu)}$.

Plane strain

If a long body is loaded by forces which are perpendicular to the longitudinal elements and do not vary along the length, it may be assumed that all cross sections are in the same condition.

There are many important problems of this kind, for instance, a long cylinder such as a tunnel or buried pipe; a laterally loaded retaining wall; a strip footing on a soil mass, etc.

Since conditions are identical at all cross sections, it is sufficient to consider only a slice between two sections unit distance apart. The components u and v of the displacement are functions of x and y . They are independent of the longitudinal coordinate z . If we further assume w , the displacement component in the z direction, remains zero at every cross section, thus the strain component ϵ_{zz} , γ_{zy} , γ_{zx} will vanish and the remaining non-zero strain components will be

$$\epsilon_{xx} = -\frac{du}{dx}, \quad \epsilon_{yy} = -\frac{dv}{dy} \quad \text{and} \quad \gamma_{xy} = -\left(\frac{dv}{dx} + \frac{du}{dy}\right)$$

The longitudinal normal stress σ_{zz} can be found in terms of σ_{xx} and σ_{yy} by means of Hooke's law

$$\sigma_{zz} = v (\sigma_{xx} + \sigma_{yy}) \quad (1.13)$$

As a result, the constitutive law for elastic isotropic material in plane strain becomes,

$$\begin{Bmatrix} \sigma_{xx} \\ \sigma_{yy} \\ \sigma_{xy} \end{Bmatrix} = \frac{E}{(1+v)(1-2v)} \begin{bmatrix} 1-v & v & 0 \\ v & 1-v & 0 \\ 0 & 0 & \frac{1-2v}{2} \end{bmatrix} \begin{Bmatrix} \epsilon_{xx} \\ \epsilon_{yy} \\ \gamma_{xy} \end{Bmatrix} \quad (1.14)$$

Differential equations of equilibrium

a) Cartesian coordinates

By considering the equilibrium of the element shown in Fig. (1.1) in the x and y directions (plane strain condition), the following two equations of equilibrium may be derived

$$\frac{\partial \sigma_{xx}}{\partial x} + \frac{\partial \sigma_{xy}}{\partial y} - \bar{x} = 0 \quad (1.15)$$

$$\frac{\partial \sigma_{xy}}{\partial x} + \frac{\partial \sigma_{yy}}{\partial y} - \bar{y} = 0$$

where \bar{x} and \bar{y} are the body forces, per unit volume, in the x and y directions.

b) Polar coordinates

By considering the equilibrium of the element shown in Fig. (1.4) in the radial and tangential directions, two equations of equilibrium are obtained,

$$\frac{\partial \sigma_{rr}}{\partial r} + \frac{1}{r} \frac{\partial \sigma_{r\theta}}{\partial \theta} + \frac{\sigma_r - \sigma_\theta}{r} - \bar{R} = 0$$

$$\frac{\partial \sigma_{r\theta}}{\partial r} + \frac{1}{r} \frac{\partial \sigma_{\theta\theta}}{\partial \theta} + 2 \frac{\sigma_{r\theta}}{r} - \bar{S} = 0 \quad (1.16)$$

where \bar{R} and \bar{S} are the body forces, per unit volume.

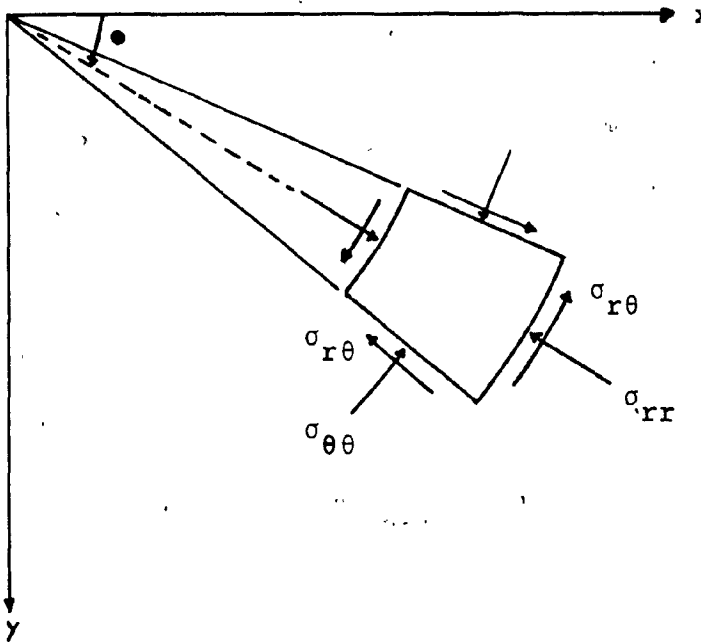


Fig. 1.4: Sign Convention for Stress in Polar coordinates

Boundary conditions

The previous equations of equilibrium must be satisfied at all points throughout the volume of the body. In addition, the stress components must be in equilibrium with the external forces at the boundary of the body.

The conditions of equilibrium at the boundary can be obtained from Fig. (1.5) where side BC coincides with the boundary of the body, and denoting \bar{x} and \bar{y} the components of the surface forces per unit area at this point of the boundary, thus

$$\bar{x} = -(\sigma_{xx} \cos Nx + \sigma_{xy} \cos Ny) \quad (1.17)$$

$$\bar{y} = -(\sigma_{yy} \cos Ny + \sigma_{xy} \cos Nx)$$

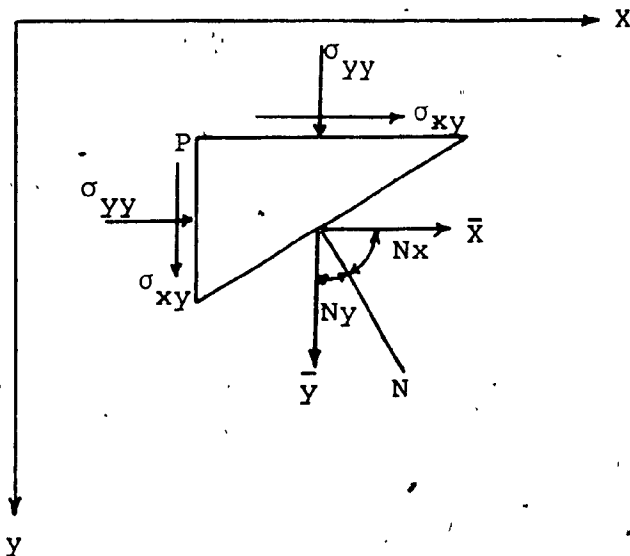


Fig. 1.5: Free body diagram of infinitesimal element at the boundary

Compatibility equation

The strain-displacement relationships for plane strain condition are given as,

$$\epsilon_x = \frac{du}{dx} \quad \epsilon_y = -\frac{dv}{dy} \quad \gamma_{xy} = -\left(\frac{dv}{dx} + \frac{du}{dy}\right)$$

Since three strain components are derived from only two displacements, the strains are not independent of each other. One further relationship can be derived (referred to as the

compatibility equation) which connects the components of strain, as follows,

$$\frac{\partial^2 \epsilon_x}{\partial y^2} + \frac{\partial^2 \epsilon_y}{\partial x^2} = \frac{\partial^2 \gamma_{xy}}{\partial x \partial y} \quad (1.17)$$

This differential equation must be satisfied by the strain components to secure the existence of functions u and v connected with the strain components by the above equations.

By using Hooke's Law, the condition of compatibility can be transformed into a relation between the stress components. In the case of plane strain we have,

$$\begin{aligned} \epsilon_x &= \frac{1}{E} [(1-v^2)\sigma_x - v(1+v)\sigma_y] \\ \epsilon_y &= \frac{1}{E} [(1-v^2)\sigma_y - v(1+v)\sigma_x] \\ \gamma_{xy} &= \frac{1}{G} \sigma_{xy} = \frac{2(1+v)}{E} \sigma_{xy} \end{aligned} \quad (1.18)$$

Substituting in Eq. (1.17) yields,

$$\begin{aligned} \frac{\partial^2}{\partial y^2} [(1-v^2)\sigma_x - v(1+v)\sigma_y] + \frac{\partial^2}{\partial x^2} [(1-v^2)\sigma_y - v(1+v)\sigma_x] \\ = 2(1+v) \frac{\partial^2 \sigma_{xy}}{\partial x \partial y} \end{aligned} \quad (1.19)$$

Using the equations of equilibrium (with zero body forces) and differentiating the first equation with respect to x , the second with respect to y and adding them yields,

$$2 \frac{\partial^2 \sigma_{xy}}{\partial x \partial y} = - \frac{\partial^2 \sigma_x}{\partial x^2} - \frac{\partial^2 \sigma_y}{\partial y^2} \quad (1.20)$$

Substituting $\frac{\partial^2 \sigma_{xy}}{\partial x \partial y}$ of Eq. (1.20) in Eq. (1.19), the compati-

bility equation in terms of stress components for plane strain condition becomes,

$$\left(\frac{\partial^2}{\partial x^2} + \frac{\partial^2}{\partial y^2} \right) (\sigma_x + \sigma_y) = 0 \quad (1.21)$$

The state of stress in a two dimensional problem can now be determined by solving the differential equations of equilibrium together with the compatibility equation and the boundary conditions.

Stress function

It has been shown that solutions of two-dimensional problems are reduced to the solution of the following equations when the weight of the body is the only body force,

$$\begin{aligned} \frac{\partial \sigma_x}{\partial x} + \frac{\partial \sigma_{xy}}{\partial y} &= 0 \\ \frac{\partial \sigma_{xy}}{\partial x} + \frac{\partial \sigma_y}{\partial y} - \rho g &= 0 \\ \left(\frac{\partial^2}{\partial x^2} + \frac{\partial^2}{\partial y^2} \right) (\sigma_x + \sigma_y) &= 0 \end{aligned} \quad (1.22)$$

together with the boundary conditions.

The usual method of solving these equations is by introducing a new function, called the stress function. Choosing any function ϕ of x and y , the equations of equilibrium will be satisfied by using the following expressions for the stress components,

$$\sigma_x = \frac{\partial^2 \phi}{\partial y^2} + \rho gy \quad \sigma_y = \frac{\partial^2 \phi}{\partial x^2} + \rho gy \quad \sigma_{xy} = - \frac{\partial^2 \phi}{\partial x \partial y} \quad (1.23)$$

substituting these expressions in the compatibility equations yields,

$$\frac{\partial^4 \phi}{\partial x^4} + 2 \frac{\partial^4 \phi}{\partial x^2 \partial y^2} + \frac{\partial^4 \phi}{\partial y^4} = 0 \quad (1.24)$$

Thus, the solution of a two dimensional problem (when weight of the body is the only body force) is reduced to finding a solution of Eq. (1.24) that satisfies the boundary conditions of the problem.

1.2 Melan's Fundamental Solution

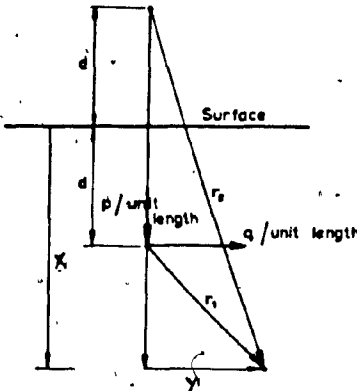
Most solutions for stress distributions in the elastic half-space may be approached using the Boussinesq and Kelvin solutions together with the principle of superposition. The Boussinesq solution describes the stress distribution in the elastic half-space due to a point load acting at its surface. The Kelvin solution, on the other hand, describes the stress distribution in the infinite space due to a point load acting within it.

For instance, the stress distribution due to a line load within the elastic half-space (Melan's Problem) can be derived by using the stress distribution produced by a line load within the infinite space (integrated Kelvin problem). The resulting stresses at the level of the straight edge of the infinite half-space can be annulled by superposing an equal and opposite system of forces at the boundary of the semi-infinite space. The stresses produced by this corrective system can be determined using

the "Integrated Boussinesq Solution", i.e., line load on the surface of semi-infinite space. The stresses produced by the corrective system are superposed on the initial stress distribution.

The stress field due to a line loading acting within semi-infinite mass is known as Melan's Problem and its solution is as follows (Poulos and Davis, 1974).

- i) Vertical Line Loading. The vertical and horizontal stresses produced by a vertical line loading ($P/\text{unit length}$) acting within the semi-infinite mass as shown in Fig. (1.6) are given by Eqs. (1.25) and (1.26) on Page (18).



$$r_1 = [(x' - d)^2 + y'^2]^{1/2}$$

$$r_2 = [(x' + d)^2 + y'^2]^{1/2}$$

Fig. 1.6: Line load within the half-space

Using a new system of axes (x, y) , as shown in Fig. (1.7) such that

$$x' = x$$

$$y' = y - \xi$$

ξ = y-coordinate of line load

Eqs. (1.25) and (1.26) are rewritten to yield Eqs. (1.27) and (1.28) on page (18).

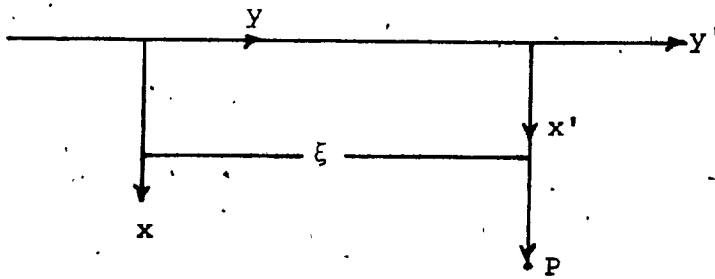


Fig. 1.7: General axes system for line load within half-space

(ii) Horizontal line loading. The vertical and horizontal stresses produced by a horizontal line load ($q/\text{unit length}$) within a semi-space are given by Eqs. (1.29) and (1.30) on page (19). Using the system of axes (x, y) of Fig. (1.7) equations (1.29) and (1.30) are rewritten to yield Eqs. (1.31) and (1.32) on page (19).

$$\sigma_x = \frac{P}{\pi} \left[\frac{m+1}{2m} \left[\frac{(x'-d)^3}{r_1^4} + \frac{(x'+d)[(x'+d)^2 + 2dx']}{r_2^4} - \frac{8dx'(d+x')y'^2}{r_2^6} \right] \right. \\ \left. + \frac{m-1}{4m} \left[\frac{(x'-d)}{r_1^2} + \frac{(3x'+d)}{r_2^2} - \frac{4x'y'^2}{r_2^4} \right] \right] \quad (1.25)$$

$$\sigma_y = \frac{P}{\pi} \left[\frac{m+1}{2m} \left[\frac{(x'-d)y^2}{r_1^4} + \frac{(x'+d)(y'^2 + 2d^2) - 2dy'^2}{r_2^4} - \frac{8dx'(d+x')y'^2}{r_2^6} \right] \right. \\ \left. + \frac{m-1}{4m} \left[\frac{(x'-d)}{r_1^2} + \frac{x'+3d}{r_2^2} + \frac{4x'y'^2}{r_2^4} \right] \right] \quad (1.26)$$

$$\sigma_x = \frac{P}{\pi} \left[\frac{m+1}{2m} \left[\frac{(x-d)^3}{[(x-d)^2 + (y-\xi)^2]^2} + \frac{(x+d)[(x+d)^2 + 2dx]}{[(x+d)^2 + (y-\xi)^2]^2} \right. \right. \\ \left. \left. - \frac{8dx(d+x)(y-\xi)^2}{[(x+d)^2 + (y-\xi)^2]^3} \right] + \frac{m-1}{4m} \left[\frac{(x-d)}{[(x-d)^2 + (y-\xi)^2]} \right. \right. \\ \left. \left. + \frac{(3x+d)}{[(x+d)^2 + (y-\xi)^2]} - \frac{4x(y-\xi)^2}{[(x+d)^2 + (y-\xi)^2]^2} \right] \right] \quad (1.27)$$

$$\sigma_y = \frac{P}{\pi} \left[\frac{m+1}{2m} \left[\frac{(x-d)(y-\xi)^2}{[(x-d)^2 + (y-\xi)^2]^2} + \frac{(x+d)^2[(y-\xi)^2 + 2d^2] - 2d(y-\xi)^2}{[(x+d)^2 + (y-\xi)^2]^2} \right. \right. \\ \left. \left. + \frac{8dx(d+x)(y-\xi)^2}{[(x+d)^2 + (y-\xi)^2]^3} \right] + \frac{m-1}{4m} \left[- \frac{(x-d)}{[(x-d)^2 + (y-\xi)^2]} \right. \right. \\ \left. \left. + \frac{(x+3d)}{[(x+d)^2 + (y-\xi)^2]} + \frac{4x(y-\xi)^2}{[(x+d)^2 + (y-\xi)^2]^2} \right] \right] \quad (1.28)$$

where,

$$m = \frac{1-v}{v}$$

$$\sigma_x = \frac{qy}{\pi} \left[\frac{m+1}{2m} \left[\frac{(x'-d)^2}{r_1^4} - \frac{d^2 - x'^2 + 6dx'}{r_2^4} + \frac{8dx'y'^2}{r_2^6} \right] \right. \\ \left. - \frac{m-1}{4m} \left[\frac{1}{r_1^2} - \frac{1}{r_2^2} - \frac{4x'(d+x')}{r_2^4} \right] \right] \quad (1.29)$$

$$\sigma_y = \frac{qy}{\pi} \left[\frac{m+1}{2m} \left[\frac{y'^2}{r_1^4} + \frac{y'^2 + 8dx' + 6d^2}{r_2^4} + \frac{8dx'(d+x')^2}{r_2^6} \right] \right. \\ \left. + \frac{m-1}{4m} \left[\frac{1}{r_1^2} + \frac{3}{r_2^2} - \frac{4x'(d+x')}{r_2^4} \right] \right] \quad (1.30)$$

$$\sigma_x = \frac{q(y-\xi)}{\pi} \left[\frac{m+1}{2m} \left[\frac{(x-d)^2}{[(x-d)^2 + (y-\xi)^2]^2} - \frac{d^2 - x^2 + 6dx}{[(x+d)^2 + (y-\xi)^2]^2} \right. \right. \\ \left. + \frac{8dx(y-\xi)^2}{[(x+d)^2 + (y-\xi)^2]^3} \right] - \frac{m-1}{4m} \left[\frac{1}{[(x-d)^2 + (y-\xi)^2]} \right. \\ \left. - \frac{1}{[(x+d)^2 + (y-\xi)^2]} - \frac{1}{[(x+d)^2 + (y-\xi)^2]^2} \right] \right] \quad (1.31)$$

$$\sigma_y = \frac{q(y-\xi)}{\pi} \left[\frac{m+1}{2m} \left[\frac{(y-\xi)^2}{[(x-d)^2 + (y-\xi)^2]^2} + \frac{(y-\xi)^2 + 8dx + 6d^2}{[(x-d)^2 + (y-\xi)^2]^2} \right. \right. \\ \left. + \frac{8dx(d+x)^2}{[(x+d)^2 + (y-\xi)^2]^3} \right] + \frac{m-1}{4m} \left[\frac{1}{[(x-d)^2 + (y-\xi)^2]} \right. \\ \left. + \frac{3}{[(x+d)^2 + (y-\xi)^2]} - \frac{4x(d+x)}{[(x+d)^2 + (y-\xi)^2]^2} \right] \right] \quad (1.32)$$

where, $m = \frac{1-v}{v}$

1.3 Ideal Soil System

The mathematical response of naturally occurring soils can be influenced by a variety of factors. These include:

- (i) The shape, size and mechanical properties of the individual particles.
- (ii) The configuration of the soil structure.
- (iii) The intergranular stresses and stress history, and
- (iv) The presence of soil moisture and the soil permeability.

These factors generally contribute to stress-strain phenomena which display markedly non-linear, irreversible and time-dependent characteristics, and to soil masses which exhibit anisotropic and non-homogeneous material properties. Thus, any attempt to solve a soil-structure interaction problem, taking into account all such material properties, is clearly a difficult task.

In order to obtain meaningful and reliable information for practical problems of soil-structure interaction it is necessary to idealize the behaviour of soil by taking into account specific aspects of its behaviour. The simplest type of idealized soil response assumes linear elastic behaviour of the soil medium. It is recognized that the assumptions of linearity and reversibility of deformations implicit in linear elastic behaviour are, of course, not always rigorously satisfied in naturally occurring soil masses.

Linear elastic behaviour, on the other hand, considerably reduces the analytical rigour needed in the solution of a particular boundary value problem and provides useful information for solving many practical problems of soil mechanics which would otherwise be intractable.

Another idealization comes from assuming continuum behaviour of the soil. The soil medium is thus represented by a homogeneous isotropic linearly elastic half space characterized by the elastic constants E and ν .

Despite the above idealization of soil behaviour, the proposed isotropic linear elastic behaviour can be very representative for work-hardened soils such as preloaded sands and overconsolidated clays. The linear elastic behaviour can be assumed until the previously established stress ratio is very nearly reached. Poorooshab et.al.(1967) have proven this phenomenon experimentally by subjecting a soil element to a series of unloading and reloading cycles. In their test, the sample is subjected to initial isotropic consolidation, then to a conventional drained test until the sample starts to yield. The test is continued by first subjecting the sample to a conventional drained unloading process, then to a $\sigma_1 = \text{constant}$, σ_3 increasing process and finally reloading it again via a conventional drained path to another yielding point. The unloading and reloading cycle is repeated several times as shown in the stress path Fig. (1.8). The corresponding axial strains (ϵ_1) are plotted against the stress parameter $t = \sqrt{\frac{2}{3}} (\sigma_1 - \sigma_3)$ as in Fig. (1.9).

From the (ϵ, t) curve in Fig. (1.9), it is noted that the soil sample behaves in a linear elastic manner upon unloading and reloading. It is also noted, from the stress path in Fig. (1.8) that this behaviour continues until the previously established stress ratio (η) is almost reached where

$$\eta \text{ (stress ratio)} = t/s$$

$$t \text{ (stress parameter)} = \sqrt{2}/3 (\sigma_1 - \sigma_3)$$

$$s \text{ (stress parameter)} = \sqrt{1}/3 (\sigma_1 + 2\sigma_3)$$

Many natural sand deposits and clays exist in an over-consolidated state, so that the mean normal stress increments imposed on them by man-made structures are often small in relation to the maximum stresses to which they have been subjected in the past. Under these circumstances and from this argument, the stress-strain relationship of such soils often resemble those of linear elastic solids. In addition, all but the very over consolidated soils decrease in volume at shear stresses well below the failure value. For these reasons, over consolidated soils can often be fairly successfully treated for the purpose of analysis as isotropic linear elastic solids.

In the case of normally consolidated soils, on the other hand, more complicated constitutive relationships which reflects more accurately the non-linear state dependent behaviour of these soils, must be used, since simple elastic treatment is likely to give unreliable results.

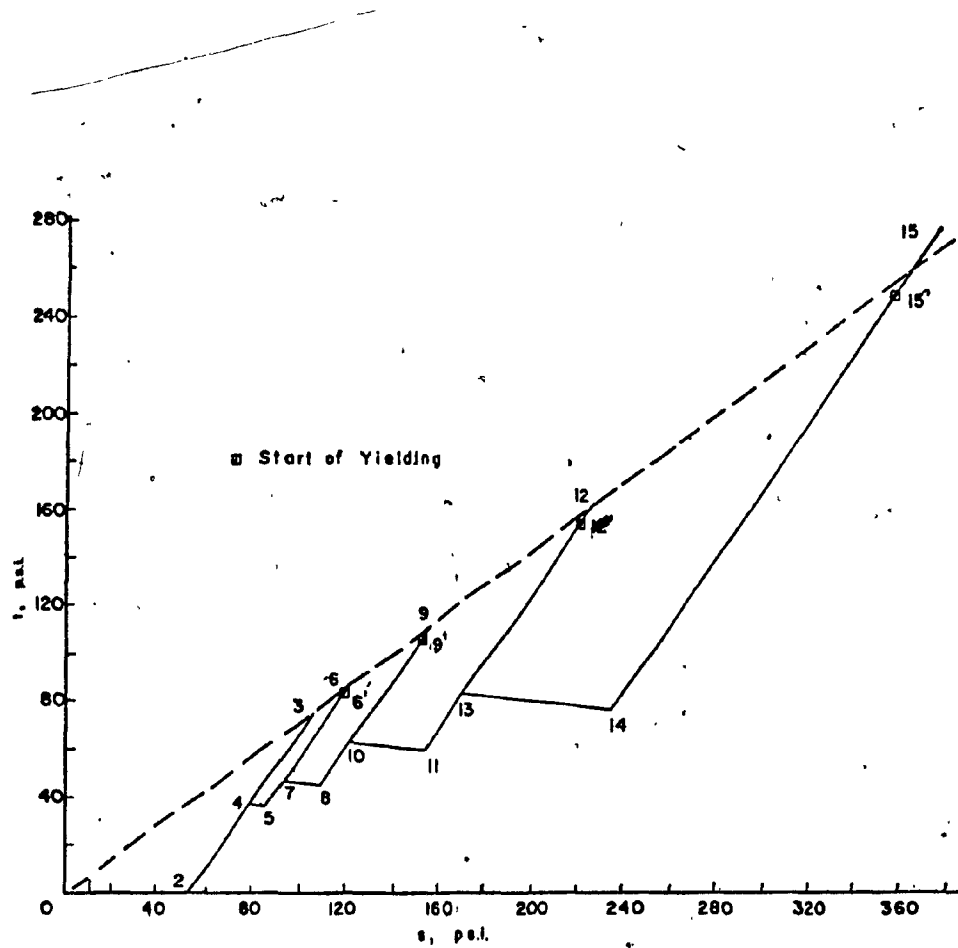


FIG. 1.8: The yield locus is a function of the stress ratio

Source: Roorooshashb et al (1967)

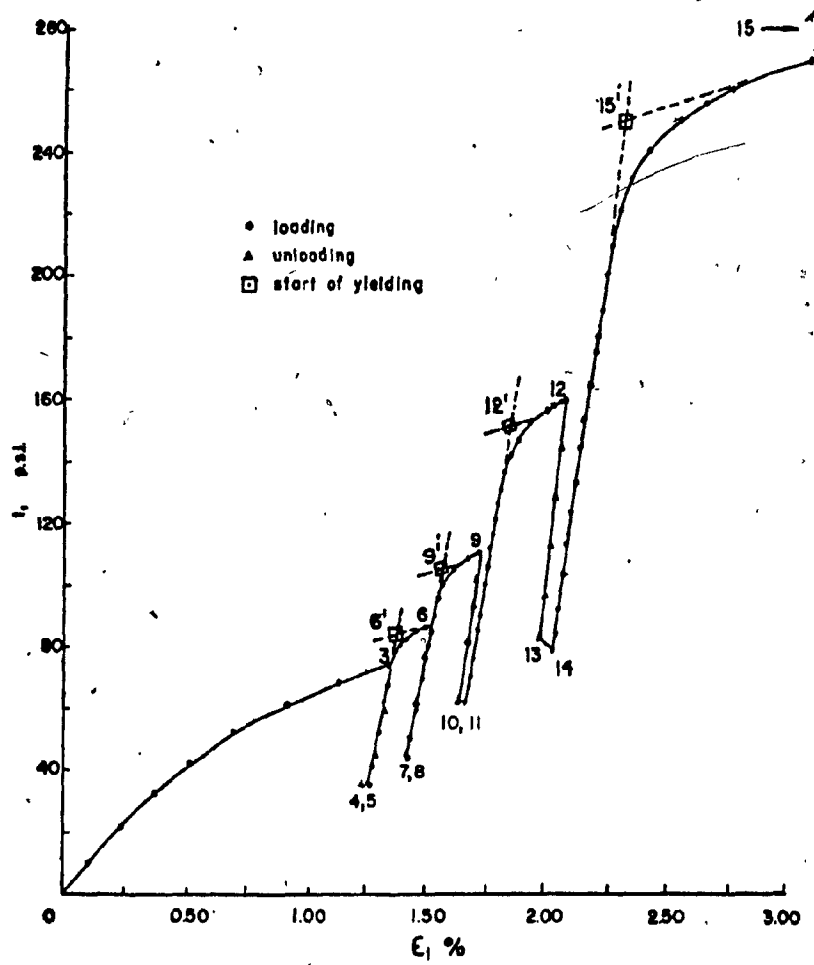


FIG. 1.9: Results from a special test studying the yield criterion

Source: Poorooshasb et al (1967)

1.4 Soil-Structure Interaction

Upon defining the deformational characteristics of the soil medium (Sec. 1.3), the flexural behaviour of the structure, and the conditions at the interface between the soil and the structure, the problem of soil-structure interaction is basically reduced to the determination of contact stress distribution at the interface. Once the contact stresses are determined, it is possible to evaluate the deflection, flexural moments and shearing forces in the structure as well as the stress and displacement fields in the idealized supporting soil medium.

The structure is assumed to be completely rigid or inflexible so that it cannot deform and it is only allowed to have rigid body motion. The deformational characteristics of the surrounding soil medium has been defined in Section (1.3). The soil is assumed isotropic and linearly elastic so that Hooke's law and the fundamental solution apply.

Regarding the conditions at the interface between the soil and the structure, it is assumed that there is no relative movement, i.e., no break away or slippage, provided that no tension is produced at the interface and the contact shear stress does not exceed the shear strength of soil.

The two problems treated in this study will focus on determining the contact stress distribution between the idealized soil medium and the following structural units:

- (i) A circular pipe embedded horizontally.
- (ii) Strip-footings of various cross-sectional shapes.

Once the contact stresses are determined the state of stress (and hence deformation) at any point within the elastic half-space can be found using the relevant fundamental solution as will become clearer in the following chapters.

CHAPTER 2

FORMULATION OF SOLUTION THEORY

The main theme of the solution method used for the problems treated in this study is explained in this chapter. Depending on the particular problem, some modifications must be applied and some techniques employed to extract the contact stresses from the solution obtained.

The displacement field in a half-space due to line traction (t_i) acting at some boundary (or contour C, since only two dimensional cases are considered) within the half-space is given by the following integral,

$$u_j(P) = \int_C t_i(s) U_{ij}(P,s) ds \quad (2.1)$$

where,

S is the arc distance of a boundary point measured from arbitrary origin on C.

ds is an element of arc length at S,

P is a point within the half-space,

$t_i(s)$ is traction function value at (S),

$U_{ij}(P,s)$ is the displacement influence function at point (P) in direction (j) due to unit line load at (S) in direction (i) as obtained from integration performed on appropriate Melan's fundamental solution.

The usual notation of Cartesian tensor analysis is used above. Latin subscripts (i) and (j) have the range (1,2)

and summation over repeated subscripts is implied.

Imposing the displacement boundary conditions on the integral Eq. (2.1), the required traction function $t_i(s)$ may be evaluated. However, it is very difficult if not impossible, to obtain the displacement field function $U_{ij}(P, S)$ in analytical form as well as solving the equation itself. Hence, U_{ij} is evaluated numerically and a numerical method is used to solve the integral equation. The contour C is divided into (n) equal segments, as shown in Fig. (2.1). The points where the unknown values are considered are called "nodes" and are taken to be at the middle of each segment. The values of U_j and t_i are assumed to be constant over each segment and equal to the values at the node of the segment.

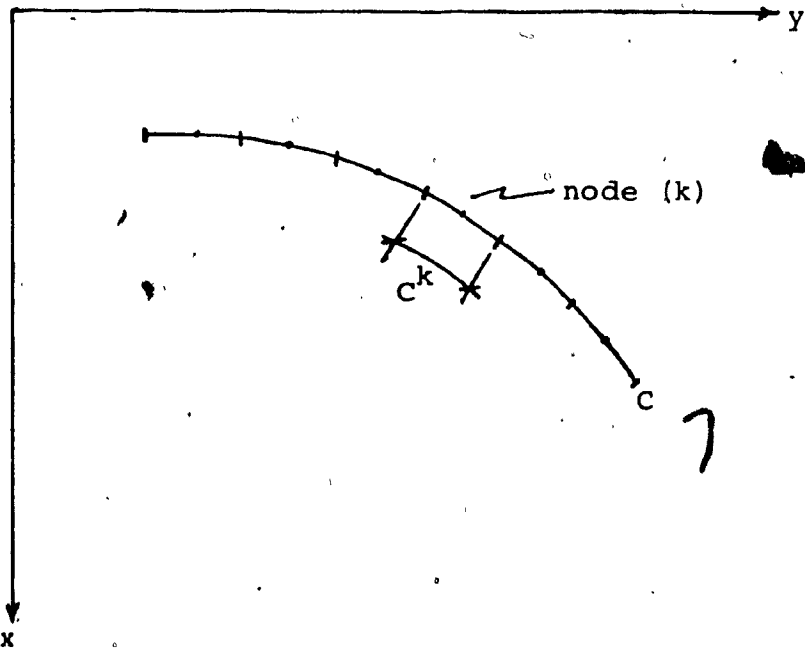


FIG. 2.1: Discretisation of boundary for numerical analysis

Following the above procedure, the integral equation is now discretized before applying the boundary conditions.

Hence, Eq. (2.1) becomes,

$$u_j(p) = \sum_{k=1}^n \int_{C^k} t_i^k u_{ij}(p, s) ds \\ = \sum_{k=1}^n t_i^k \int_{C^k} u_{ij}(p, s) ds \quad (2.2)$$

where C^k = segment arc length.

Applying the boundary conditions yields

$$u_j^l = \sum_{k=1}^n t_i^k \int_{C^k} u_{ij}(s) ds, \quad (l=1, 2, \dots, n) \quad (2.3)$$

where,

u_j^l is the displacement of node (l) in (j) direction

t_i^k is the traction value at segment (k), in (i)
direction

$u_{ij}(s)$ is influence function of displacement in direct-
ion (j) of node l , due to unit line load at s in
direction (i).

The above equation is basically a system of $(2n)$ linear
equations in the $(2n)$ unknown tractions t_i^k .

In each of these equations one of the integrals is
singular, namely when $(k=l)$. The singular integral is under-
stood in the sense of Cauchy principal value, (Kreyszig, 1979).

The numerical evaluation of the displacement influence
factors $\int_{C^k} u_{ij}^t(s) ds$ is elaborated in the following

paragraphs. The integral $[\int_k^C u_{ij}^\ell(s) ds]$ in Eq. (2.3) is the influence factor for the displacement in direction (j) at node (ℓ) due to a uniformly distributed line load in direction (i) at segment (k) which may be referred to as $v_{ij}^{\ell/k}$ and hence Eq. (2.3) is rewritten as,

$$u_j^\ell = \sum_{k=1}^n t_i^k v_{ij}^{\ell/k} \quad (2.4)$$

Expanding Eq. (2.4) and writing it in matrix form results in

$$\begin{bmatrix} v_{11}^{\ell/k} & v_{21}^{\ell/k} \\ v_{12}^{\ell/k} & v_{22}^{\ell/k} \end{bmatrix}_{2n \times 2n} \begin{bmatrix} t_1^k \\ t_2^k \end{bmatrix}_{2n \times 1} = \begin{bmatrix} u_1^\ell \\ u_2^\ell \end{bmatrix}_{2n \times 1} \quad (2.5)$$

In the above system of simultaneous linear algebraic equations the contour displacement values u_j^ℓ are prescribed and the traction values t_i^k are unknowns. Hence evaluation of the influence factors $v_{ij}^{\ell/k}$ remains.

To obtain a tractable solution, it is necessary to assume the existence of a rigid boundary (in a practical situation, this is represented by bedrock) sufficiently distant from the surface, for Melan's solution to be applied. The vertical displacement, relative to the bedrock, of any point except the point of application of the load is evaluated by integrating the corresponding vertical strain (ϵ_{xx}).

For plane strain condition, the stress and strain components are related through the equation,

$$\epsilon_{xx} = \frac{1-v^2}{E} [\sigma_{xx} - \frac{v}{1-v} \sigma_{yy}] \quad (2.6)$$

however,

$$\epsilon_{xx} = - \frac{du_x}{dx}$$

hence,

$$u_x^l = - \int_H^{x^l} \epsilon_{xx} dx = \int_{x^l}^H \epsilon_{xx} dx$$

$$= \frac{1-v^2}{E} \int_{x^l}^H [\sigma_{xx} - \frac{v}{1-v} \sigma_{yy}] dx \quad (2.7)$$

If the horizontal displacement is calculated relative to some stationary reference, say the x-axis, then it can be obtained by integrating the corresponding horizontal strain ϵ_{yy} from $y = 0$ to the y coordinate of the point as follows

$$u_y^l = - \int_0^{y^l} \epsilon_{yy} dy = \frac{1-v^2}{E} \int_{y^l}^0 [\sigma_{yy} - \frac{v}{1-v} \sigma_{xx}] dy \quad (2.8)$$

At this point it remains to evaluate the horizontal and vertical strains ϵ_{yy} , ϵ_{xx} respectively due to unit horizontal line load ($q=1$) and unit vertical line load ($P=1$). Substituting σ_x and σ_y for ($P=1$) from Eqs. (1.27) and (1.28) yields ϵ_x^P and ϵ_y^P given by Eqs. (2.9) and (2.10) respectively. Substituting σ_x and σ_y for ($q=1$) from Eqs. (1.31) and (1.32) yields ϵ_x^q and ϵ_y^q given by Eqs. (2.11) and (2.12) respectively.

$$\epsilon_x^P = \frac{1-v^2}{\pi E} \left[\frac{m+1}{2m} \left[\frac{(x-d)^3}{[(x-d)^2 + (y-\xi)]^2} + \frac{(x+d)[(x+d)^2 + 2dx]}{[(x+d)^2 + (y-\xi)]^2} - \frac{8dx(d+x)(y-\xi)^2}{[(x+d)^2 + (y-\xi)]^3} \right] \right.$$

$$+ \frac{m-1}{4m} \left[\frac{(x-d)}{[(x-d)^2 + (y-\xi)]^2} + \frac{(3x+d)}{[(x+d)^2 + (y-\xi)]^2} - \frac{4x(y-\xi)^2}{[(x+d)^2 + (y-\xi)]^2} \right]$$

$$- \frac{v}{1-v} \left[\frac{\frac{m+1}{2m} \left[\frac{(x-d)(y-\xi)^2}{[(x+d)^2 + (y-\xi)]^2} + \frac{(x+d)[(y-\xi)^2 2d^2] - 2d(y-\xi)}{[(x+d)^2 + (y-\xi)]^2} + \frac{8dx(d+x)(y-\xi)^2}{[(x+d)^2 + (y-\xi)]^3} \right]}{[(x-d)^2 + (y-\xi)^2]^{1/2}} \right.$$

$$+ \frac{m-1}{4m} \left[- \frac{(x-d)}{[(x-d)^2 + (y-\xi)]^2} + \frac{(x+3d)}{[(x+d)^2 + (y-\xi)]^2} + \frac{4x(y-\xi)^2}{[(x+d)^2 + (y-\xi)]^2} \right] \left. \right] \quad (2.9)$$

$$\epsilon_y^P = \frac{1-v^2}{\pi E} \left[\frac{m+1}{2m} \left[\frac{(x-d)(y-\xi)^2}{[(x-d)^2 + (y-\xi)]^2} + \frac{(x+d)[(y-\xi)^2 + 2d(y-\xi)]^2}{[(x+d)^2 + (y-\xi)]^2} + \frac{8dx(x+d)(y-\xi)^2}{[(x+d)^2 + (y-\xi)]^3} \right] \right.$$

$$+ \frac{m-1}{4m} \left[\frac{(x-d)}{[(x-d)^2 + (y-\xi)]^2} + \frac{(x+3d)}{[(x+d)^2 + (y-\xi)]^2} + \frac{4x(y-\xi)^2}{[(x+d)^2 + (y-\xi)]^2} \right]$$

$$- \frac{v}{1-v} \left[\frac{\frac{m+1}{2m} \left[\frac{(x-d)^3}{[(x-d)^2 + (y-\xi)]^2} + \frac{(x+d)[(x+d)^2 + 3dx]}{[(x+d)^2 + (y-\xi)]^2} - \frac{8dx(d+x)(y-\xi)^2}{[(x+d)^2 + (y-\xi)]^3} \right]}{[(x-d)^2 + (y-\xi)^2]^{1/2}} \right.$$

$$+ \frac{m-1}{4m} \left[- \frac{(x-d)}{[(x-d)^2 + (y-\xi)]^2} + \frac{(3x+d)}{[(x+d)^2 + (y-\xi)]^2} - \frac{4x(y-\xi)^2}{[(x+d)^2 + (y-\xi)]^2} \right] \left. \right] \quad (2.10)$$

$$\varepsilon_x^q = \frac{(1-v)^2(y-\xi)}{\pi E} \left[\frac{m+1}{2m} \left[\frac{(x-d)^2}{[(x-d)^2 + (y-\xi)^2]^2} - \frac{d^2 - x^2 + 6dx}{[(x+d)^2 + (y-\xi)^2]^2} + \frac{8dx(y-\xi)^2}{[(x+d)^2 + (y-\xi)^2]^3} \right] \right.$$

$$- \frac{m-1}{4m} \left[\frac{1}{[(x-d)^2 + (y-\xi)^2]} - \frac{1}{[(x+d)^2 + (y-\xi)^2]} - \frac{4x(d+x)}{[(x+d)^2 + (y-\xi)^2]^2} \right]$$

$$- \frac{v}{1-v} \left[\frac{m+1}{2m} \left[\frac{(y-\xi)^2}{[(x-d)^2 + (y-\xi)^2]^2} + \frac{(y-\xi)^2 + 8dx + 6d^2}{[(x+d)^2 + (y-\xi)^2]^2} + \frac{8dx(d+x)^2}{[(x+d)^2 + (y-\xi)^2]^3} \right] \right.$$

$$+ \frac{m-1}{4m} \left[\frac{1}{[(x-d)^2 + (y-\xi)^2]} + \frac{3}{[(x+d)^2 + (y-\xi)^2]} - \frac{4x(d+x)}{[(x+d)^2 + (y-\xi)^2]^2} \right] \left. \right]. \quad (2.11)$$

33

$$\varepsilon_y^q = \frac{(1-v^2)(y-\xi)}{\pi E} \left[\frac{m+1}{2m} \left[\frac{(y-\xi)^2}{[(x-d)^2 + (y-\xi)^2]^2} + \frac{(y-\xi)^2 + 8dx + 6d^2}{[(x+d)^2 + (y-\xi)^2]^2} + \frac{8dx(y-\xi)^2}{[(x+d)^2 + (y-\xi)^2]^3} \right] \right.$$

$$+ \frac{m-1}{4m} \left[\frac{1}{[(x-d)^2 + (y-\xi)^2]} + \frac{3}{[(x+d)^2 + (y-\xi)^2]} - \frac{4x(d+x)}{[(x+d)^2 + (y-\xi)^2]^2} \right]$$

$$- \frac{v}{1-v} \frac{m+1}{2m} \left[\frac{(x-d)^2}{[(x-d)^2 + (y-\xi)^2]^2} - \frac{d^2 - x^2 + 6dx}{[(x+d)^2 + (y-\xi)^2]^2} + \frac{8dx(y-\xi)^2}{[(x+d)^2 + (y-\xi)^2]^3} \right]$$

$$- \frac{m-1}{4m} \left[\frac{1}{[(x-d)^2 + (y-\xi)^2]} - \frac{3}{[(x+d)^2 + (y-\xi)^2]} - \frac{4x(d+x)}{[(x+d)^2 + (y-\xi)^2]^2} \right] \left. \right]. \quad (2.12)$$

Resolving the unit traction ($t_i^k = 1$) corresponding to $v_{ij}^{l/k}$ into horizontal and vertical components as shown in Fig. (2.2)

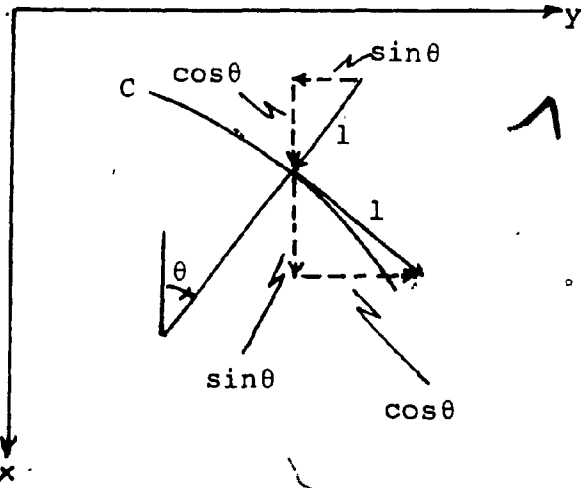


Fig. 2.2: Vertical and horizontal components of boundary traction

we obtain,

$$v_{1j}^{l/k} = \int_{C^k} \int_x^H [\cos(\theta) \epsilon_{jj}^P - \sin(\theta) \epsilon_{jj}^Q] dx ds \quad (2.13)$$

$$v_{2j}^{l/k} = \int_{C^k} \int_y^0 [\sin(\theta) \epsilon_{jj}^P + \cos(\theta) \epsilon_{jj}^Q] dx ds \quad (2.14)$$

where,

θ is the angle between the normal at S and the positive x-axis.

A numerical double integration subroutine, available at the IMSL library of Concordia University's main computer, is used to evaluate the above integrals. The routine uses the cautious Romberg adaptive method to evaluate single integrals involved in its procedure (IMSL, 1982).

Once t_i are evaluated, the displacements of any point in the half space can be calculated using Eq.(2.2) and the state of stress found using the following equations,

$$\sigma_x(P) = \sum_{k=1}^n t_i^k \int_{C^k} x_i(s) ds$$

$$\sigma_y(P) = \sum_{k=1}^n t_i^k \int_{C^k} y_i(s) ds$$

$$\sigma_{xy}(P) = \sum_{k=1}^n t_i^k \int_{C^k} XY_i(s) ds \quad (2.15)$$

where,

x_i^k , y_i^k and XY_i^k are influence functions for the vertical, horizontal and shear stresses respectively at point (P) due to unit load in the direction (i) at s.

CHAPTER 3

APPLICATIONS

The problems of the magnitude and distribution of static stresses on horizontal pipes and on strip footings (of semi-circular, triangular and flat cross-sections) embedded in a homogeneous and isotropic semi-infinite elastic soil will be treated in this chapter to demonstrate the use of the method established previously.

The various structural units are considered to be embedded horizontally with their horizontal axes parallel to the z-axis of a rectangular coordinate system x,y,z as shown in Fig. (2.1). The surrounding material has as its upper surface the plane $x = 0$, but otherwise it is unbounded. Technically, such a body is known as a semi-infinite solid. The x-axis penetrates in its positive direction vertically downward and bisects the cross-section of the unit. The semi-infinite ground has a uniform solid weight per unit volume (γ), so that the problem involves only constant body forces acting in the positive x-direction.

The length of the structure is assumed to be very great in comparison with the dimensions of its cross-section. This factor and the uniformity of the body forces permit a treatment of the problem as one of plane strain.

The problem is then, that of finding the contact normal and shear stresses between the structural unit and the surrounding soil that satisfies the problem's boundary

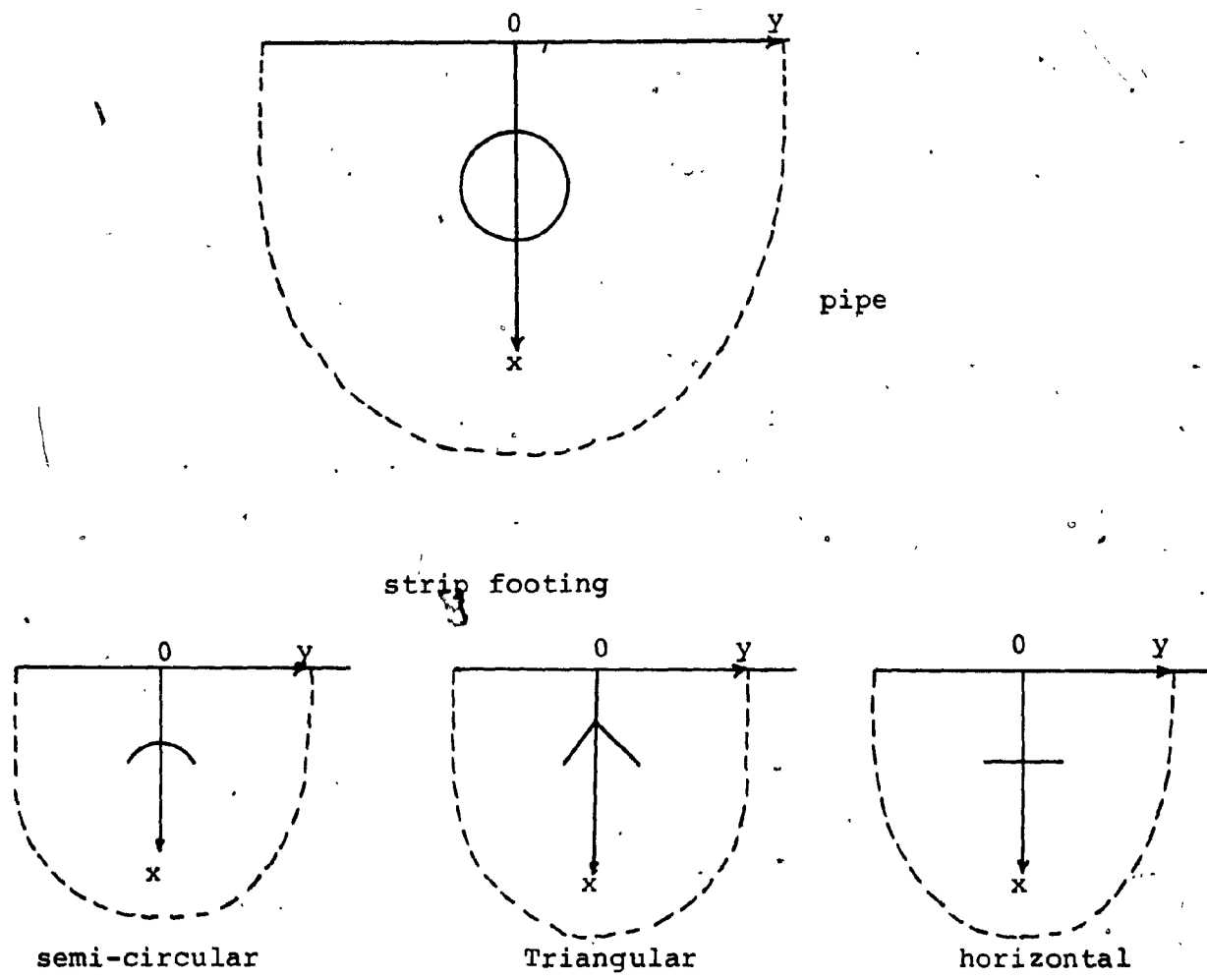


FIG. 3.1: Idealization of the structural units treated

conditions. The boundary conditions are: zero stresses at the bounding straight surface ($x=0$), no slippage at the soil-structure interface and only translation movement of the unit, implied by its rigidity. The stress distribution is assumed to be symmetrical about the unit's vertical axis and the contact surface is rough enough to prevent any slippage.

Theoretical modelling of the problems treated and application of the solution method are to follow.

3.1 Contact Stresses on Horizontally Embedded Rigid Pipes

The development of the mathematical model used for this problem follows the solution method established in Chapter (2). A set of tractions at the pipe-soil interface is sought. The tractions are to be symmetric with a vertical force component equal to the weight of the soil displaced by the pipe. In addition, the solution must satisfy the following displacement conditions for points at the contact surface,

- (i) zero horizontal displacement,
- (ii) all points have the same vertical displacements.

In this sense the tractions to be found are the changes in the stresses existing on an immaginary circumference in the location where the pipe is to be installed. However, no fundamental solution exists for the half-space with the discontinuity created by the pipe. In modelling the problem, discontinuity is avoided by considering a circular contour

C in a half space with zero body forces at the same depth
(D) and of the same radius (R) as those of the pipe.

Let the half space Ω consist of two separate regions: the region Ω_1 outside C and the region Ω_2 bounded by C. If \underline{t} and \bar{t} are external tractions acting on C of Ω_1 and Ω_2 respectively such that they produce the same displacement field on C, then, a traction $t = \underline{t} + \bar{t}$ acting on C of Ω will produce the same displacement and stress fields in Ω_1 and Ω_2 , due to \underline{t} and \bar{t} respectively. If tractions t is solved for under a prescribed set of displacement conditions on C of Ω following the method of Chapter (2), the traction \underline{t} can be found such that it satisfies the same displacement conditions on C of Ω_1 . \underline{t} is extracted from t by considering the boundary equilibrium equations on C of Ω_1 under the stress field produced by t in Ω .

Parameter \underline{t} is obviously the required disturbance traction of the original problem.

Dividing C into (n) segments as shown in Fig. (3.2) and applying Eq. (2.5) of Chapter (2) with the above prescribed displacement conditions yields

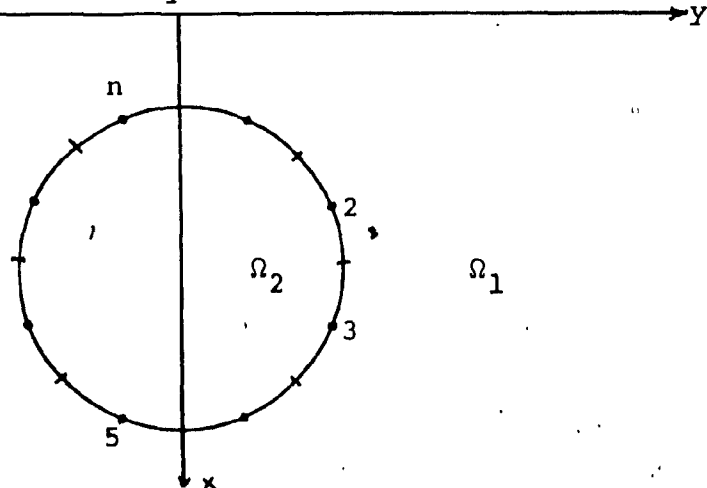


FIG. 3.2: Discretisation of the pipe boundary

$$\begin{bmatrix} v_{11}^{\ell/k} & v_{21}^{\ell/k} \\ \hline v_{12}^{\ell/k} & v_{22}^{\ell/k} \end{bmatrix} \begin{bmatrix} t_1^k \\ t_2^k \end{bmatrix} = \begin{bmatrix} \bar{u} \\ 0 \end{bmatrix} \quad (3.1)$$

where,

t_1^k are radial tractions

t_2^k are tangential tractions

\bar{u} unknown constant vertical displacement

Eq. (3.1) results in $(2n)$ equations and $(2n+1)$ unknowns.

One more equation is obtained from the condition imposed on \underline{t} such that,

$$\sum_{k=1}^n [\underline{t}_1^k \int_{C_k} \cos \theta \, ds + \underline{t}_2^k \int_{C_k} \sin \theta \, ds] = -W = -\pi R^2 \gamma \quad (3.2)$$

i.e., the vertical component of the disturbance traction is equal to the weight of material displacement.

But,

$$\underline{t}_i^k = t_i^k - \bar{t}_i^k \quad , (3.3)$$

and by equating the vertical component of \underline{t}_i^k to zero to satisfy the equilibrium of Ω_2 yields,

$$\sum_{k=1}^n [t_1^k \int_{C_k} \cos \theta \, ds + t_2^k \int_{C_k} \sin \theta \, ds] = -\pi R^2 \gamma \quad (3.4)$$

Thus a system of $(2n+1)$ simultaneous linear algebraic equations in $(2n+1)$ unknowns is obtained. Consequently \underline{t}_i remains to be evaluated.

Since the tractions t_i are symmetrical about the vertical axis of C , the number of unknowns is reduced to $(n+1)$ by considering only the displacement equations for nodes on one side of C . In this manner the influence factor $\bar{v}_{ij}^{\ell/k}$ will be defined as the displacement at node ℓ in direction (j) due to unit uniform loads at segments k and k' . Here segment k' is the mirror segment of segment k about the x -axis, that is

$$v_{1j}^{\ell/k} = v_{ij}^{\ell/k} + v_{ij}^{\ell/k'} \quad (3.5)$$

$$v_{2j}^{\ell/k} = v_{2j}^{\ell/k} - v_{2j}^{\ell/k'} \quad (3.6)$$

where the range of ℓ and k is $(1, 2, \dots, n/2)$.

The equilibrium equation becomes,

$$\sum_{k=1}^{n/2} 2[t_1^k \int_{C_k} \cos ds + t_2^k \int_{C_k} \sin ds] = -\pi R^2 \gamma \quad (3.7)$$

Numerical integration is used to evaluate the influence factors. An IMSL library subroutine called (LEQT1F) available on Concordia University's main computer is used to solve the resulting system of linear equations. LEQT1F performs Gaussian elimination with equilibrium and partial pivoting (IMSL, 1982).

The last stage in the analysis is extracting the t_i 's acting on C of Ω_1 from the now known traction t_i , using the boundary equilibrium equations on C of Ω_1 under the stress field of t_i 's. Referring to Fig. (3.3), the following expressions for t_i^k are obtained

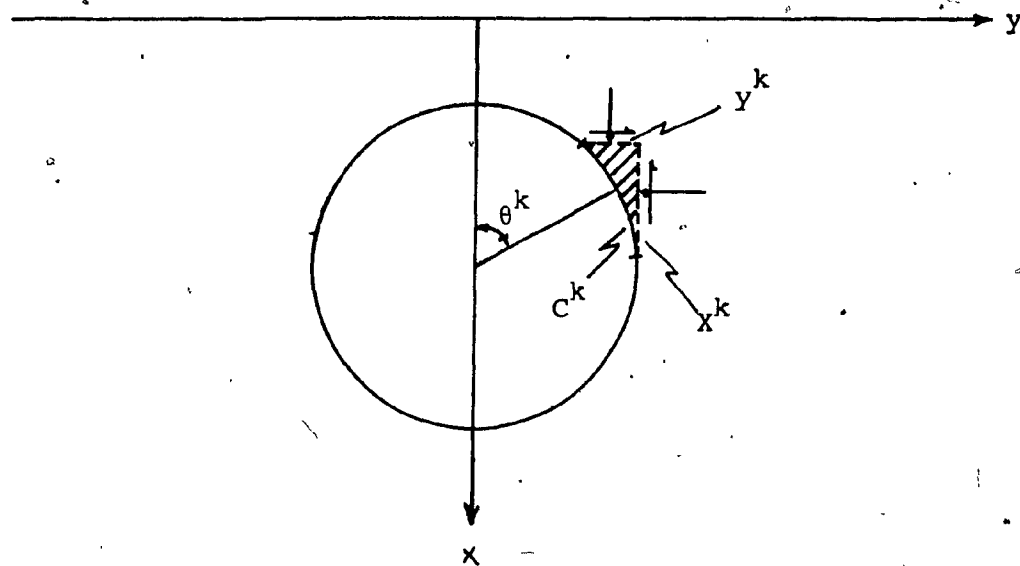


FIG. 3.3: Resolving tractions for pipe problems

$$t_1^k = \left[\int_k^y \sigma_x \cos \theta^k dy - \int_k^x \sigma_{xy} \cos \theta^k dx \right. \\ \left. + \int_k^x \sigma_y \sin \theta^k dx - \int_k^y \sigma_{xy} \sin \theta^k dy \right] / C^k \quad (3.8)$$

$$t_2^k = \left[- \int_k^y \sigma_x \sin \theta^k dy + \int_k^x \sigma_{xy} \sin \theta^k dx \right. \\ \left. + \int_k^x \sigma_y \cos \theta^k dx - \int_k^y \sigma_{xy} \cos \theta^k dy \right] / C^k \quad (3.9)$$

where,

C^k arc length of segment k

x^k projection of C^k on x-axis

y^k projection of C^k on y-axis

$\sigma_x, \sigma_y, \sigma_{xy}$ are values of the stress field induced by the vertical and horizontal components of the tractions t_i obtained from Melan's fundamental solution.

The final contact stress is now found by superposing the disturbance tractions t_i on the original stresses at the same depth prior to the installation of the pipe. The displacement and state of stress at any point in Ω_1 can now be found by using the same values for the same point in Ω produced by t_i 's.

3.2 Contact Stresses on Strip Footings of Various Shapes

The development of the mathematical model used for solving the problem considered here follows the solution method of Chapter (2) with the following boundary conditions,

- (i) The set of symmetric tractions on the contact surface have a vertical force component equal to the applied load (W),
- (ii) zero horizontal displacement,
- (iii) fixed vertical displacement for all points on the interface.

To obtain the final contact pressure, these tractions must be superposed on the pressure acting before applying the load (W).

In modelling the problem, it is assumed that the footing is of negligible thickness, so that the embedding half-space remains continuous. Thus, the footing is represented by a contour C of the same dimensions as those of the footing. Let t_i be the set of tractions acting on C in such a way to satisfy the boundary conditions of the problem stated above. In the real problem, t_i is equal to the sum of the traction t_i and the traction \bar{t}_i acting on the bottom

and top faces of the footing, respectively.

t_i and \bar{t}_i are found, as for the pipe problem, from the boundary equilibrium equations applied to the bottom and top faces of C under the stress field of t_i .

Dividing C into (n) segments as shown in Fig. (3.4) and applying Eq. (2.5) of Chapter (2) with the prescribed displacements on the boundary C yields,

$$\begin{bmatrix} v_{11}^{\ell/k} & v_{21}^{\ell/k} \\ \cdots & \cdots \\ v_{12}^{\ell/k} & v_{22}^{\ell/k} \end{bmatrix} \begin{bmatrix} t_1^k \\ t_2^k \end{bmatrix} = \begin{bmatrix} \bar{u} \\ 0 \end{bmatrix} \quad (3.10)$$

where,

\bar{u} is the unknown vertical displacement of the footing,

$v_{ij}^{\ell/k}$ and t_i areas defined before.

One more equation is obtained by applying the equilibrium equation in the vertical direction, as in the pipe problem. This yields,

$$\sum_{k=1}^n [t_1^k \int_C^k \cos\theta ds + t_2^k \int_C^k \sin\theta ds] = w \quad (3.11)$$

Eqs. (3.10) and (3.11) create the desired $(2n+1)$ system of simultaneous algebraic equations in the $(2n)$ unknown tractions t_i and the unknown vertical displacement \bar{u} .

By considering the symmetry of the tractions, the system is reduced to $(n+1)$ simultaneous algebraic equations, as in the pipe problem as follows,

$$\begin{bmatrix} \bar{v}_{11}^{\ell/k} & \bar{v}_{21}^{\ell/k} \\ \bar{v}_{12}^{\ell/k} & \bar{v}_{22}^{\ell/k} \end{bmatrix} \begin{bmatrix} t_1^k \\ t_2^k \end{bmatrix} = \begin{bmatrix} \bar{u} \\ 0 \end{bmatrix} \quad (3.12)$$

and,

$$\sum_{k=1}^n 2[t_1^k \int_{C^k} \cos ds + t_2^k \int_{C^k} \sin ds] = w \quad (3.13)$$

where all the parameters are as defined for the pipe problem.

Eqs. (3.8) and (3.9) of Sec. (3.1) are used to extract \bar{t}_i from the now known tractions t_i as shown in Fig. (3.4).

$$\begin{aligned} \bar{t}_1^k &= [\int_y^k \sigma_x \cos \theta^k dy - \int_x^k \sigma_{xy} \cos \theta^k ddx \\ &\quad + \int_x^k \sigma_y \sin \theta^k dx - \int_y^k \sigma_{xy} \sin \theta^k dy]/c^k \end{aligned} \quad (3.14)$$

$$\begin{aligned} \bar{t}_2^k &= [-\int_y^k \sigma_x \sin \theta^k dy + \int_x^k \sigma_{xy} \sin \theta^k dx \\ &\quad + \int_x^k \sigma_y \cos \theta^k dx - \int_y^k \sigma_{xy} \cos \theta^k dy]/c^k \end{aligned} \quad (3.15)$$

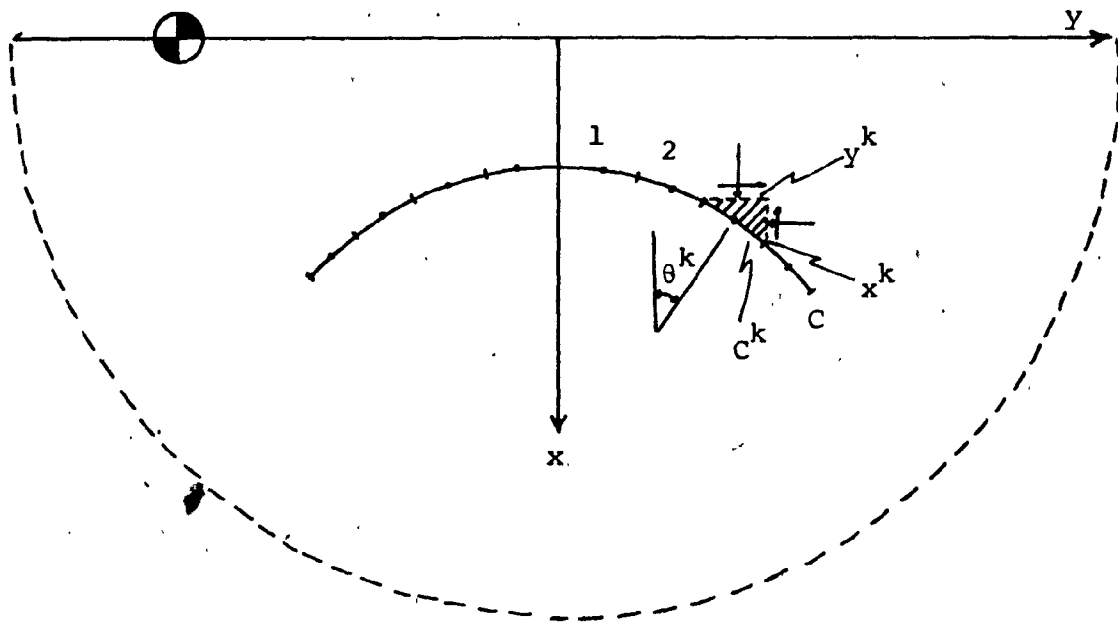


FIG. 3.4: Resolving tractions for strip footing problem
where,

x^k, y^k, c^k are as defined before

$\sigma_x, \sigma_y, \sigma_{xy}$ are the stress field values due to t_i

Since,

$$t_i^k = t_i^k + \bar{t}_i^k$$

hence,

$$\bar{t}_i^k = t_i^k - \bar{t}_i^k \quad (3.16)$$

The final contact pressure is determined by superposing the disturbance tractions \bar{t}_i and t_i on the original stresses prior to applying the load (W).

The displacement and state of stress of any point within the half-space can be found by using Eqs. (2.2) and (2.15) respectively with the stress field induced by the total traction t_i .

CHAPTER 4

NUMERICAL RESULTS

The method of analysis presented in the previous chapters may be used to determine the stresses and displacements anywhere within the elastic soil mass due to soil-structure interaction. However attention will be restricted here to determining the contact pressures and the displacement of the structure. As stated previously, the elastic soil is assumed to have self-weight or applied surcharge sufficient to prevent breakaway at the soil structure interface and the structure surface is rough enough to prevent slip.

Application of the analytical technique, previously mentioned, to the prediction of contact pressures, involves numerical approximation regarding the number of segments which are necessary to simulate the rigid structure's behaviour. In this regard it was found that the results could be obtained with sufficient degree of accuracy by using a relatively small number of segments. The adoption of a larger number of segments did not alter the results significantly.

The contact pressure problem of the rigid circular pipe is considered first. Later, those of rigid strip footings of semi-circular, triangular, and flat cross-sections are considered.

A single program is written for each problem, depending on its geometry. This program is used to calculate the influence factors. It forms and solves the desired system of linear algebraic equations and proceeds to calculate contact stresses as well as the vertical displacement of the structural unit.

4.1 Horizontal Pipe

The pipe considered is of radius (R) and its centre is at depth (D) below the ground surface. The underlying bedrock is at depth (H) below the ground surface.

The boundary of the pipe is first divided into 20 equal segments numbered in clockwise direction. The first end point of the first segment coincides with the crown of the pipe. Each segment is assigned a single node at its midpoint.

The program developed for this problem is called "PIPE". It calculates the coordinates of each node in the x-y axis system and the arc distances of the end points for all segments. The origin of the arc distance is taken at the crown of the pipe. Its positive direction is clockwise. The program also calculates the displacement influence factors for nodes falling on the right-hand side of the pipe's axis due to uniform unit normal and tangential loads acting on each segment. The desired system of linear algebraic equations is assembled and solved to obtain the vertical displacement of the pipe, as well as, the set of

tractions (t_i) acting on each segment as defined in Chapter (3).

Finally, the actual disturbance in contact pressure \underline{t}_i is extracted from t_i and superposed on the original pressure to obtain the final contact pressure at the interface.

The first computer run for this problem is done with $R = 3^m$, $D = 15^m$, $H = 30^m$, $\gamma = 1800 \text{ KG/m}^3$, $E = 1.5 \times 10^6 \text{ KG/m}^2$, $\nu = .3$, $K_o = .5$. Because of its symmetry, the results for half the pipe are given in Table (4.1).

The results of Table (4.1) are plotted in Fig. (4.1), using the "Centre for Building Studies" Megatic graphics system. Lagrange interpolation formula is used to interpolate pressure between nodal values.

A second run of this problem is obtained with 40 segments and the same parameters used for the first run.

Results are given in Table (4.2) and plotted in Fig. (4.2). It should be noted that the adoption of a larger number of segments did not significantly alter the results.

The two programs used for solving and plotting the results of this problem are given in the appendix under the names "PIPE" and "PIPELO" respectively.

The user of program "PIPE" needs only to give the following data: R , D , H , γ , E , ν , K_o and the desired number of segments (n).

TABLE 4.1
RESULTS OF "PIPE" (N=20)

[DATA]		[RESULTANT STRESS DISTRIBUTION]		[STRESS DIST. ON OUTER SURFACE]	
ANGLE	RAD.	TAN.	RAD.	TAN.	
9.00	-1782.5	-372.6	1639.3	-324.2	
27.00	-1559.4	-1077.4	1497.3	-1008.5	
45.00	-1149.8	-1673.9	1174.3	-1641.8	
63.00	-602.7	-2138.5	663.8	-2189.1	
81.00	58.6	-2462.6	42.2	-2568.0	
99.00	830.1	-2630.4	-903.6	-22742.5	
117.00	1700.7	-2584.1	-1761.7	-2630.8	
135.00	2601.5	-2240.5	-2620.8	-2201.2	
153.00	3377.4	-1544.7	-3305.9	-1470.3	
171.00	3838.9	-553.9	-3679.1	-487.8	
VERTICAL DISPLACEMENT IS: [-.016502]					

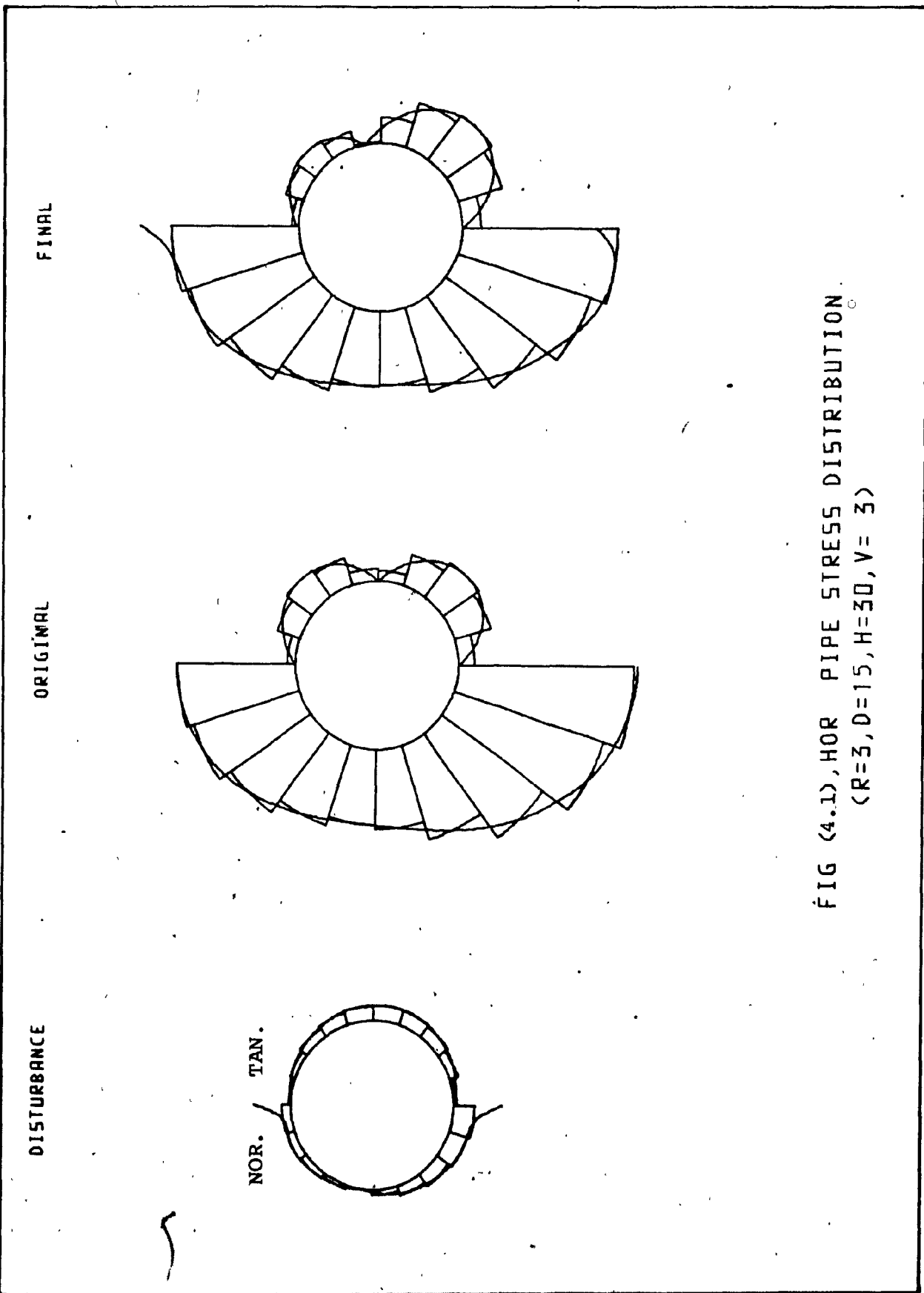
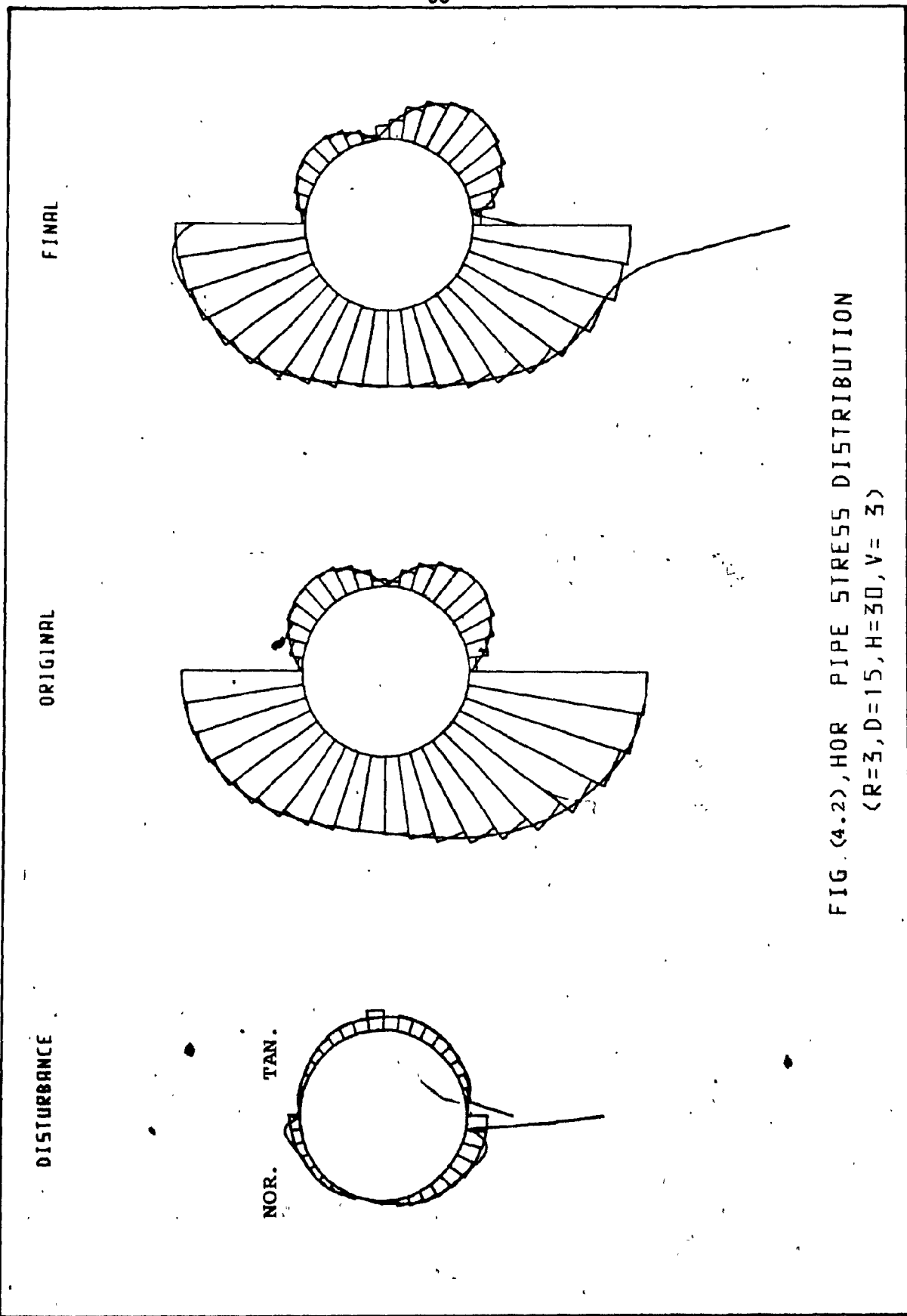


TABLE 4.2

RESULTS OF "PIPE" (N=40)

[DATA]		[RESULTANT STRESS DISTRIBUTION]		[STRESS DIST. ON OUTER SURFACE]	
ANGLE	RAD.	TAN.	RAD.	TAN.	
4.50	-1786.0	-185.6	1649.9	-159.4	
13.50	-1729.4	-551.5	1616.7	-506.3	
22.50	-1621.0	-902.9	1543.5	-840.5	
31.50	-1555.8	-1227.5	1425.7	-1167.4	
40.50	-1426.7	-1519.4	1262.6	-1082.4	
49.50	-1005.0	-1780.1	1055.3	-1780.5	
58.50	-725.2	-1993.9	796.2	-2046.8	
67.50	-415.6	-2167.8	500.0	-2272.8	
76.50	39.1	-1706.2	-18.0	-2180.1	
85.50	99.8	-4317.6	-81.2	-352.4	
94.50	586.2	-1902.6	544.3	-2163.0	
103.50	1021.7	-2571.3	-1087.3	-2714.1	
112.50	1850.7	-2568.0	-1530.8	-2666.8	
121.50	1913.6	-2499.3	-1982.5	-2542.6	
130.50	2367.4	-2337.4	-2415.7	-2331.6	
139.50	2798.7	-2077.6	-2809.6	-2037.2	
148.50	3186.6	-1735.3	-3155.6	-1672.4	
157.50	3509.6	-1308.5	-3431.5	-3218.4	
166.50	3738.9	-814.5	-3623.5	-767.9	
175.50	3859.3	-276.5	-3715.5	-239.7	
VERTICAL DISPLACEMENT IS: [-0.016488]					



4.2 Strip Footings

Rigid strip footings with three different cross-sections are considered here. The cross-sectional figures are as follows: the semi-circular, the triangular and the horizontal.

The semi-circular and triangular footings considered are of angular size (ANG) and their bottom is at depth (HB) and of breadth (BR). The underlying bedrock is at depth (H). The same applies to the horizontal strip footing but with (ANG) = 180°.

The boundary of each footing is first divided into 20 segments. The first end-point of the first segment coincides with the crest of the footing for the semi-circular and triangular shapes and with the mid point for the flat shape. Each segment is assigned a single node at its midpoint.

A single program is developed for each shape, "CIRFDN" for the semi-circular, "TRIFDN" for the triangular and "FLAFDN" for the flat shape.

As in program "PIPE", each of these programs calculates the coordinates of each node in the x-y system and the arc distances of the end-points for all segments. The origin of the arc distance coincides with the crest of the footing for both the circular and triangular shapes and with the midpoint for the flat shape. Its positive direction coincides with that of increasing numbering of the nodes.

"CIRFDN", "TRIFDN", and "FLAFDN" calculate the displacement influence factors for nodes falling on the right-hand side of the footing axis of symmetry due to uniform unit normal and tangential loads on each segment. The desired system of linear algebraic equations is assembled and solved for the vertical displacement of the footing and the set of tractions (t_i) (total tractions) as defined in Chapter (3). Finally, the actual disturbances in contact pressures \bar{t}_i and t_i acting on the top and bottom faces of the footing, respectively, are extracted from t_i using Eqs. (3.14) and (3.15) of Chapter (3).

For the purpose of comparison, the parameters used are identical for all three shapes: $BR = 1^m$, $HB = 3^m$, $H = 10^m$, $E = 1.5 \times 10^6 \text{ KG/m}^2$, $\nu = .3$, $W = 30000 \text{ KG/m}$, $\text{ANG} = 120^\circ$ is used for the circular and triangular shapes.

Again, because of their symmetry, the results for one half the footing are given. Compressive normal stress and tangential stress of a clockwise direction are considered positive. Results are plotted using the "CBS" graphics system as in the pipe problem, and Lagrange interpolation formula is used to interpolate stresses between nodal values.

Results of the first run for the semi-circular, triangular and flat shapes are given in Tables (4.3), (4.4), (4.5) and illustrated in Figs. (4.3), (4.4), (4.5) respectively.

A second run for these problems is obtained with (40) segments and the same parameters used in the first run.

Results are given in Tables (4.6), (4.7), (4.8) and are plotted in Figs.(4.6), (4.7), (4.8) for the semi-circular, triangular and flat shapes, respectively.

There were no significant differences, noted in the results for an increase in the number of segments. Listings of "CIRFDN", "TRIFDN" and "FLAFDN", the plotting programs "CIRPLO" for plotting "CIRFDN" results, and "TRIPLO" for plotting "TRIFDN" and "FLAFDN" results are given in the appendix.

The user of the preceeding programs must supply the following: BR, HB, H, E, v, W and the desired number of segments.

The pressures plotted in Figs. (4.3-4.8) rise to high values near the edges of the footing. With the numerical method employed, it is impossible to calculate the pressures immediately adjacent to the edges. The curves in these figures are extrapolated beyond the limits of the numerical analysis, however this is not reliable.

TABLE 4.3

RESULTS OF "CIFRDN" (N=20)

[DATA]			[STRESS DIST. ON LOWER SURFACE]			[STRESS DIST. ON UPPER SURFACE]		
ANG.	RAD.	TAN.	RAD.	TAN.	RAD.	TAN.	RAD.	TAN.
3.0	7990.7	339.6	5423.0	147.2	-2567.7	192.4		
9.0	8095.0	1037.2	5342.7	334.5	-2752.3	702.8		
15.0	8194.2	1763.4	5356.5	572.2	-2837.7	1191.2		
21.0	8360.1	2560.2	5392.6	831.7	-2967.5	1736.6		
27.0	8566.4	3439.3	5448.3	1106.0	-3118.1	2333.2		
33.0	8920.4	4505.7	5581.9	1467.4	-3338.5	3038.2		
39.0	9285.1	5709.1	5742.4	1875.9	-3542.7	3833.3		
45.0	10139.4	7573.4	6164.4	2607.5	-3975.0	4966.0		
51.0	11341.0	10084.5	6948.0	3492.1	-4393.1	6592.4		
57.0	23128.3	24825.3	11168.6	12235.7	-11959.7	12589.7		
							[VERTICAL DISPLACEMENT IS: [.016648]	

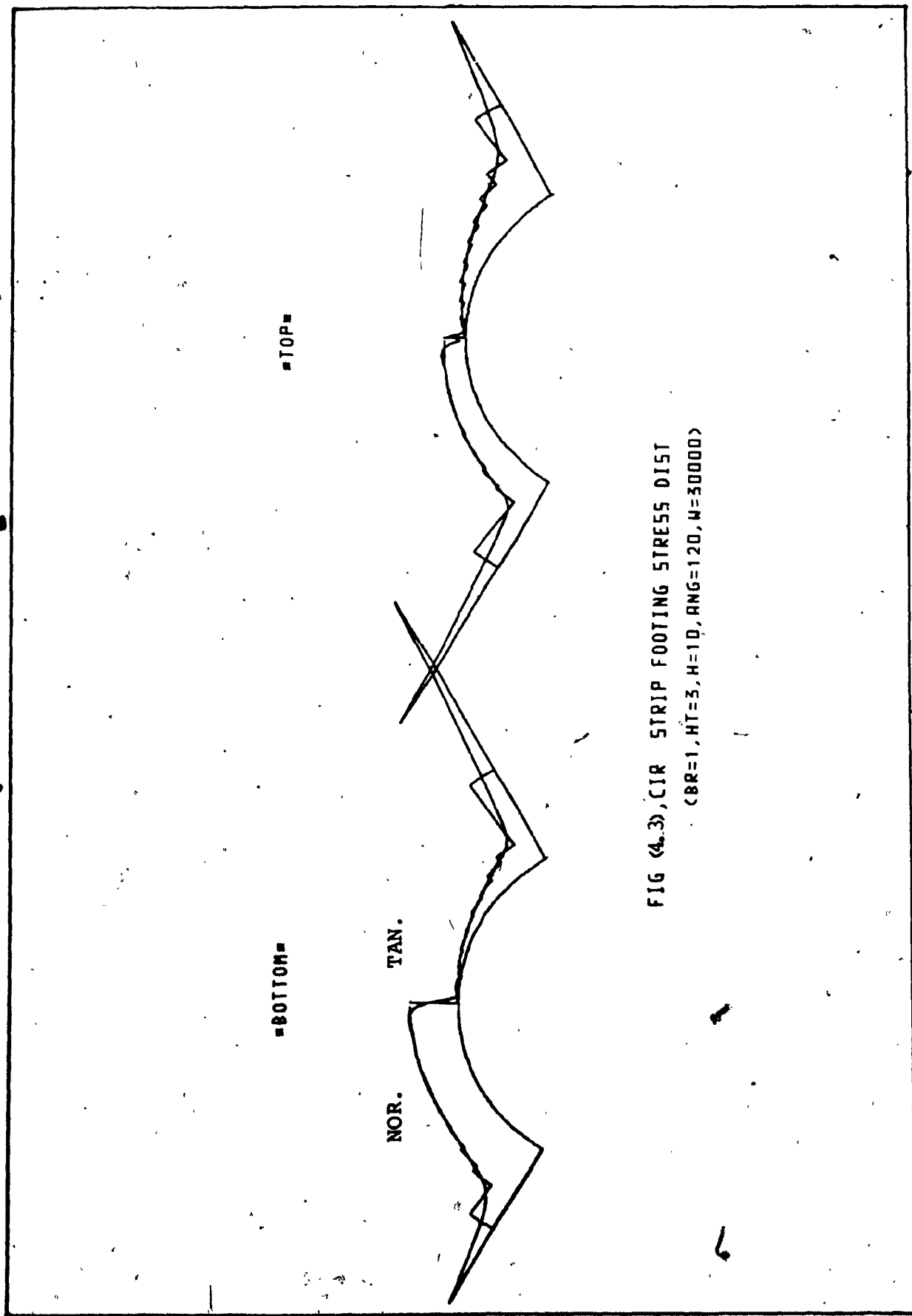


FIG (4.3), CIR STRIP FOOTING STRESS DIST
($CBR=1, HT=3, H=10, RNG=120, W=30000$)

TABLE 4.4
RESULTS OF "TRIFDN" (N=20)

[DATA]					
LEN.	RAD.	TAN.	RAD.	TAN.	RAD.
.1	6738.2	2245.8	35555.6	786.9	-3182.6
.2	7070.5	2437.2	4605.3	1038.2	-2465.2
.3	7601.8	2734.2	5153.8	1247.0	-2447.9
.4	7909.9	2893.7	5149.0	1364.3	-2460.9
.5	8689.7	3327.3	5908.3	1612.8	-2781.4
.6	9428.4	3694.8	6297.3	1840.4	-3127.1
.7	10503.7	4293.3	6837.5	2164.2	-3666.2
.8	12341.7	5114.2	7743.6	2591.8	-4598.1
.9	15481.6	6560.2	9411.0	3092.9	-6070.6
1.0	35811.3	15937.0	18404.2	10346.2	-17407.1
					5590.8
					■ VERTICAL DISPLACEMENT IS: [.016599]

[RESULTANT STRESS DISTRIBUTION] [STRESS DIST. ON LOWER SURFACE] [STRESS DIST. ON UPPER SURFACE]

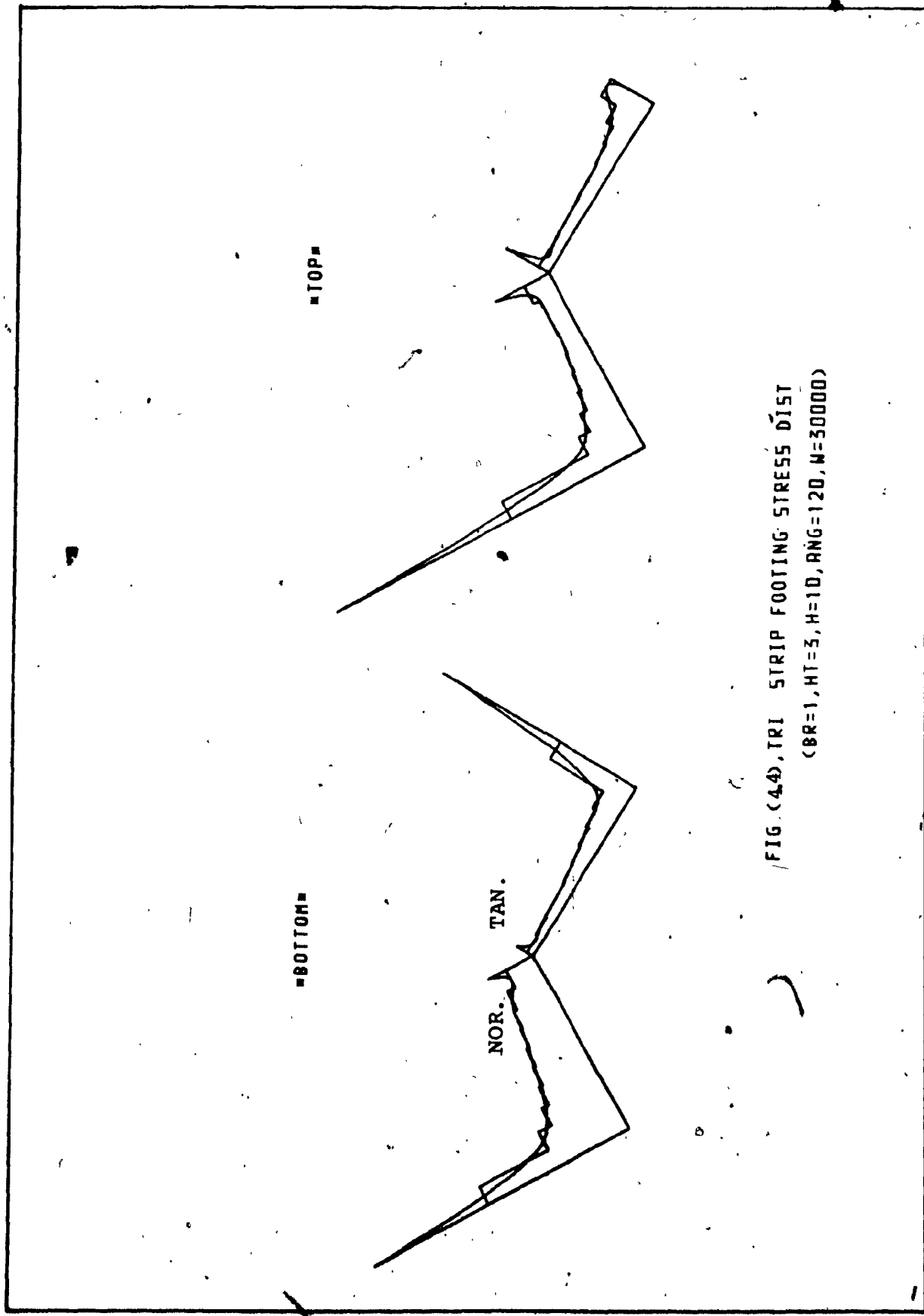


FIG. (4.4), TRI STRIP FOOTING STRESS DIST
(BR=1, HT=5, H=10, RNG=120, W=30000)

TABLE 4.5
RESULTS OF "FLAFDN" (N=20)

[DATA]			
RADIUS OF FOOTING IN METERS :	1.00		
DEPTH OF FOOTING BOTTOM IN METERS :	3.00		
ANGULAR SIZE OF FOOTING	180.00		
DEPTH OF UNDERLYING ROCK LAYER :	10.00		
ELASTIC GROUND E-MODULUS IN KG/S.M. :	15000000.00		
DENSITY OF GROUND IN KG/C.M. :	1800.00		
POISONS RATIO: .30			
COEFF. OF LATERAL PRESSURE : .50			
LOAD ON FOOTING IN KG. :	30000.00		
NUMBER OF SECTIONS (N) :	20		

[RESULTANT STRESS DISTRIBUTION]		[STRESS DIST. ON LOWER SURFACE]		[STRESS DIST. ON UPPER SURFACE]	
LEN.	RAD.	TAN.	RAD.	TAN.	RAD.
.0	9460.9	4.2	6826.8	12.2	-2634.1
.2	9575.6	15.6	-6881.6	38.4	-2694.0
.3	9805.4	30.4	6990.8	66.2	-2814.7
.4	10182.7	44.2	7170.7	93.2	-3012.0
.5	10746.0	56.6	7442.6	118.8	-3303.5
.6	11588.3	113.4	7848.6	166.1	-3739.8
.7	12862.0	120.7	8467.6	186.3	-4394.3
.8	15020.4	187.0	9528.8	247.1	-5491.6
.9	18407.4	271.8	11207.0	22.4	-7200.4
1.0	42351.2	802.1	23093.7	3289.8	-19257.5

* VERTICAL DISPLACEMENT IS: [.016309]

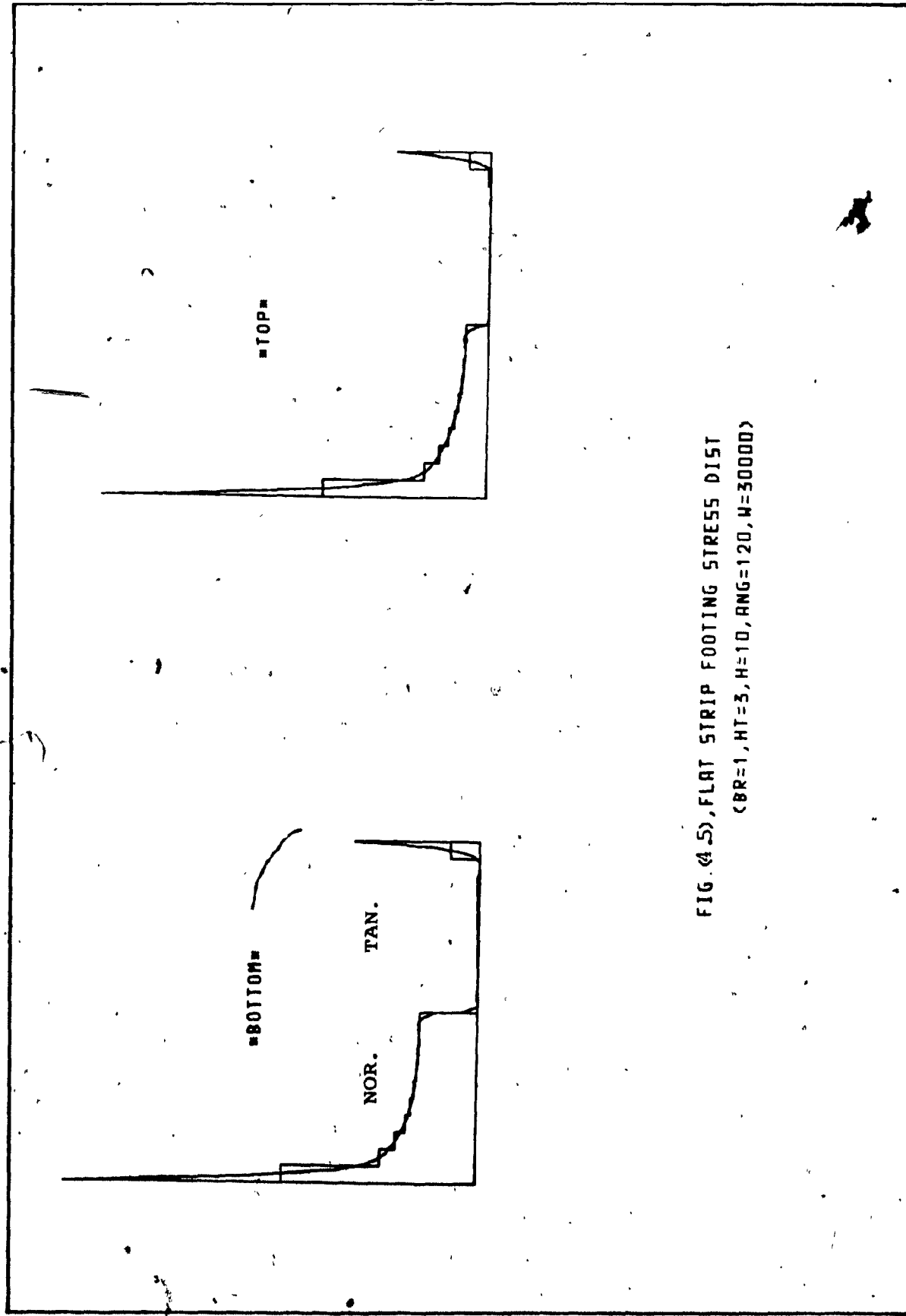


FIG. (4.5), FLAT STRIP FOOTING STRESS DIST
($B/R=1$, $H/T=3$, $H=10$, $RNG=120$, $W=300000$)

TABLE 4.6
RESULTS OF "CIRFDN" (N=40)

[DATA]				[STRESS DIST. ON LOWER SURFACE]				[STRESS DIST. ON UPPER SURFACE]			
ANG.	HAD.	TAN.	NAD.	TAN.	NAD.	TAN.	NAD.	TAN.	NAD.	TAN.	NAD.
1.5	7872.9	166.7	5122.2	75.8	-2450.6	90.8					
4.5	7883.1	506.5	5283.4	149.5	-2639.6	357.1					
7.5	8080.0	856.7	5317.9	269.8	-2722.1	586.9					
10.5	8039.9	1204.4	5300.8	390.2	-2739.2	814.1					
13.5	7997.4	1587.9	5264.0	487.0	-2733.5	1060.9					
16.5	8248.3	1966.3	5366.2	627.8	-2882.1	1338.5					
19.5	8266.0	2277.5	5360.2	724.2	-2905.6	1553.3					
22.5	8280.2	2914.2	5336.0	963.6	-2944.1	1950.6					
25.5	8418.2	3121.0	5376.3	973.7	-3011.9	2147.3					
28.5	8738.0	3785.0	5516.6	1216.3	-3221.4	2528.7					
31.5	8672.0	4126.1	5461.6	1325.6	-3210.4	2800.5					
34.5	8988.2	4837.0	5593.4	1605.3	-3339.8	3251.7					
37.5	8860.3	5188.5	5523.4	1644.4	-3336.9	3504.2					
40.5	9485.7	6155.6	5825.3	2032.9	-3600.4	4122.6					
43.5	9800.2	7024.4	5980.1	2386.8	-3820.1	4645.6					
46.5	10215.9	7898.7	6192.8	2720.7	-4033.1	5174.0					
49.5	10903.0	9384.4	6568.8	3349.8	-4334.2	6034.6					
52.5	12348.2	11726.1	7286.5	4908.1	-5061.7	7318.0					
55.5	11560.7	14477.5	6672.5	5461.8	-5888.3	9012.7					
58.5	31589.1	35571.7	14743.7	18117.1	-16855.4	17454.6					
					*	VERTICAL DISPLACEMENT 15: [.016602]					

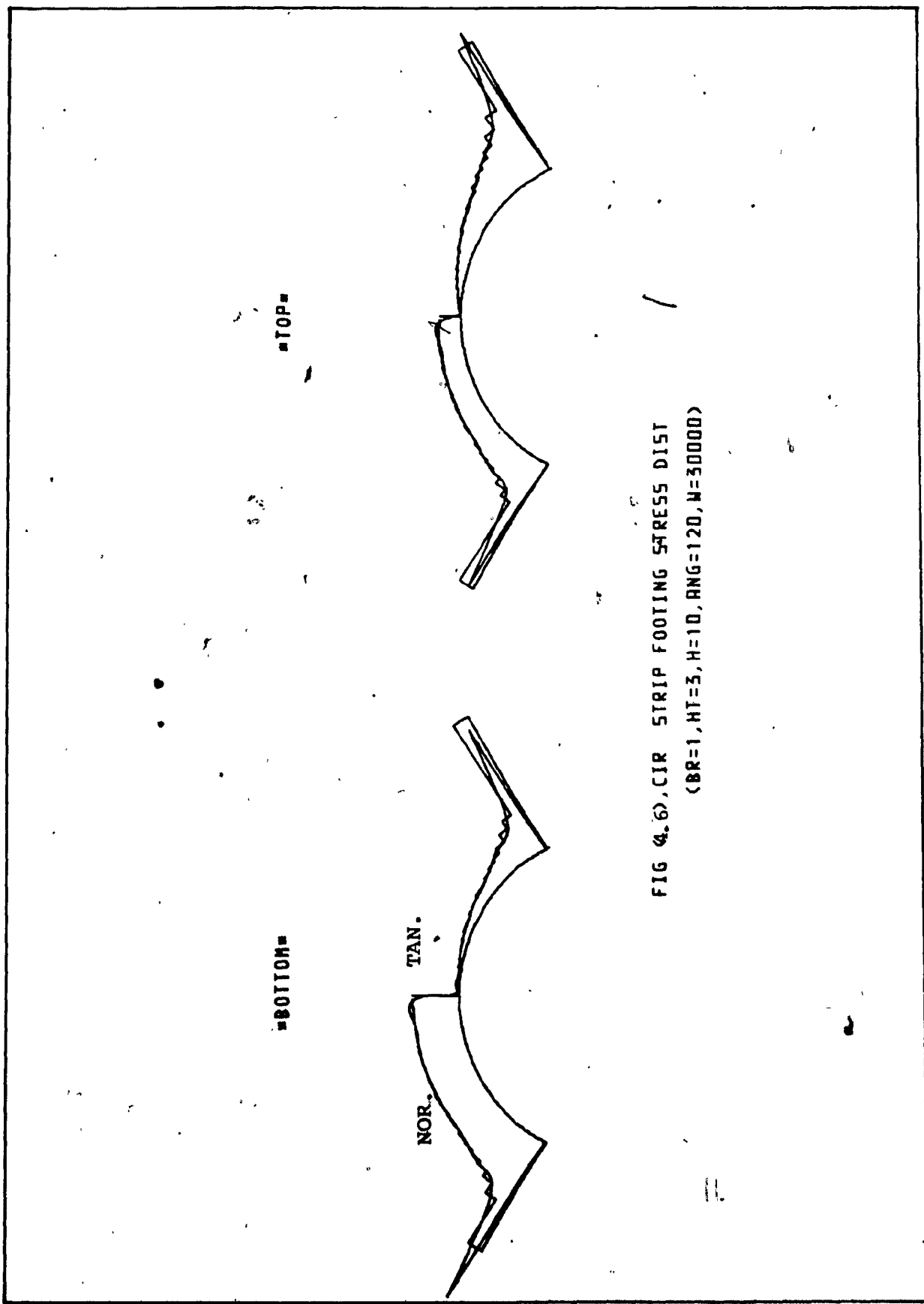


FIG 4.6, CIR STRIP FOOTING STRESS DIST
(BR=1, HT=5, H=10, RANG=120, N=300000)

TABLE 4.7

RESULTS OF "TRIFDN" (N=40)

[DATA]			[STRESS DIST. ON LOWER SURFACE] (STRESS DIST. ON UPPER SURFACE)		
LENGTH	RAD.	TAN.	RAD.	TAN.	RAD.
.03	6617.9	2191.0	3068.3	678.8	-3549.5
.09	6652.0	2232.5	3958.2	875.8	-2694.6
.18	6831.3	2331.7	4305.6	967.0	-2445.7
.20	7133.9	2492.6	4740.6	1078.1	-2393.3
.26	7346.2	2607.8	4979.4	1165.3	-2364.8
.32	7580.4	2721.9	5194.9	1247.9	-2385.5
.38	7874.0	2932.6	5804.7	1374.6	-2469.4
.43	8091.2	3017.8	5553.9	1444.6	-2540.3
.49	8288.6	3089.9	5691.5	1491.0	-2593.2
.55	8746.7	3446.5	5941.0	1684.5	-2805.7
.61	9053.7	3500.2	6101.1	1731.2	-2952.6
.68	9567.2	3808.3	6365.9	1902.1	-3201.3
.72	10015.0	3990.8	6592.9	2007.4	-3422.1
.78	10683.8	4117.0	6932.5	2211.3	-3751.3
.84	11994.8	5000.3	7556.2	2549.2	-4438.2
.89	12342.2	5086.8	7735.3	2583.7	-4606.9
.95	14006.5	6336.3	8974.9	3180.1	-5831.6
1.01	17473.5	7467.9	10270.3	3816.8	-7203.2
1.07	21243.9	9377.4	12298.9	4405.4	-8944.9
1.13	50744.4	22528.9	25442.3	10568.1	-25302.1
					7960.8
					VERMIL DISPLACEMENT IS: (.016539)

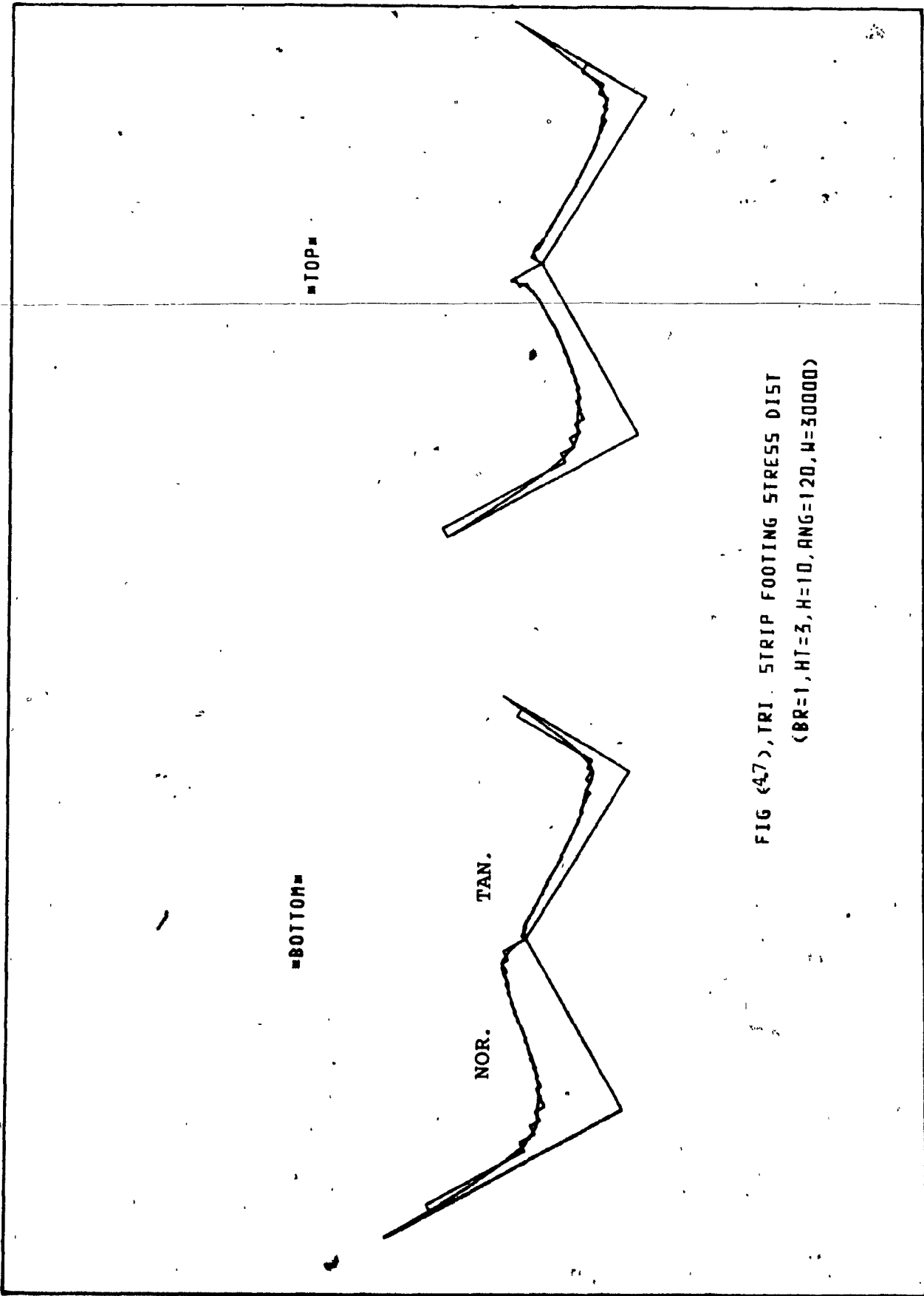


FIG (4.7), TRI. STRIP FOOTING STRESS DIST
($B/R=1$, $H/T=3$, $H=10$, $RNG=120$, $W=30000$)

TABLE 4.8

RESULTS OF "FLA FDN" (N=40)

[DATA]

BREEDTH OF FOOTING IN METERS : 1.00
 DEPTH OF FOOTING BOTTOM IN METERS : 3.00
 ANGULAR SIZE OF FOOTING : 180.00
 DEPTH OF UNDERLYING ROCK LAYER : 10.00
 ELASTIC GROUND E-MODULUS IN KG/S.M. : 15000000.00
 DENSITY OF GROUND IN KG/C.M. : 1800.00
 POISONS RATIO : .30
 COEFF. OF LATENT PRESSURE : 1.50
 LOAD ON FOOTING IN KG. : 30000.00
 NUMBER OF SECTIONS (N) : 40

RESULANT STRESS DISTRIBUTION]				[STRESS DIST. ON LOWER SURFACE] [STRESS DIST. ON UPPER SURFACE]			
LENGTH	RAD.	TAN.	RAD.	TAN.	RAD.	TAN.	
.03	9370.7	.9	6780.7	5.9	-2590.0	-4.9	
.08	9394.1	5.8	6792.2	18.6	-2011.9	-12.8	
.13	9457.1	17.6	6822.0	34.9	-2635.1	-17.3	
.18	9577.9	16.6	6880.2	57.8	-2697.7	-41.2	
.23	9355.9	27.2	6766.8	51.2	-2589.2	-28.0	
.28	9948.4	36.8	7059.0	54.8	-2889.4	-17.9	
.33	9999.2	38.7	7080.1	67.3	-2919.2	-40.6	
.38	10210.1	49.3	7180.8	99.5	-3029.2	-50.2	
.43	10502.7	61.1	7320.9	115.9	-3181.8	-51.8	
.48	10812.8	60.0	7470.1	125.6	-3382.7	-65.6	
.53	11231.4	62.6	7672.7	145.6	-3588.7	-63.1	
.58	11730.6	67.2	7912.8	158.5	-3877.6	-71.3	
.63	12338.7	15.6	8221.6	132.2	-4114.1	-116.6	
.68	13116.5	394.1	8590.2	328.4	-4526.3	65.6	
.73	14175.3	64.1	9095.1	175.2	-5080.2	-111.1	
.78	15489.6	158.5	9762.9	232.1	-5726.7	-73.6	
.83	17476.4	326.7	10739.4	310.1	-6137.0	6.6	
.88	20694.8	277.8	12332.1	317.7	-8362.7	-39.9	
.93	25580.2	374.4	14786.3	-26.9	-10793.9	40.3	
.98	59537.6	1283.2	31661.7	4644.9	-27815.9	-3361.7	

* VERTICAL DISPLACEMENT IS: [-0.16262]

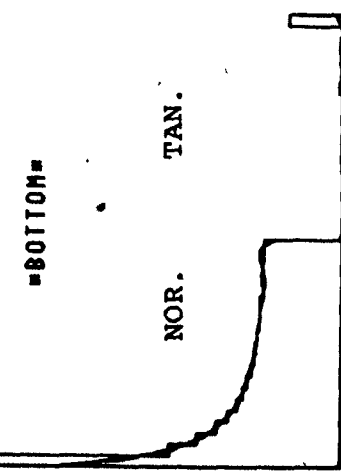
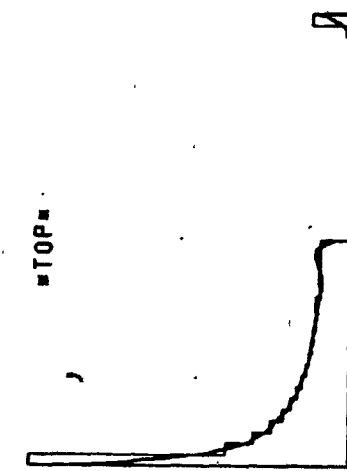


FIG. (48), FLAT STRIP FOOTING STRESS DIST
($B/R=1$, $H=10$, $RNG=120$, $W=30000$)

CHAPTER 5

DISCUSSION AND CONCLUSION

In this study a solution method has been presented for the prediction of contact pressures and movements of simple rigid structural units embedded in an elastic isotropic semi-infinite soil medium.

The approach has been applied to horizontal circular pipes and strip footings of various cross-sectional configurations. The method presented may be used to predict both immediate and final movements of the structural units. The immediate movement is calculated from an elastic modulus in terms of total stresses and the final movement is calculated from an elastic modulus in terms of effective stresses.

It is commonly accepted that the use of elastic theory to predict the behaviour of soil masses must be used with care. According to Davis and Poulos (1963), the properties of real soils depart from those of ideal elastic materials in two important respects; first: strain is not linearly dependent on stress, and secondly, the relation between stress and strain may differ for an increase in compressive stress from that of a decrease. This, however, may be handled by employing an approximate elastic modulus determined with oedemeter or triaxial tests on the soil for a range of stress appropriate to the problem. If necessary, the soil mass may be considered to be divided into a number

of layers, a different modulus being selected for each layer.

Hence, in using this approach, it would be necessary to employ great care in determining the appropriate approximate elastic modulus. This is due to the changes in stress within the soil which covers a wide range and involve increases and decreases.

The solutions for the problems treated in this study presume no breakaway at the soil-structure interface. This is reasonable as it is generally accepted (e.g. Douglas and Davis, 1964) that fully bonded condition corresponds to the most practical limiting case for the application of elastic solutions, since at working loads the compression stresses (due to overburden pressure and surcharge) will be sufficient to prevent the development of tensile stresses between the structural unit and soil.

Regarding the strip footings application, the actual footings differ from the models used in that the actual footing will have a finite thickness. From this point of view the theory should tend to over estimate the movements by neglecting the restraints at the ends. However, a real model may be used to simulate the actual footing but, an ill-conditioned system of linear algebraic equations is expected to result for small breadth to thickness ratios. This has yet to be investigated.

In applying the method, an obvious test for a given problem is to start with (n) small and examine the computed

data as (n) increases. The successful results presented for so few nodal points surely are, in some measure, due to the simple geometries of the structural units treated. The numbers (n) used were chosen for convenience. Attention in the trials was focussed on convergence and validity of the method, rather than on optimum programming or error analysis.

The extent to which (n) may be increased, above which ill-conditioning may result was not examined for the problems treated. This was due to the fact that increasing (n) dramatically requires additional computer storage and execution time which were not available for this study.

Segment size or spacing of nodes was made equal. This is desirable for optimum conditioning of the equations and ease of programming. It is believed that unequal intervals may be used to handle pressure concentrations more effectively but this is yet to be investigated.

The use of the method of analysis presented requires only the solution of a small number of equations, whereas alternative approaches which involve sub-division of the soil into numerous finite elements require the solution of quite large systems of equations. Thus for analysis of competitive accuracy, the proposed method leads to significant computational savings.

In summary, it is believed that the solution method presented provides a useful approach to predicting the order of contact pressures and movements of structural units

embedded in elastic soil in general, but considerable care in determining the appropriate properties of the soil would be necessary. Furthermore, having established the soundness of the approach for the particular cases analysed in this study, i.e., rigid structural units with plane strain condition, one may proceed to more general soil-structure problems. A step further would be to consider flexible structural units embedded in non-linear elastic and perhaps even anisotropic soil systems by using appropriate displacement configurations of the structural unit and incremental analysis to handle the non-linear soil behaviour.

REFERENCES

- [1] Brebbia, C.A., and S. Walker. Boundary Element Techniques in Engineering. London: Newnes-Butterworths, 1980.
- [2] Burden, R.L., J.D. Faires, and A.C. Reynolds. Numerical Analysis. 2d ed. Boston: Weber and Schmidt, 1981.
- [3] Davis, E.H., and H.G. Poulos, "Triaxial Testing and Three Dimensional Settlement Analysis". Proceedings of the 4th Australia-New Zealand Confr. on Soil Mechanics, 1963.
- [4] Douglass, D.J., and E.H. Davis, "The Movement of Burried Footings Due to Moment and Horizontal Load and the Movement of Anchor Plates." Geotechnique, 14:115-32. February, 1964.
- [5] IMSL Libraries. International Mathematics and Statistics Library Reference Manual. 9th ed. Houston, 1982.
- [6] Kreyszig, E. Advanced Engineering Mathematics. New York: John Wiley and Sons, 1979.
- [7] Melan, E. "Der Spannungszustand der Durch Eine Einzelkraft im Innern Beanspruchten Halbschiebe". Z. Agnew Math. Mech., 12:343-46. December, 1932.
- [8] Poorooshashb, H.B., I. Holubec, and A.N. Sherbourne, "Yielding and Flow of Sand in Triaxial Compression". Canadian Geotechnical Journal. 4:376-88. November, 1967.

- [9] Poulos, H.G., and E.H. Davis, Elastic Solutions for Soil and Rock Mechanics, New York: John Wiley and Sons, 1974.
- [10] Timoshenko, S.P., and J.N. Goodier. Theory of Elasticity. 3d ed. New York: McGraw-Hill, 1970.

APPENDIX

```
*****  
PROGRAM "PIPE"  
PROGRAM "PIPE" EVALUATES THE DISPLACEMENT OF , AND THE  
CONTACT STRESS OF A RIGID CIRCULAR PIPE INSTALLED  
IN LINEARLY ELASTIC GROUND .  
THESE STRESS ARE AN APPROXIMATION TO THE REAL CONTACT  
STRESS DISTRIBUTION.  
THE METHOD USED IS PRESENTED IN THIS THESIS.  
-----  
PROGRAM PIPE(INPUT,OUTPUT)  
IMPLICIT REAL (A-H,O-Z)  
COMMON X,Y,D,R,PI,V,H  
COMMON /O/ X1,Y1,X2,Y2  
CCC X,Y ARE COORDINATES OF THE POINT AT WHICH STRESS ARE  
CCC CALCULATED.  
CCC DF,Z ARE COORDINATES OF THE FORCE UNDER CONSIDERATION  
PARAMETER (N=20,K=21,L=10)  
CCC N IS NUMBER OF SECTION TO WHICH PIPE IS DIVIDED.  
REAL A(K,K),BRS(L),BTS(L),URS(L),UTS(L),XF(N),YF(N),  
$SP(N),SF(N),ANP(L),XP(L),YP(L)  
CCC A IS THE MATRIX OF DISPLACEMENT INFLUENCE  
CCC FACTORS, AND LATER OF STRESS INFLUENCE FACTORS.  
CCC VS' & HS ARE VECTORS OF TOTAL VER. AND HOR.  
CCC FORCES ACTING AT EACH SECTION, AND LATER VECTORS  
CCC OF RAD. AND TAN. STRESS AT EACH SECTION.  
CCC XF & YF ARE VECTORS OF END-POINTS COORDINATES  
CCC OF EACH SECTION.  
CCC XP & YP ARE VECTORS OF MID-POINT COORDINATES  
CCC OF EACH SECTION.  
REAL B(K,1),WKAREA(K),WK(130)  
INTEGER M,O,IA,IDGT,IERR  
REAL INC,K0  
INTEGER IER  
CCC INC IS THE SIZE OF THE ELEMENTAL PIPE SECTION .  
REAL DBLIN  
CCC DBLIN IS A DOUBLE INTEGRATION SUBROUTINE FROM IMSL LIBRARY.  
EXTERNAL POLY  
EXTERNAL FSXPR,FSXQR,FSYPR,FSYQR  
CCC THESE ARE THE STRAIN FUNCTIONS UPON WHICH DOUBLE  
CCC INTEGRATION IS PERFORMED TO GET DISP. INFLUENCE  
CCC FACTORS DUE TO A UNIT NORMAL STRESS.  
EXTERNAL FSXPT,FSXQT,FSYPT,FSYQT  
CCC THESE ARE THE STRAIN FUNCTIONS UPON WHICH DOUBLE  
CCC INTEGRATION IS PERFORMED TO GET DISP. INFLUENCE  
CCC FACTORS DUE TO A UNIT TANGENTIAL STRESS.  
EXTERNAL AX,BX,AY,BY  
CCC INTEGRATION LIMIT FUNCTIONS FOR DBLIN SUBROUTINE.  
EXTERNAL FVSPR,FHSPR,FSSPVR,FSSPHR,  
$FVSQR,FHSQR,FSSQVR,FSSQHR,  
$FVSPT,FHSPT,FSSPVT,FSSPHT,  
$FVSQT,FHSQT,FSSQVT,FSSQHT  
CCC THESE ARE STRESS FUNCTIONS IN TERMS OF VER. AND  
CCC HOR. COMPONENTS OF NORMAL AND TANGENTIAL STRESS.  
EXTERNAL XL1,XL2,YL1,YL2
```



```
SP(1)=INC/2.  
CCC 7 GENERATION OF ANGULAR COOD. OF MID-POINTS AND  
CCC END-POINTS OF EACH SECTION.  
DO 5,I=1,L  
SP(I+1)=SP(I)+INC  
SF(I+1)=SF(I)+INC  
5 CONTINUE  
CCC 8 GENERATION OF POINTS COOD.  
DO 10,I=1,L  
XP(I)=D-R*COS(SP(I)/R)  
YP(I)=R*SIN(SP(I)/R)  
10 CONTINUE  
DO 11,I=1,L+1  
XF(I)=D-R*COS(SF(I)/R)  
YF(I)=R*SIN(SF(I)/R)  
11 CONTINUE  
CCC 9 GENERATION OF DISPLACEMENT INFLUENCE FACTORS.  
DO 30,J=1,L  
X=XP(J)  
Y=YP(J)  
DO 35,I=1,L  
T1=SF(I)  
T11=SP(I)-EPS  
T22=SP(I)+EPS  
T2=SF(I+1)  
IF((I.EQ.J).OR.(((I+J).EQ.(L+1)).AND.(I.GT.J)))THEN  
VDP1=DBLIN(FSXPR,T1,T11,AX,BX,AERR,ERROR,IER)  
$-DBLIN(FSXQR,T1,T11,AX,BX,AERR,ERROR,IER)  
$+DBLIN(FSXPR,T22,T2,AX,BX,AERR,ERROR,IER)  
$-DBLIN(FSXQR,T22,T2,AX,BX,AERR,ERROR,IER)  
HDP1=DBLIN(FSYPR,T1,T11,AY,BY,AERR,ERROR,IER)  
$-DBLIN(FSYQR,T1,T11,AY,BY,AERR,ERROR,IER)  
$+DBLIN(FSYPR,T22,T2,AY,BY,AERR,ERROR,IER)  
$-DBLIN(FSYQR,T22,T2,AY,BY,AERR,ERROR,IER)  
VDQ1=DBLIN(FSXPT,T1,T11,AX,BX,AERR,ERROR,IER)  
$+DBLIN(FSXQT,T1,T11,AX,BX,AERR,ERROR,IER)  
$+DBLIN(FSXPT,T22,T2,AX,BX,AERR,ERROR,IER)  
$+DBLIN(FSXQT,T22,T2,AX,BX,AERR,ERROR,IER)  
HDQ1=DBLIN(FSYPT,T1,T11,AY,BY,AERR,ERROR,IER)  
$+DBLIN(FSYQT,T1,T11,AY,BY,AERR,ERROR,IER)  
$+DBLIN(FSYPT,T22,T2,AY,BY,AERR,ERROR,IER)  
$+DBLIN(FSYQT,T22,T2,AY,BY,AERR,ERROR,IER)  
ELSE  
VDP1=DBLIN(FSXPR,T1,T2,AX,BX,AERR,ERROR,IER)  
$-DBLIN(FSXQR,T1,T2,AX,BX,AERR,ERROR,IER)  
HDP1=DBLIN(FSYPR,T1,T2,AY,BY,AERR,ERROR,IER)  
$-DBLIN(FSYQR,T1,T2,AY,BY,AERR,ERROR,IER)  
VDQ1=DBLIN(FSXPT,T1,T2,AX,BX,AERR,ERROR,IER)  
$+DBLIN(FSXQT,T1,T2,AX,BX,AERR,ERROR,IER)  
HDQ1=DBLIN(FSYPT,T1,T2,AY,BY,AERR,ERROR,IER)  
$+DBLIN(FSYQT,T1,T2,AY,BY,AERR,ERROR,IER)  
ENDIF  
T1=-T1  
T2=-T2
```

```
VDP2=DBLIN(FSXPR,T2,T1,AX,BX,AERR,ERROR,IER)
$-DBLIN(FSXQR,T2,T1,AX,BX,AERR,ERROR,IER)
HDP2=DBLIN(FSYPR,T2,T1,AY,BY,AERR,ERROR,IER)
$-DBLIN(FSYQR,T2,T1,AY,BY,AERR,ERROR,IER)
VDQ2=-DBLIN(FSXPT,T2,T1,AX,BX,AERR,ERROR,IER)
$-DBLIN(FSXQT,T2,T1,AX,BX,AERR,ERROR,IER)
HDQ2=-DBLIN(FSYPT,T2,T1,AY,BY,AERR,ERROR,IER)
$-DBLIN(FSYQT,T2,T1,AY,BY,AERR,ERROR,IER)
A(J,I)=VDP1+VDP2
A(J,I+L)=VDQ1+VDQ2
A(J+L,I)=HDP1+HDP2
A(J+L,I+L)=HDQ1+HDQ2
35 CONTINUE
30 CONTINUE
DO 90 ,J=1,N/2
A(J,K)=-1*E
90 CONTINUE
DO 95,J=N/2+1,K
95 A(J,K)=0.0
DO 100,I=1,N/2
A(K,I)=2.*R*(SIN(SF(I+1)/R)-SIN(SF(I)/R))
A(K,I+N/2)=-2.*R*(COS(SF(I+1)/R)-COS(SF(I)/R))
100 CONTINUE
DO 105,I=1,K-1
105 B(I,1)=0.0
B(K,1)=-PI*R**2*DE
CCC LEQT1F IS AN IMSL LIBRARY SUBROUTINE TO SOLVE
CCC A SYSTEM OF LINEAR EQUATIONS.
CALL LEQT1F(A,M,O,IA,B,IDL,WKAREA,IER)
CCC GENERATING STRESS INFLUENCE FACTORS.
DO 40,J=1,N/2
X1=XF(J)
Y1=YF(J)
X2=XF(J+1)
Y2=YF(J+1)
IF(J.LE.N/4)THEN
X=X1
Y=Y2
ELSE
X=X2
Y=Y1
ENDIF
DO 45,I=1,N/2
T1=SF(I)+EPS
T2=SF(I+1)-EPS
VSP1=DBLIN(FVSPR,T1,T2,YL1,YL2,AERR,ERROR,IER)
$-DBLIN(FSSPVR,T1,T2,XL1,XL2,AERR,ERROR,IER)
$-DBLIN(FVSQR,T1,T2,YL1,YL2,AERR,ERROR,IER)
$+DBLIN(FSSQVR,T1,T2,XL1,XL2,AERR,ERROR,IER)
HSP1=-DBLIN(FHSPR,T1,T2,XL1,XL2,AERR,ERROR,IER)
$+DBLIN(FSSPHR,T1,T2,YL1,YL2,AERR,ERROR,IER)
$+DBLIN(FHSQR,T1,T2,XL1,XL2,AERR,ERROR,IER)
$-DBLIN(FSSQHR,T1,T2,YL1,YL2,AERR,ERROR,IER)
VSQ1=-DBLIN(FVSPR,T1,T2,YL1,YL2,AERR,ERROR,IER)
```

```
$-DBLIN(FSSPVT,T1,T2,XL1,XL2,AERR,ERROR,IER)
$+DBLIN(FVSQL,T1,T2,YL1,YL2,AERR,ERROR,IER)
$-DBLIN(FSSQVT,T1,T2,XL1,XL2,AERR,ERROR,IER)
HSQ1=-DBLIN(FHSPPT,T1,T2,XL1,XL2,AERR,ERROR,IER)
$+DBLIN(FSSPHT,T1,T2,YL1,YL2,AERR,ERROR,IER)
$-DBLIN(FHSQT,T1,T2,XL1,XL2,AERR,ERROR,IER)
$+DBLIN(FSSQHT,T1,T2,YL1,YL2,AERR,ERROR,IER)
T1=-T1
T2=-T2
VSP2=DBLIN(FVSPR,T2,T1,YL1,YL2,AERR,ERROR,IER)
$-DBLIN(FSSPVR,T2,T1,XL1,XL2,AERR,ERROR,IER)
$-DBLIN(FVSQR,T2,T1,YL1,YL2,AERR,ERROR,IER)
$+DBLIN(FSSQVR,T2,T1,XL1,XL2,AERR,ERROR,IER)
HSP2=-DBLIN(FHSPR,T2,T1,XL1,XL2,AERR,ERROR,IER)
$+DBLIN(FSSPHR,T2,T1,YL1,YL2,AERR,ERROR,IER)
$+DBLIN(FHSQR,T2,T1,XL1,XL2,AERR,ERROR,IER)
$-DBLIN(FSSQHR,T2,T1,YL1,YL2,AERR,ERROR,IER)
VSQ2=-DBLIN(FVSPT,T2,T1,YL1,YL2,AERR,ERROR,IER)
$+DBLIN(FSSPVT,T2,T1,XL1,XL2,AERR,ERROR,IER)
$-DBLIN(FVSQL,T2,T1,YL1,YL2,AERR,ERROR,IER)
$+DBLIN(FSSQVT,T2,T1,XL1,XL2,AERR,ERROR,IER)
HSQ2=DBLIN(FHSPPT,T2,T1,XL1,XL2,AERR,ERROR,IER)
$-DBLIN(FSSPHT,T2,T1,YL1,YL2,AERR,ERROR,IER)
$+DBLIN(FHSQT,T2,T1,XL1,XL2,AERR,ERROR,IER)
$-DBLIN(FSSQHT,T2,T1,YL1,YL2,AERR,ERROR,IER)
A(J,I)=VSP1+VSP2
A(J,I+L)=VSQ1+VSQ2
A(J+L,I)=HSP1+HSP2
A(J+L,I+L)=HSQ1+HSQ2
45 CONTINUE
40 CONTINUE
CCC CALCULATING TOTAL VER. & HOR. FORCES
CCC ON BOTH SIDES OF EACH SECTION.
DO 110,J=1,N/2
DO 115,I=1,N/2
A(J,I)=B(I,1)*A(J,I)+B(I+L,1)*A(J,I+L)
A(J+L,I)=B(I,1)*A(J+L,I)+B(I+L,1)*A(J+L,I+L)
115 CONTINUE
110 CONTINUE
DO 120,I=1,N/2
URS(I)=0.
UTS(I)=0.
20 CONTINUE
DO 125,J=1,N/2
DO 130,I=1,N/2
URS(J)=URS(J)+A(J,I)
UTS(J)=UTS(J)+A(J+L,I)
130 CONTINUE
125 CONTINUE
AREA=INC
CCC RESOLVING FORCES INTO NOR. & TAN. STRESS.
DO 165,I=1,N/2
RS=(URS(I)*COS(SP(I)/R)-UTS(I)*SIN(SP(I)/R))/AREA
TS=-(URS(I)*SIN(SP(I)/R)+UTS(I)*COS(SP(I)/R))/AREA
```

```
URS(I)=RS
UTS(I)=TS
165 CONTINUE
DO 166,I=1,N/2
BRS(I)=B(I,1)+URS(I)
BTS(I)=B(I+L,1)-UTS(I)
166 CONTINUE
PRINT2050
2050 FORMAT(//1X,'[ RESULTANT STRESS DISTRIBUTION ]')
PRINT3000
PRINT1700
PRINT3000
DO 190,I=1,N/2
PRINT1800,ANP(I),B(I,1),B(I+L,1)
190 PRINT3000
PRINT2060
2060 FORMAT(//1X,'[ STRESS DISTRIBUTION ON INNER SURFACE ]')
PRINT3000
PRINT1700
PRINT3000
DO 191,I=1,N/2
PRINT1800,ANP(I),BRS(I),BTS(I)
191 PRINT3000
PRINT2070
2070 FORMAT(//1X,'[ STRESS DISTRIBUTION ON OUTER SURFACE ]')
PRINT3000
PRINT1700
PRINT3000
DO 192,I=1,N/2
PRINT1800,ANP(I),URS(I),UTS(I)
192 PRINT3000
1700 FORMAT(1X,'*', 'ANGLE',T16,'RAD.',T31,'TAN.',T41,'*')
1800 FORMAT(1X,'*',F6.2,T10,F10.1,T25,F10.1,T41,'*')
PRINT2900,B(K,1)
2900 FORMAT(1X,'*', 'VERTICAL DISPLACEMENT IS ','[',F8.6,']',
$T41,'*')
PRINT3000
3000 FORMAT(1X,'-----*')
STOP
END
REAL FUNCTION FSXPR(T,X1)
IMPLICIT REAL (A-H,O-Z)
COMMON DUMMY,Y,D,R,PI,V,H
REAL M
M=(1-V)/V
DF=D-R*COS(T/R)
Z=R*SIN(T/R)
A1=(X1-DF)**3/((X1-DF)**2+(Y-Z)**2)**2
A2=(X1+DF)*((X1+DF)**2+2*DF*X1)/((X1+DF)**2+(Y-Z)**2)**2
A3=8*DF*X1*(DF+X1)*(Y-Z)**2/((X1+DF)**2+(Y-Z)**2)**3
A4=(X1-DF)/((X1-DF)**2+(Y-Z)**2)
A5=(3*X1+DF)/((X1+DF)**2+(Y-Z)**2)
A6=4*X1*(Y-Z)**2/((X1+DF)**2+(Y-Z)**2)**2
A7=(X1-DF)*(Y-Z)**2/((X1-DF)**2+(Y-Z)**2)**2
```

```
A8=((X1+DF)**2+(Y-Z)**2+2*DF**2)-2*DF*(Y-Z)**2)/  
$((X1+DF)**2+(Y-Z)**2)**2  
A9=8*DF*X1*((DF+X1)*(Y-Z)**2)/((X1+DF)**2+(Y-Z)**2)**3  
A10=-1*(X1-DF)/((X1-DF)**2+(Y-Z)**2)  
A11=(X1+3*DF)/((X1+DF)**2+(Y-Z)**2)  
A12=4*X1*(Y-Z)**2/((X1+DF)**2+(Y-Z)**2)**2  
A123=(M+1)/(2*M)*(A1+A2-A3)  
A456=(M-1)/(4*M)*(A4+A5-A6)  
A789=(M+1)/(2*M)*(A7+A8+A9)  
A101112=(M-1)/(4*M)*(A10+A11+A12)  
FSXPR=(1-V**2)/(PI)*(A123+A456-V/(1-V)*(A789+A101112))  
$*COS(T/R)  
RETURN  
END  
REAL FUNCTION FSXQR(T,X1)  
IMPLICIT REAL (A-H,O-Z)  
COMMON DUMMY,Y,D,R,PI,V,H  
REAL M  
M=(1-V)/V  
DF=D-R*COS(T/R)  
Z=R*SIN(T/R)  
A1=(X1-DF)**2/((X1-DF)**2+(Y-Z)**2)**2  
A2=(DF**2-X1**2+6*DF*X1)/((X1+DF)**2+(Y-Z)**2)**2  
A3=8*DF*X1*(Y-Z)**2/((X1+DF)**2+(Y-Z)**2)**3  
A4=1/((X1-DF)**2+(Y-Z)**2)  
A5=1/((X1+DF)**2+(Y-Z)**2)  
A6=4*X1*((DF+X1))/((X1+DF)**2+(Y-Z)**2)**2  
A7=(Y-Z)**2/((X1-DF)**2+(Y-Z)**2)**2  
A8=(Y-Z)**2+8*DF*X1+6*DF**2)/((X1+DF)**2+(Y-Z)**2)**2  
A9=8*DF*X1*((DF+X1)**2/((X1+DF)**2+(Y-Z)**2)**3  
A10=1/((X1-DF)**2+(Y-Z)**2)  
A11=3/((X1+DF)**2+(Y-Z)**2)  
A12=4*X1*(DF+X1)/((X1+DF)**2+(Y-Z)**2)**2  
A123=(M+1)/(2*M)*(A1-A2+A3)  
A456=(M-1)/(4*M)*(A4-A5-A6)  
A789=(M+1)/(2*M)*(A7+A8+A9)  
A101112=(M-1)/(4*M)*(A10+A11-A12)  
FSXQR=(Y-Z)/(PI)*(A123-A456-V/(1-V)*(A789+A101112))  
$*SIN(T/R)*(1-V**2)  
RETURN  
END  
REAL FUNCTION FSYPR(T,Y1)  
IMPLICIT REAL (A-H,O-Z) <  
COMMON X,DUMMY,D,R,PI,V,H  
REAL M  
M=(1-V)/V  
DF=D-R*COS(T/R)  
Z=R*SIN(T/R)  
A1=(X-DF)*(Y1-Z)**2/((X-DF)**2+(Y1-Z)**2)**2  
A2=((X+DF)*((Y1-Z)**2+2*DF**2)-2*DF*(Y1-Z)**2)/  
$((X+DF)**2+(Y1-Z)**2)**2  
A3=8*DF*X*(DF+X)*(Y1-Z)**2/((X+DF)**2+(Y1-Z)**2)**3  
A4=-1*(X-DF)/((X-DF)**2+(Y1-Z)**2)  
A5=(X+3*DF)/((X+DF)**2+(Y1-Z)**2)
```

```
A6=4*X*(Y1-Z)**2/((X+DF)**2+(Y1-Z)**2)**2
A7=(X-DF)**3/((X-DF)**2+(Y1-Z)**2)**2
A8=(X+DF)*((X+DF)**2+2*DF*X)/((X+DF)**2+(Y1-Z)**2)**2
A9=8*DF*X*(DF+X)*(Y1-Z)**2/((X+DF)**2+(Y1-Z)**2)**3
A10=(X-DF)/((X-DF)**2+(Y1-Z)**2)
A11=(3*X+DF)/((X+DF)**2+(Y1-Z)**2)
A12=4*X*(Y1-Z)**2/((X+DF)**2+(Y1-Z)**2)**2
A123=(M+1)/(2*M)*(A1+A2+A3)
A456=(M-1)/(4*M)*(A4+A5+A6)
A789=(M+1)/(2*M)*(A7+A8-A9)
A101112=(M-1)/(4*M)*(A10+A11-A12)
FSYPR=(1-V**2)/(PI)*(A123+A456-V/(1-V)*(A789+A101112))
$#COS(T/R)
RETURN
END
REAL FUNCTION FSYQR(T,Y1)
IMPLICIT REAL (A-H,O-Z)
COMMON X,DUMMY,D,R,PI,V,H
REAL M
M=(1-V)/V
DF=D-R*COS(T/R)
Z=R*SIN(T/R)
A1=(Y1-Z)**2/((X-DF)**2+(Y1-Z)**2)**2
A2=((Y1-Z)**2+8*DF*X+6*DF**2)/((X+DF)**2+(Y1-Z)**2)**2
A3=8*DF*X*(DF+X)**2/((X+DF)**2+(Y1-Z)**2)**3
A4=1/((X-DF)**2+(Y1-Z)**2)
A5=3/((X+DF)**2+(Y1-Z)**2)
A6=4*X*(DF+X)/((X+DF)**2+(Y1-Z)**2)**2
A7=(X-DF)**2/((X-DF)**2+(Y1-Z)**2)**2
A8=(DF**2-X**2+6*DF*X)/((X+DF)**2+(Y1-Z)**2)**2
A9=8*DF*X*(Y1-Z)**2/((X+DF)**2+(Y1-Z)**2)**3
A10=1/((X-DF)**2+(Y1-Z)**2)
A11=1/((X+DF)**2+(Y1-Z)**2)
A12=4*X*(DF+X)/((X+DF)**2+(Y1-Z)**2)**2
A123=(M+1)/(2*M)*(A1+A2+A3)
A456=(M-1)/(4*M)*(A4+A5-A6)
A789=(M+1)/(2*M)*(A7-A8+A9)
A101112=(M-1)/(4*M)*(A10-A11-A12)
FSYQR=(Y1-Z)/(PI)*(A123+A456-V/(1-V)*(A789-A101112))
$#SIN(T/R)*(1-V**2)
RETURN
END
REAL FUNCTION FSKPT(T,X1)
IMPLICIT REAL (A-H,O-Z)
COMMON DUMMY,Y,D,R,PI,V,H
REAL M
M=(1-V)/V
DF=D-R*COS(T/R)
Z=R*SIN(T/R)
A1=(X1-DF)**3/((X1-DF)**2+(Y-Z)**2)**2
A2=(X1+DF)*((X1+DF)**2+2*DF*X1)/((X1+DF)**2+(Y-Z)**2)**2
A3=8*DF*X1*(DF+X1)*(Y-Z)**2/((X1+DF)**2+(Y-Z)**2)**3
A4=(X1-DF)/((X1-DF)**2+(Y-Z)**2)
A5=(3*X1+DF)/((X1+DF)**2+(Y-Z)**2)
```

```
A6=4*X1*(Y-Z)**2/((X1+DF)**2+(Y-Z)**2)**2
A7=(X1-DF)*(Y-Z)**2/((X1-DF)**2+(Y-Z)**2)**2
A8=((X1+DF)*((Y-Z)**2+2*DF**2)-2*DF*(Y-Z)**2)/
$((X1+DF)**2+(Y-Z)**2)**2
A9=8*DF*X1*(DF+X1)*(Y-Z)**2/((X1+DF)**2+(Y-Z)**2)**3
A10=-1*((X1-DF)/((X1-DF)**2+(Y-Z)**2))
A11=(X1+3*DF)/((X1+DF)**2+(Y-Z)**2)
A12=4*X1*(Y-Z)**2/((X1+DF)**2+(Y-Z)**2)**2
A123=(M+1)/(2*M)*(A1+A2-A3)
A456=(M-1)/(4*M)*(A4+A5-A6)
A789=(M+1)/(2*M)*(A7+A8+A9)
A101112=(M-1)/(4*M)*(A10+A11+A12)
FSXPT=(1-V**2)/(PI)*(A123+A456-V/(1-V)*(A789+A101112))
**SIN(T/R)
RETURN
END
REAL FUNCTION FSXQT(T,X1)
IMPLICIT REAL (A-H,O-Z)
COMMON DUMMY,Y,D,R,PI,V,H
REAL M
M=(1-V)/V
DF=D-R*COS(T/R)
Z=R*SIN(T/R)
A1=(X1-DF)**2/((X1-DF)**2+(Y-Z)**2)**2
A2=(DF**2-X1**2+6*DF*X1)/((X1+DF)**2+(Y-Z)**2)**2
A3=8*DF*X1*(Y-Z)**2/((X1+DF)**2+(Y-Z)**2)**3
A4=1/((X1-DF)**2+(Y-Z)**2)
A5=1/((X1+DF)**2+(Y-Z)**2)
A6=4*X1*(DF+X1)/((X1+DF)**2+(Y-Z)**2)**2
A7=(Y-Z)**2/((X1-DF)**2+(Y-Z)**2)**2
A8=((Y-Z)**2+8*DF*X1+6*DF**2)/((X1+DF)**2+(Y-Z)**2)**2
A9=8*DF*X1*(DF+X1)**2/((X1+DF)**2+(Y-Z)**2)**3
A10=1/((X1-DF)**2+(Y-Z)**2)
A11=3/((X1+DF)**2+(Y-Z)**2)
A12=4*X1*(DF+X1)/((X1+DF)**2+(Y-Z)**2)**2
A123=(M+1)/(2*M)*(A1-A2+A3)
A456=(M-1)/(4*M)*(A4-A5-A6)
A789=(M+1)/(2*M)*(A7+A8+A9)
A101112=(M-1)/(4*M)*(A10+A11-A12)
FSXQT=(Y-Z)/(PI)*(A123-A456-V/(1-V)*(A789+A101112))
**COS(T/R)*(1-V**2)
RETURN
END
REAL FUNCTION FSYPT(T,Y1)
IMPLICIT REAL (A-H,O-Z)
COMMON X,DUMMY,D,R,PI,V,H
REAL M
M=(1-V)/V
DF=D-R*COS(T/R)
Z=R*SIN(T/R)
A1=(X-DF)*(Y1-Z)**2/((X-DF)**2+(Y1-Z)**2)**2
A2=((X+DF)*((Y1-Z)**2+2*DF**2)-2*DF*(Y1-Z)**2)/
$((X+DF)**2+(Y1-Z)**2)**2
A3=8*DF*X*(DF+X)*(Y1-Z)**2/((X+DF)**2+(Y1-Z)**2)**3
```

```
A4=-1*(X-DF)/((X-DF)**2+(Y1-Z)**2)
A5=(X+3*DF)/((X+DF)**2+(Y1-Z)**2)
A6=4*X*(Y1-Z)**2/((X+DF)**2+(Y1-Z)**2)**2
A7=(X-DF)**3/((X-DF)**2+(Y1-Z)**2)**2
A8=(X+DF)*((X+DF)**2+2*DF*X)/((X+DF)**2+(Y1-Z)**2)**2
A9=8*DF*X*(DF+X)*(Y1-Z)**2/((X+DF)**2+(Y1-Z)**2)**3
A10=(X-DF)/((X-DF)**2+(Y1-Z)**2)
A11=(3*X+DF)/((X+DF)**2+(Y1-Z)**2)
A12=4*X*(Y1-Z)**2/((X+DF)**2+(Y1-Z)**2)**2
A123=(M+1)/(2*M)*(A1+A2+A3)
A456=(M-1)/(4*M)*(A4+A5+A6)
A789=(M+1)/(2*M)*(A7+A8-A9)
A101112=(M-1)/(4*M)*(A10+A11-A12)
FSYPT=(1-V**2)/(PI)*(A123+A456-V/(1-V)*(A789+A101112))
*SIN(T/R)
RETURN
END
REAL FUNCTION FSYQT(T,Y1)
IMPLICIT REAL (A-H,O-Z)
COMMON X,DUMMY,D,R,PI,V,H
REAL M
M=(1-V)/V
DF=D-R*COS(T/R)
Z=R*SIN(T/R)
A1=(Y1-Z)**2/((X-DF)**2+(Y1-Z)**2)**2
A2=((Y1-Z)**2+8*DF*X+6*DF**2)/((X+DF)**2+(Y1-Z)**2)**2
A3=8*DF*X*(DF+X)**2/((X+DF)**2+(Y1-Z)**2)**3
A4=1/((X-DF)**2+(Y1-Z)**2)
A5=3/((X+DF)**2+(Y1-Z)**2)
A6=4*X*(DF+X)/((X+DF)**2+(Y1-Z)**2)**2
A7=(X-DF)**2/((X-DF)**2+(Y1-Z)**2)**2
A8=(DF**2-X**2+6*DF*X)/((X+DF)**2+(Y1-Z)**2)**2
A9=8*DF*X*(Y1-Z)**2/((X+DF)**2+(Y1-Z)**2)**3
A10=1/((X+DF)**2+(Y1-Z)**2)
A11=1/((X+DF)**2+(Y1-Z)**2)
A12=4*X*(DF+X)/((X+DF)**2+(Y1-Z)**2)**2
A123=(M+1)/(2*M)*(A1+A2+A3)
A456=(M-1)/(4*M)*(A4+A5-A6)
A789=(M+1)/(2*M)*(A7-A8+A9)
A101112=(M-1)/(4*M)*(A10-A11-A12)
FSYQT=(Y1-Z)/(PI)*(A123+A456-V/(1-V)*(A789-A101112))
*COS(T/R)*(1-V**2)
RETURN
END
REAL FUNCTION AX(T)
COMMON X,Y,D,R,PI,V,H
AX=X
RETURN
END
REAL FUNCTION BX(T)
COMMON X,Y,D,R,PI,V,H
BX=H
RETURN
END
```

```
REAL FUNCTION AY(T)
COMMON X,Y,D,R,PI,V,H
AY=0.
RETURN
END
REAL FUNCTION BY(T)
COMMON X,Y,D,R,PI,V,H
BY=Y
RETURN
END
REAL FUNCTION FSSPVR(T,X)
IMPLICIT REAL (A-H,O-Z)
COMMON DUM1,Y,D,R,PI,V,H
REAL M
M=(1-V)/V
DF=D-R*COS(T/R)
Z=R*SIN(T/R)
R1=((X-DF)**2+(Y-Z)**2)
R2=((X+DF)**2+(Y-Z)**2)
A1=(X-DF)**2/R1**2
A2=(X**2-2*DF*X-DF**2)/R2**2
A3=8*DF*X*(DF+X)**2/R2**3
A4=1/R1
A5=1/R2
A6=4*X*(X+DF)/R2**2
A123=(M+1)/(2*M)*(A1+A2+A3)
A456=(M-1)/(4*M)*(A4-A5+A6)
FSSPVR=COS(T/R)*(Y-Z)*(A123+A456)/PI
RETURN
END
REAL FUNCTION FVSPR(T,Y)
IMPLICIT REAL (A-H,O-Z)
COMMON X,DUM2,D,R,PI,V,H
REAL M
M=(1-V)/V
DF=D-R*COS(T/R)
Z=R*SIN(T/R)
R1=((X-DF)**2+(Y-Z)**2)
R2=((X+DF)**2+(Y-Z)**2)
A1=(X-DF)**3/R1**2
A2=(X+DF)*((X+DF)**2+2*DF*X)/R2**2
A3=8*DF*X*(DF+X)*(Y-Z)**2/R2**3
A4=(X-DF)/R1
A5=(3*X+DF)/R2
A6=4*X*(Y-Z)**2/R2**2
A123=(M+1)/(2*M)*(A1+A2-A3)
A456=(M-1)/(4*M)*(A4+A5-A6)
FVSPR=COS(T/R)*(A123+A456)/PI
RETURN
END
REAL FUNCTION FHSPR(T,X)
IMPLICIT REAL (A-H,O-Z)
COMMON DUM1,Y,D,R,PI,V,H
REAL M
```

```
M=(1-V)/V
DF=D-R*COS(T/R)
Z=R*SIN(T/R)
R1=((X-DF)**2+(Y-Z)**2)
R2=((X+DF)**2+(Y-Z)**2)
A1=(X-DF)*(Y-Z)**2/R1**2
A2=((X+DF)**2+(Y-Z)**2+2*DF*(Y-Z)**2)-2*DF*(Y-Z)**2)/R2**2
A3=8*DF*X*(DF+X)*(Y-Z)**2/R2**3
A4=-1*(X-DF)/R1
A5=(X+3*DF)/R2
A6=4*X*(Y-Z)**2/R2**2
A123=(M+1)/(2*M)*(A1+A2+A3)
A456=(M-1)/(4*M)*(A4+A5+A6)
FHSPR=COS(T/R)*(A123+A456)/PI
RETURN
END
REAL FUNCTION FSSQVR(T,X)
IMPLICIT REAL (A-H,O-Z)
COMMON DUM1,Y,D,R,PI,V,H
REAL M
M=(1-V)/V
DF=D-R*COS(T/R)
Z=R*SIN(T/R)
R1=((X-DF)**2+(Y-Z)**2)
R2=((X+DF)**2+(Y-Z)**2)
A1=(X-DF)*(Y-Z)**2/R1**2
A2=(2*DF*X+(Y-Z)**2)*(DF+X)/R2**2
A3=8*DF*X*(DF+X)*(Y-Z)**2/R2**3
A4=(X-DF)/R1
A5=(3*X+DF)/R2
A6=4*X*(DF+X)**2/R2**2
A123=(M+1)/(2*M)*(A1+A2-A3)
A456=(M-1)/(4*M)*(A4+A5-A6)
FSSQVR=SIN(T/R)*(A123+A456)/PI
RETURN
END
REAL FUNCTION FVSQR(T,Y)
IMPLICIT REAL (A-H,O-Z)
COMMON X,DUM2,D,R,PI,V,H
REAL M
M=(1-V)/V
DF=D-R*COS(T/R)
Z=R*SIN(T/R)
R1=((X-DF)**2+(Y-Z)**2)
R2=((X+DF)**2+(Y-Z)**2)
A1=(X-DF)**2/R1**2
A2=(DF**2-X**2+6*X*DF)/R2**2
A3=8*DF*X*(Y-Z)**2/R2**3
A4=1/R1
A5=1/R2
A6=4*X*(DF+X)/R2**2
A123=(M+1)/(2*M)*(A1-A2+A3)
A456=(M-1)/(4*M)*(A4-A5-A6)
FVSQR=SIN(T/R)*(A123-A456)/PI
```

```
RETURN
END
REAL FUNCTION FHSQR(T,X)
IMPLICIT REAL (A-H,O-Z)
COMMON DUM1,Y,D,R,PI,V,H
REAL M
M=(1-V)/V
DF=D-R*COS(T/R)
Z=R*SIN(T/R)
R1=((X-DF)**2+(Y-Z)**2)
R2=((X+DF)**2+(Y-Z)**2)
A1=(Y-Z)**2/R1**2
A2=((Y-Z)**2+8*DF*X+6*DF**2)/R2**2
A3=8*DF*X*(DF+X)**2/R2**3
A4=1/R1
A5=3/R2
A6=4*X*(DF+X)/R2**2
A123=(M+1)/(2*M)*(A1+A2+A3)
A456=(M-1)/(4*M)*(A4+A5-A6)
FHSQR=SIN(T/R)*(Y-Z)*(A123+A456)/PI
RETURN
END
REAL FUNCTION FSSPHR(T,Y)
IMPLICIT REAL (A-H,O-Z)
COMMON X,DUM2,D,R,PI,V,H
REAL M
M=(1-V)/V
DF=D-R*COS(T/R)
Z=R*SIN(T/R)
R1=((X-DF)**2+(Y-Z)**2)
R2=((X+DF)**2+(Y-Z)**2)
A1=(X-DF)**2/R1**2
A2=(X**2-2*DF*X-DF**2)/R2**2
A3=8*DF*X*(DF+X)**2/R2**3
A4=1/R1
A5=1/R2
A6=4*X*(X+DF)/R2**2
A123=(M+1)/(2*M)*(A1+A2+A3)
A456=(M-1)/(4*M)*(A4-A5+A6)
FSSPHR=COS(T/R)*(Y-Z)*(A123+A456)/PI
RETURN
END
REAL FUNCTION FSSQHR(T,Y)
IMPLICIT REAL (A-H,O-Z)
COMMON X,DUM2,D,R,PI,V,H
REAL M
M=(1-V)/V
DF=D-R*COS(T/R)
Z=R*SIN(T/R)
R1=((X-DF)**2+(Y-Z)**2)
R2=((X+DF)**2+(Y-Z)**2)
A1=(X-DF)*(Y-Z)**2/R1**2
A2=(2*DF*X+(Y-Z)**2)*(DF+X)/R2**2
A3=8*DF*X*(DF+X)*(Y-Z)**2/R2**3
```

```
A4=(X-DF)/R1
A5=(3*X+DF)/R2
A6=4*X*(DF+X)**2/R2**2
A123=(M+1)/(2*M)*(A1+A2-A3)
A456=(M-1)/(4*M)*(A4+A5-A6)
FSSQHR=SIN(T/R)*(A123+A456)/PI
RETURN
END
REAL FUNCTION FSSPVT(T,X)
IMPLICIT REAL (A-H,O-Z)
COMMON DUM1,Y,D,R,PI,V,H
REAL M
M=(1-V)/V
DF=D-R*COS(T/R)
Z=R*SIN(T/R)
R1=((X-DF)**2+(Y-Z)**2)
R2=((X+DF)**2+(Y-Z)**2)
A1=(X-DF)**2/R1**2
A2=(X**2-2*DF*X-DF**2)/R2**2
A3=8*DF*X*(DF+X)**2/R2**3
A4=1/R1
A5=1/R2
A6=4*X*(X+DF)/R2**2
A123=(M+1)/(2*M)*(A1+A2+A3)
A456=(M-1)/(4*M)*(A4-A5+A6)
FSSPVT=SIN(T/R)*(Y-Z)*(A123+A456)/PI
RETURN
END
REAL FUNCTION FVSPT(T,Y)
IMPLICIT REAL (A-H,O-Z)
COMMON X,DUM2,D,R,PI,V,H
REAL M
M=(1-V)/V
DF=D-R*COS(T/R)
Z=R*SIN(T/R)
R1=((X-DF)**2+(Y-Z)**2)
R2=((X+DF)**2+(Y-Z)**2)
A1=(X-DF)**3/R1**2
A2=(X+DF)*((X+DF)**2+2*DF*X)/R2**2
A3=8*DF*X*(DF+X)*(Y-Z)**2/R2**3
A4=(X-DF)/R1
A5=(3*X+DF)/R2
A6=4*X*(Y-Z)**2/R2**2
A123=(M+1)/(2*M)*(A1+A2-A3)
A456=(M-1)/(4*M)*(A4+A5-A6)
FVSPT=SIN(T/R)*(A123+A456)/PI
RETURN
END
REAL FUNCTION FHSPT(T,X)
IMPLICIT REAL (A-H,O-Z)
COMMON DUM1,Y,D,R,PI,V,H
REAL M
M=(1-V)/V
DF=D-R*COS(T/R)
```

```
Z=R*SIN(T/R)
R1=((X-DF)**2+(Y-Z)**2)
R2=((X+DF)**2+(Y-Z)**2)
A1=(X-DF)**2/R1**2
A2=((X+DF)**2+(Y-Z)**2+2*DF**2)-2*DF*(Y-Z)**2)/R2**2
A3=8*DF*X*(DF+X)*(Y-Z)**2/R2**3
A4=-1*(X-DF)/R1
A5=(X+3*DF)/R2
A6=4*X*(Y-Z)**2/R2**2
A123=(M+1)/(2*M)*(A1+A2+A3)
A456=(M-1)/(4*M)*(A4+A5+A6)
FHSPT=SIN(T/R)*(A123+A456)/PI
RETURN
END
REAL FUNCTION FSSQVT(T,X)
IMPLICIT REAL (A-H,O-Z)
COMMON DUM1,Y,D,R,PI,V,H
REAL M
M=(1-V)/V
DF=D-R*COS(T/R)
Z=R*SIN(T/R)
R1=((X-DF)**2+(Y-Z)**2)
R2=((X+DF)**2+(Y-Z)**2)
A1=(X-DF)**2/R1**2
A2=(2*DF*X+(Y-Z)**2)*(DF+X)/R2**2
A3=8*DF*X*(DF+X)*(Y-Z)**2/R2**3
A4=(X-DF)/R1
A5=(3*X+DF)/R2
A6=4*X*(DF+X)**2/R2**2
A123=(M+1)/(2*M)*(A1+A2-A3)
A456=(M-1)/(4*M)*(A4+A5-A6)
FSSQVT=COS(T/R)*(A123+A456)/PI
RETURN
END
REAL FUNCTION FVSQT(T,Y)
IMPLICIT REAL (A-H,O-Z)
COMMON X,DUM2,D,R,PI,V,H
REAL M
M=(1-V)/V
DF=D-R*COS(T/R)
Z=R*SIN(T/R)
R1=((X-DF)**2+(Y-Z)**2)
R2=((X+DF)**2+(Y-Z)**2)
A1=(X-DF)**2/R1**2
A2=(DF**2-X**2+6*X*DF)/R2**2
A3=8*DF*X*(Y-Z)**2/R2**3
A4=1/R1
A5=1/R2
A6=4*X*(DF+X)/R2**2
A123=(M+1)/(2*M)*(A1-A2+A3)
A456=(M-1)/(4*M)*(A4-A5-A6)
FVSQT=COS(T/R)*(Y-Z)*(A123-A456)/PI
RETURN
END
```

```
REAL FUNCTION FHSQT(T,X)
IMPLICIT REAL (A-H,O-Z)
COMMON DUM1,Y,D,R,PI,V,H
REAL M
M=(1-V)/V
DF=D-R*COS(T/R)
Z=R*SIN(T/R)
R1=((X-DF)**2+(Y-Z)**2)
R2=((X+DF)**2+(Y-Z)**2)
A1=(Y-Z)**2/R1**2
A2=((Y-Z)**2+8*DF*X+6*DF**2)/R2**2
A3=8*DF*X*(DF+X)**2/R2**3
A4=1/R1
A5=3/R2
A6=4*X*(DF+X)/R2**2
A123=(M+1)/(2*M)*(A1+A2+A3)
A456=(M-1)/(4*M)*(A4+A5-A6)
FHSQT=COS(T/R)*(Y-Z)*(A123+A456)/PI,
RETURN
END
REAL FUNCTION FSSPHT(T,Y)
IMPLICIT REAL (A-H,O-Z)
COMMON X,DUM2,D,R,PI,V,H
REAL M
M=(1-V)/V
DF=D-R*COS(T/R)
Z=R*SIN(T/R)
R1=((X-DF)**2+(Y-Z)**2)
R2=((X+DF)**2+(Y-Z)**2)
A1=(X-DF)**2/R1**2
A2=(X**2-2*DF*X-DF**2)/R2**2
A3=8*DF*X*(DF+X)**2/R2**3
A4=1/R1
A5=1/R2
A6=4*X*(X+DF)/R2**2
A123=(M+1)/(2*M)*(A1+A2+A3)
A456=(M-1)/(4*M)*(A4-A5+A6)
FSSPHT=SIN(T/R)*(Y-Z)*(A123+A456)/PI
RETURN
END
REAL FUNCTION FSSQHT(T,Y)
IMPLICIT REAL (A-H,O-Z)
COMMON X,DUM2,D,R,PI,V,H
REAL M
M=(1-V)/V
DF=D-R*COS(T/R)
Z=R*SIN(T/R)
R1=((X-DF)**2+(Y-Z)**2)
R2=((X+DF)**2+(Y-Z)**2)
A1=(X-DF)*(Y-Z)**2/R1**2
A2=(2*DF*X+(Y-Z)**2)*(DF+X)/R2**2
A3=8*DF*X*(DF+X)*(Y-Z)**2/R2**3
A4=(X-DF)/R1
A5=(3*X+DF)/R2
```

```
A6=4*X*(DF+X)**2/R2**2
A123=(M+1)/(2*M)*(A1+A2-A3),
A456=(M-1)/(4*M)*(A4+A5-A6)
FSSQHT=COS(T/R)*(A123+A456)/PI
RETURN
END
REAL FUNCTION XL1(T)
COMMON /0/ X1,Y1,X2,Y2
XL1=X1
RETURN
END
REAL FUNCTION XL2(T)
COMMON /0/ X1,Y1,X2,Y2
XL2=X2
RETURN
END
REAL FUNCTION YL1(T)
COMMON /0/ X1,Y1,X2,Y2
YL1=Y1
RETURN
END
REAL FUNCTION YL2(T)
COMMON /0/ X1,Y1,X2,Y2
YL2=Y2
RETURN
END
REAL FUNCTION POLY(K,X)
IMPLICIT REAL (A-H,O-Z)
INTEGER K
P=K
POLY=X**(P-1.)
RETURN
END
```

PROGRAM "CIRFDN"
PROGRAM "CIRFDN" EVALUATE THE DISPLACEMENT OF ,AND THE
CONTACT STRESS OF A RIGID ANNULAR STRIP FOOTING
IN LINEARLY ELASTIC GROUND .
THESE STRESS ARE AN APPROXIMATION TO THE REAL CONTACT
STRESS DISTRIBUTION.
THE METHOD USED IS PRESENTED IN THIS THESIS.

```
-----  
PROGRAM CIRFDN(INPUT,OUTPUT)  
IMPLICIT REAL (A-H,O-Z)  
COMMON X,Y,D,R,PI,V,H  
COMMON /O/ X1,Y1,X2,Y2  
CCC X,Y ARE COORDINATES OF THE POINT AT WHICH STRESS ARE  
CALCULATED.  
CCC DF,Z ARE COORDINATES OF THE FORCE UNDER CONSIDERATION  
PARAMETER (N=20,K=21,L=10)  
CCC N IS NUMBER OF SECTION TO WHICH PIPE IS DIVIDED,  
REAL A(K,K),BRS(L),BTS(L),URS(L),UTS(L),XF(N),YF(N),  
$SP(N),SF(N),ANP(L),XP(L),YP(L)  
CCC A IS THE MATRIX OF DISPLACEMENT INFLUENCE  
FACTORS, AND LATER OF STRESS INFLUENCE FACTORS.  
CCC VS & HS ARE VECTORS OF TOTAL VER. AND HOR.  
CCC FORCES ACTING AT EACH SECTION, AND LATER VECTORS  
CCC OF RAD. AND TAN. STRESS AT EACH SECTION.  
CCC XF & YF ARE VECTORS OF END-POINTS COORDINATES  
CCC OF EACH SECTION.  
CCC XP & YP ARE VECTORS OF MID-POINT COORDINATES  
CCC OF EACH SECTION.  
REAL B(K,1),WKAREA(K),WK(130)  
INTEGER M,O,IA,IDGT,IERR  
REAL INC,KO  
INTEGER IER  
CCC INC IS THE SIZE OF THE ELEMENTAL PIPE SECTION  
REAL DBLIN  
CCC DBLIN IS A DOUBLE INTEGRATION SUBROUTINE FROM IMSL LIBRARY.  
EXTERNAL POLY  
EXTERNAL FSXPR,FSXQR,FSYPR,FSYQR  
CCC THESE ARE THE STRAIN FUNCTIONS UPON WHICH DOUBLE  
CCC INTEGRATION IS PERFORMED TO GET DISP. INFLUENCE  
CCC FACTORS DUE TO A UNIT NORMAL STRESS.  
EXTERNAL FSXPT,FSXQT,FSYPT,FSYQT  
CCC THESE ARE THE STRAIN FUNCTIONS UPON WHICH DOUBLE  
CCC INTEGRATION IS PERFORMED TO GET DISP. INFLUENCE  
CCC FACTORS DUE TO A UNIT TANGENTIAL STRESS.  
EXTERNAL AX,BX,AY,BY  
CCC INTEGRATION LIMIT FUNCTIONS FOR DBLIN SUBROUTINE.  
EXTERNAL FVSPR,FHSPR,FSSPVR,FSSPHR,  
$FVSQR,FHSQR,FSSQVR,FSSQHR,  
$FVSPT,FHSPT,FSSPVT,FSSPHT,  
$FVSQT,FHSQT,FSSQVT,FSSQHT  
CCC THESE ARE STRESS FUNCTIONS IN TERMS OF VER. AND  
CCC HOR. COMPONENTS OF NORMAL AND TANGENTIAL STRESS.  
EXTERNAL XL1,XL2,YL1,YL2
```



```

DO 4,I=1,L
4 ANP(I)=I*ANG/N-.5*ANG/N
IANG=ANG/2
ANG=ANG*PI/360.
R=BR/SIN(ANG)
D=HT+R*COS(ANG)
INC=2.*R*ANG/N
SF(1)=0.
SP(1)=INC/2.

CCC/ GENERATION OF ANGULAR COOD. OF MID-POINTS AND
CCC/ END-POINTS OF EACH SECTION.
DO 5,I=1,L
SP(I+1)=SP(I)+INC
SF(I+1)=SF(I)+INC
5 CONTINUE

CCC GENERATION OF POINTS COOD.
DO 10,I=1,L
XP(I)=D-R*COS(SP(I)/R)
YP(I)=R*SIN(SP(I)/R)

10 CONTINUE
DO 11,I=1,L+1
XF(I)=D-R*COS(SF(I)/R)
YF(I)=R*SIN(SF(I)/R)

11 CONTINUE

CCC GENERATION OF DISPLACEMENT INFLUENCE FACTORS.
DO 30,J=1,L
X=XP(J)
Y=YP(J)
DO 35,I=1,L
T1=SF(I)
T11=SP(I)-EPS
T22=SP(I)+EPS
T2=SF(I+1)
IF(I.EQ.J)THEN
VDP1=DBLIN(FSXPR,T1,T11,AX,BX,AERR,ERROR,IER)
$-DBLIN(FSXQR,T1,T11,AX,BX,AERR,ERROR,IER).
$+DBLIN(FSXPR,T22,T2,AX,BX,AERR,ERROR,IER)
$-DBLIN(FSXQR,T22,T2,AX,BX,AERR,ERROR,IER)
HDP1=DBLIN(FSYPR,T1,T11,AY,BY,AERR,ERROR,IER)
$-DBLIN(FSYQR,T1,T11,AY,BY,AERR,ERROR,IER)
$+DBLIN(FSYPR,T22,T2,AY,BY,AERR,ERROR,IER)
$-DBLIN(FSYQR,T22,T2,AY,BY,AERR,ERROR,IER)
VDQ1=DBLIN(FSXPT,T1,T11,AX,BX,AERR,ERROR,IER)
$+DBLIN(FSXQT,T1,T11,AX,BX,AERR,ERROR,IER)
$+DBLIN(FSXPT,T22,T2,AX,BX,AERR,ERROR,IER)
$+DBLIN(FSXQT,T22,T2,AX,BX,AERR,ERROR,IER)
HDQ1=DBLIN(FSYPT,T1,T11,AY,BY,AERR,ERROR,IER)
$+DBLIN(FSYQT,T1,T11,AY,BY,AERR,ERROR,IER)
$+DBLIN(FSYPT,T22,T2,AY,BY,AERR,ERROR,IER)
$+DBLIN(FSYQT,T22,T2,AY,BY,AERR,ERROR,IER)
ELSE
VDP1=DBLIN(FSXPR,T1,T2,AX,BX,AERR,ERROR,IER)

```

```
$-DBLIN(FSXQR,T1,T2,AX,BX,AERR,ERROR,IER)
HDP1=DBLIN(FSYPR,T1,T2,AY,BY,AERR,ERROR,IER)
$-DBLIN(FSYQR,T1,T2,AY,BY,AERR,ERROR,IER)
VDQ1=DBLIN(FSXPT,T1,T2,AX,BX,AERR,ERROR,IER)
$+DBLIN(FSXQT,T1,T2,AX,BX,AERR,ERROR,IER)
HDQ1=DBLIN(FSYPT,T1,T2,AY,BY,AERR,ERROR,IER)
$+DBLIN(FSYQT,T1,T2,AY,BY,AERR,ERROR,IER)
ENDIF
T1=-T1
T2=-T2
VDP2=DBLIN(FSXPR,T2,T1,AX,BX,AERR,ERROR,IER)
$-DBLIN(FSXQR,T2,T1,AX,BX,AERR,ERROR,IER)
HDP2=DBLIN(FSYPR,T2,T1,AY,BY,AERR,ERROR,IER)
$-DBLIN(FSYQR,T2,T1,AY,BY,AERR,ERROR,IER)
VDQ2=-DBLIN(FSXPT,T2,T1,AX,BX,AERR,ERROR,IER)
$-DBLIN(FSXQT,T2,T1,AX,BX,AERR,ERROR,IER)
HDQ2=-DBLIN(FSYPT,T2,T1,AY,BY,AERR,ERROR,IER)
$-DBLIN(FSYQT,T2,T1,AY,BY,AERR,ERROR,IER)
A(J,I)=VDP1+VDP2
A(J,I+L)=VDQ1+VDQ2
A(J+L,I)=HDP1+HDP2
A(J+L,I+L)=HDQ1+HDQ2
35 CONTINUE
30 CONTINUE
DO 90 ,J=1,N/2
A(J,K)=-1#E
90 CONTINUE
DO 95,J=N/2+1,K
95 A(J,K)=0.0
DO 100,I=1,N/2
A(K,I)=2.*R*(SIN(SF(I+1)/R)-SIN(SF(I)/R))
A(K,I+N/2)=-2.*R*(COS(SF(I+1)/R)-COS(SF(I)/R))
100 CONTINUE
DO 105,I=1,K-1
105 B(I,1)=0.0
B(K,1)=W
CCC LEQT1F IS AN IMSL LIBRARY SUBROUTINE TO SOLVE
CCC A SYSTEM OF LINEAR EQUATIONS.
CALL LEQT1F(A,M,O,IA,B,IDL,WKAREA,IER)
CCC GENERATING STRESS INFLUENCE FACTORS.
DO 40,J=1,N/2
X1=XF(J)
Y1=YF(J)
X2=XF(J+1)
Y2=YF(J+1)
X=X1
Y=Y2
DO 45,I=1,N/2
T1=SF(I)+EPS
T2=SF(I+1)-EPS
VSP1=DBLIN(FVSPR,T1,T2,YL1,YL2,AERR,ERROR,IER)
$-DBLIN(FSSPVR,T1,T2,XL1,XL2,AERR,ERROR,IER)
$-DBLIN(FVSQR,T1,T2,YL1,YL2,AERR,ERROR,IER)
$+DBLIN(FSSQVR,T1,T2,XL1,XL2,AERR,ERROR,IER)
```

```
HSP1=-DBLIN(FHSPR,T1,T2,XL1,XL2,AERR,ERROR,IER)
$+DBLIN(FSSPHR,T1,T2,YL1,YL2,AERR,ERROR,IER)
$+DBLIN(FHSQR,T1,T2,XL1,XL2,AERR,ERROR,IER)
$-DBLIN(FSSQHR,T1,T2,YL1,YL2,AERR,ERROR,IER)
VSQ1=-DBLIN(FVSPT,T1,T2,YL1,YL2,AERR,ERROR,IER)
$-DBLIN(FSSPVT,T1,T2,XL1,XL2,AERR,ERROR,IER)
$+DBLIN(FVSQT,T1,T2,YL1,YL2,AERR,ERROR,IER)
$-DBLIN(FSSQVT,T1,T2,XL1,XL2,AERR,ERROR,IER)
HSQ1=-DBLIN(FHSPT,T1,T2,XL1,XL2,AERR,ERROR,IER)
$+DBLIN(FSSPHT,T1,T2,YL1,YL2,AERR,ERROR,IER)
$-DBLIN(FHSQT,T1,T2,XL1,XL2,AERR,ERROR,IER)
$+DBLIN(FSSQHT,T1,T2,YL1,YL2,AERR,ERROR,IER)
T1=-T1
T2=-T2
VSP2=DBLIN(FVSPR,T2,T1,YL1,YL2,AERR,ERROR,IER)
$-DBLIN(FSSPVR,T2,T1,XL1,XL2,AERR,ERROR,IER)
$-DBLIN(FVSQR,T2,T1,YL1,YL2,AERR,ERROR,IER)
$+DBLIN(FSSQVR,T2,T1,XL1,XL2,AERR,ERROR,IER)
HSP2=-DBLIN(FHSPR,T2,T1,XL1,XL2,AERR,ERROR,IER)
$+DBLIN(FSSPHR,T2,T1,YL1,YL2,AERR,ERROR,IER)
$+DBLIN(FHSQR,T2,T1,XL1,XL2,AERR,ERROR,IER)
$-DBLIN(FSSQHR,T2,T1,YL1,YL2,AERR,ERROR,IER)
VSQ2=-DBLIN(FVSPT,T2,T1,YL1,YL2,AERR,ERROR,IER)
$+DBLIN(FSSPVT,T2,T1,XL1,XL2,AERR,ERROR,IER)
$-DBLIN(FVSQT,T2,T1,YL1,YL2,AERR,ERROR,IER)
$+DBLIN(FSSQVT,T2,T1,XL1,XL2,AERR,ERROR,IER)
HSQ2=DBLIN(FHSPT,T2,T1,XL1,XL2,AERR,ERROR,IER)
$-DBLIN(FSSPHT,T2,T1,YL1,YL2,AERR,ERROR,IER)
$+DBLIN(FHSQT,T2,T1,XL1,XL2,AERR,ERROR,IER)
$-DBLIN(FSSQHT,T2,T1,YL1,YL2,AERR,ERROR,IER)
A(J,I)=VSP1+VSP2
A(J,I+L)=VSQ1+VSQ2
A(J+L,I)=HSP1+HSP2
A(J+L,I+L)=HSQ1+HSQ2
45 CONTINUE
40 CONTINUE
CCC CALCULATING TOTAL VER. & HOR. FORCES
CCC ON BOTH SIDES OF EACH SECTION.
DO 110,J=1,N/2
DO 115,I=1,N/2
A(J,I)=B(I,1)*A(J,I)+B(I+L,1)*A(J,I+L)
A(J+L,I)=B(I,1)*A(J+L,I)+B(I+L,1)*A(J+L,I+L)
115 CONTINUE
110 CONTINUE
DO 120,I=1,N/2
URS(I)=0.
UTS(I)=0.
120 CONTINUE
DO 125,J=1,N/2
DO 130,I=1,N/2
URS(J)=URS(J)+A(J,I)
UTS(J)=UTS(J)+A(J+L,I)
130 CONTINUE
125 CONTINUE
```

```
      AREA=INC
CCC RESOLVING FORCES INTO NOR. & TAN. STRESS.
DO 165,I=1,N/2
RS=(URS(I)*COS(SP(I)/R)-UTS(I)*SIN(SP(I)/R))/AREA
TS=-(URS(I)*SIN(SP(I)/R)+UTS(I)*COS(SP(I)/R))/AREA
URS(I)=RS
UTS(I)=TS
165 CONTINUE
DO 166,I=1,N/2
BRS(I)=B(I,1)+URS(I)
BTS(I)=B(I+L,1)-UTS(I)
166 CONTINUE
PRINT2050
2050 FORMAT(//1X,'[ RESULTANT STRESS DISTRIBUTION ]')
PRINT3000
PRINT1700
PRINT3000
DO 190,I=1,N/2
PRINT1800,ANP(I),B(I,1),B(I+L,1)
190 PRINT3000
PRINT2060
2060 FORMAT(//1X,'[ STRESS DISTRIBUTION ON LOWER SURFACE ]')
PRINT3000
PRINT1700
PRINT3000
DO 191,I=1,N/2
PRINT1800,ANP(I),BRS(I),BTS(I)
191 PRINT3000
PRINT2070
2070 FORMAT(//1X,'[ STRESS DISTRIBUTION ON UPPER SURFACE ]')
PRINT3000
PRINT1700
PRINT3000
DO 192,I=1,N/2
PRINT1800,ANP(I),URS(I),UTS(I)
192 PRINT3000
1700 FORMAT(1X,'*', 'ANG.',T16,'RAD.',T31,'TAN.',T41,'**')
1800 FORMAT(1X,'**',F4.1,T10,F10.1,T25,F10.1,T41,'**')
PRINT2900,B(K,1)
2900 FORMAT(1X,'**','VERTICAL DISPLACEMENT IS ','[',F8.6,']','
$T41,'**')
PRINT3000
3000 FORMAT(1X,'-----')
STOP
END
```

PROGRAM "TRIFDN"
PROGRAM "TRIFDN" EVALUATE THE DISPLACEMENT OF , AND THE
CONTACT STRESS OF A RIGID TRIANGULAR STRIP FOOTING
IN LINEARLY ELASTIC GROUND .
THESE STRESS ARE AN APPROXIMATION TO THE REAL CONTACT
STRESS DISTRIBUTION.
THE METHOD USED IS PRESENTED IN THIS THESIS.

```
PROGRAM TRIFDN(INPUT,OUTPUT)
IMPLICIT REAL (A-H,O-Z)
COMMON X,Y,HT,AN,PI,V,H
COMMON /O/ X1,Y1,X2,Y2
CCC X,Y ARE COORDINATES OF THE POINT AT WHICH STRESS ARE
CCC CALCULATED.
CCC DF,Z ARE COORDINATES OF THE FORCE UNDER CONSIDERATION
PARAMETER (N=20,K=21,L=10)
CCC N IS NUMBER OF SECTION TO WHICH PIPE IS DIVIDED.
REAL A(K,K),BRS(L),BTS(L),URS(L),UTS(L),XF(N),YF(N),
$SP(L),SF(N),XP(L),YP(L)
CCC A IS THE MATRIX OF DISPLACEMENT INFLUENCE
CCC FACTORS, AND LATER OF STRESS INFLUENCE FACTORS.
CCC VS & HS ARE VECTORS OF TOTAL.VER. AND HOR.
CCC FORCES ACTING AT EACH SECTION, AND LATER VECTORS
CCC OF RAD. AND TAN. STRESS AT EACH SECTION.
CCC XF & YF ARE VECTORS OF END-POINTS COORDINATES
CCC OF EACH SECTION.
CCC XP & YP ARE VECTORS OF MID-POINT COORDINATES
CCC OF EACH SECTION.
REAL B(K,1),WKAREA(K),WK(130)
INTEGER M,O,IA, IDGT, IERR
REAL INC,K0
INTEGER IER
CCC INC IS THE SIZE OF THE ELEMENTAL PIPE SECTION
REAL DBLIN
CCC DBLIN IS A DOUBLE INTEGRATION SUBROUTINE FROM IMSL LIBRARY.
EXTERNAL POLY
EXTERNAL FSXPR,FSXQR,FSYPR,FSYQR
CCC THESE ARE THE STRAIN FUNCTIONS UPON WHICH DOUBLE
GCC INTEGRATION IS PERFORMED TO GET DISP. INFLUENCE
CCC FACTORS DUE TO A UNIT NORMAL STRESS.
EXTERNAL FSXPT,FSXQT,FSYPT,FSYQT
CCC THESE ARE THE STRAIN FUNCTIONS UPON WHICH DOUBLE
CCC INTEGRATION IS PERFORMED TO GET DISP. INFLUENCE
CCC FACTORS DUE TO A UNIT TANGENTIAL STRESS.
EXTERNAL AX,BX,AY,BY
CCC INTEGRATION LIMIT FUNCTIONS FOR DBLIN SUBROUTINE.
EXTERNAL FVSPR,FHSPR,FSSPVR,FSSPHR,
$FVSQR,FHSQR,FSSQVR,FSSQHR,
$FVSPT,FHSPT,FSSPVT,FSSPHT,
$FVSQT,FHSQT,FSSQVT,FSSQHT
CCC THESE ARE STRESS FUNCTIONS IN TERMS OF VER. AND
CCC HOR. COMPONENTS OF NORMAL AND TANGENTIAL STRESS.
EXTERNAL XL1,XL2,YL1,YL2
```



```
$+DBLIN(FSXQT,T1,T2,AX,BX,AERR,ERROR,IER)
HDQ1=DBLIN(FSYPT,T1,T2,AY,BY,AERR,ERROR,IER)
$+DBLIN(FSYQT,T1,T2,AY,BY,AERR,ERROR,IER)
ENDIF
AN=-1.*ANG
T1=-T1
T2=-T2
VDP2=DBLIN(FSXPR,T2,T1,AX,BX,AERR,ERROR,IER)
$-DBLIN(FSXQR,T2,T1,AX,BX,AERR,ERROR,IER)
HDP2=DBLIN(FSYPR,T2,T1,AY,BY,AERR,ERROR,IER)
$-DBLIN(FSYQR,T2,T1,AY,BY,AERR,ERROR,IER)
VDQ2=-DBLIN(FSXPT,T2,T1,AX,BX,AERR,ERROR,IER)
$-DBLIN(FSXQT,T2,T1,AX,BX,AERR,ERROR,IER)
HDQ2=-DBLIN(FSYPT,T2,T1,AY,BY,AERR,ERROR,IER)
$-DBLIN(FSYQT,T2,T1,AY,BY,AERR,ERROR,IER)
A(J,I)=VDP1+VDP2
A(J,I+L)=VDQ1+VDQ2
A(J+L,I)=HDP1+HDP2
A(J+L,I+L)=HDQ1+HDQ2
35 CONTINUE
30 CONTINUE
DO 90 ,J=1,N/2
A(J,K)=-1.*E
90 CONTINUE
DO 95,J=N/2+1,K
95 A(J,K)=0.0
DO 100,I=1,N/2.
A(K,I)=2.*INC*COS(ANG)
A(K,I+L)=2.*INC*SIN(ANG)
100 CONTINUE
DO 105,I=1,K-1
105 B(I,1)=0.0
B(K,1)=W
CCC LEQT1F IS AN IMSL LIBRARY SUBROUTINE TO SOLVE
CCC A SYSTEM OF LINEAR EQUATIONS.
CALL LEQT1F(A,M,O,IA,B,IDLGT,WKAREA,IER)
PRINT*, 'IER IS '
PRINT*, IER
CCC GENERATING STRESS INFLUENCE FACTORS.
DO 40,J=1,N/2
X1=XF(J)
Y1=YF(J)
X2=XF(J+1)
Y2=YF(J+1)
X=X1
Y=Y2
DO 45,I=1,N/2
AN=ANG
T1=SF(I)+EPS
T2=SF(I+1)-EPS
VSP1=DBLIN(FVSPR,T1,T2,YL1,YL2,AERR,ERROR,IER)
$-DBLIN(FSSPVR,T1,T2,XL1,XL2,AERR,ERROR,IER)
$-DBLIN(FVSQR,T1,T2,YL1,YL2,AERR,ERROR,IER)
$+DBLIN(FSSQVR,T1,T2,XL1,XL2,AERR,ERROR,IER)
```

```
HSP1=-DBLIN(FHSPR,T1,T2,XL1,XL2,AERR,ERROR,IER)
$+DBLIN(FSSPHR,T1,T2,YL1,YL2,AERR,ERROR,IER)
$+DBLIN(FHSQR,T1,T2,XL1,XL2,AERR,ERROR,IER)
$-DBLIN(FSSQHR,T1,T2,YL1,YL2,AERR,ERROR,IER)
VSQ1=DBLIN(FVSPT,T1,T2,YL1,YL2,AERR,ERROR,IER)
$-DBLIN(FSSPVT,T1,T2,XL1,XL2,AERR,ERROR,IER)
$+DBLIN(FVSPQT,T1,T2,YL1,YL2,AERR,ERROR,IER)
$-DBLIN(FSSQVT,T1,T2,XL1,XL2,AERR,ERROR,IER)
HSQ1=-DBLIN(FHSPT,T1,T2,XL1,XL2,AERR,ERROR,IER)
$+DBLIN(FSSPHT,T1,T2,YL1,YL2,AERR,ERROR,IER)
$-DBLIN(FHSQQT,T1,T2,XL1,XL2,AERR,ERROR,IER)
$+DBLIN(FSSQHT,T1,T2,YL1,YL2,AERR,ERROR,IER)
AN=-1.*ANG
T1=-T1
T2=-T2
VSP2=DBLIN(FVSPR,T2,T1,YL1,YL2,AERR,ERROR,IER)
$-DBLIN(FSSPVR,T2,T1,XL1,XL2,AERR,ERROR,IER)
$-DBLIN(FVSQR,T2,T1,YL1,YL2,AERR,ERROR,IER)
$+DBLIN(FSSQVR,T2,T1,XL1,XL2,AERR,ERROR,IER)
HSP2=-DBLIN(FHSPR,T2,T1,XL1,XL2,AERR,ERROR,IER)
$+DBLIN(FSSPHR,T2,T1,YL1,YL2,AERR,ERROR,IER)
$+DBLIN(FHSQR,T2,T1,XL1,XL2,AERR,ERROR,IER)
$-DBLIN(FSSQHR,T2,T1,YL1,YL2,AERR,ERROR,IER)
VSQ2=-DBLIN(FVSPT,T2,T1,YL1,YL2,AERR,ERROR,IER)
$+DBLIN(FSSPVT,T2,T1,XL1,XL2,AERR,ERROR,IER)
$-DBLIN(FVSPQT,T2,T1,YL1,YL2,AERR,ERROR,IER)
$+DBLIN(FSSQVT,T2,T1,XL1,XL2,AERR,ERROR,IER)
HSQ2=DBLIN(FHSPT,T2,T1,XL1,XL2,AERR,ERROR,IER)
$-DBLIN(FSSPHT,T2,T1,YL1,YL2,AERR,ERROR,IER)
$+DBLIN(FHSQQT,T2,T1,XL1,XL2,AERR,ERROR,IER)
$-DBLIN(FSSQHT,T2,T1,YL1,YL2,AERR,ERROR,IER)
A(J,I)=VSP1+VSP2
A(J,I+L)=VSQ1+VSQ2
A(J+L,I)=HSP1+HSP2
A(J+L,I+L)=HSQ1+HSQ2
45 CONTINUE
40 CONTINUE
CCC CALCULATING TOTAL V&R. & HOR. FORCES
CCC ON BOTH SIDES OF EACH SECTION.
DO 110,J=1,N/2
DO 115,I=1,N/2
A(J,I)=B(I,1)*A(J,I)+B(I+L,1)*A(J,I+L)
A(J+L,I)=B(I,1)*A(J+L,I)+B(I+L,1)*A(J+L,I+L)
115 CONTINUE
110 CONTINUE
DO 120,I=1,N/2
URS(I)=0.
UTS(I)=0.
120 CONTINUE
DO 125,J=1,N/2
DO 130,I=1,N/2
URS(J)=URS(J)+A(J,I)
UTS(J)=UTS(J)+A(J+L,I)
130 CONTINUE
```

```
125 CONTINUE
  AREA=INC
CCC  RESOLVING FORCES INTO NOR. & TAN. STRESS.
  DO 165,I=1,N/2
    RS=(URS(I)*COS(ANG)-UTS(I)*SIN(ANG))/AREA
    TS=-(URS(I)*SIN(ANG)+UTS(I)*COS(ANG))/AREA
    URS(I)=RS
    UTS(I)=TS
165 CONTINUE
  DO 166,I=1,N/2
    BRS(I)=B(I,1)+URS(I)
    BTS(I)=B(I+L,1)-UTS(I)
166 CONTINUE
PRINT2050
2050 FORMAT(//1X,'[ RESULTANT STRESS DISTRIBUTION ]')
PRINT3000
PRINT1700
PRINT3000
DO 190,I=1,N/2
PRINT1800,SP(I),B(I,1),B(I+L,1)
190 PRINT3000
PRINT2060
2060 FORMAT(//1X,'[ STRESS DISTRIBUTION ON LOWER SURFACE ]')
PRINT3000
PRINT1700
PRINT3000
DO 191,I=1,N/2
PRINT1800,SP(I),BRS(I),BTS(I)
191 PRINT3000
PRINT2070
2070 FORMAT(//1X,'[ STRESS DISTRIBUTION ON UPPER SURFACE ]')
PRINT3000
PRINT1700
PRINT3000
DO 192,I=1,N/2
PRINT1800,SP(I),URS(I),UTS(I)
192 PRINT3000
1700 FORMAT(1X,'*', 'LENGTH',T16,'RAD.',T31,'TAN.',T41,'**')
1800 FORMAT(1X,'*',F5.2,T10,F10.1,T25,F10.1,T41,'**')
PRINT2900,B(K,1)
2900 FORMAT(1X,'*', 'VERTICAL DISPLACEMENT IS ',',[',F8.6,'],',
$T41,'**')
PRINT3000
3000 FORMAT(1X,'-----')
STOP
END
```

PROGRAM "FLAFDN"

PROGRAM "FLAFDN" EVALUATE THE DISPLACEMENT OF , AND THE CONTACT STRESS OF A RIGID FLAT STRIP FOOTING INSTALLED IN LINEARLY ELASTIC GROUND . THESE STRESS ARE AN APPROXIMATION TO THE REAL CONTACT STRESS DISTRIBUTION.

THE METHOD USED IS PRESENTED IN THIS THESIS.

PROGRAM FLAFDN(INPUT,OUTPUT)

IMPLICIT REAL (A-H,O-Z)

COMMON X,Y,HT,AN,PI,V,H

COMMON /O/ X1,Y1,X2,Y2

CCC X,Y ARE COORDINATES OF THE POINT AT WHICH STRESS ARE CALCULATED.

CCC DF,Z ARE COORDINATES OF THE FORCE UNDER CONSIDERATION PARAMETER (N=20,K=21,L=10)

CCC N IS NUMBER OF SECTION TO WHICH PIPE IS DIVIDED.

REAL A(K,K),BRS(L),BTS(L),URS(L),UTS(L),XF(N),YF(N),
\$SP(L),SF(N),XP(L),YP(L)

CCC A IS THE MATRIX OF DISPLACEMENT INFLUENCE

CCC FACTORS, AND LATER OF STRESS INFLUENCE FACTORS.

CCC VS & HS ARE VECTORS OF TOTAL VER. AND HOR.

CCC FORCES ACTING AT EACH SECTION, AND LATER VECTORS

CCC OF RAD. AND TAN. STRESS AT EACH SECTION.

CCC XF & YF ARE VECTORS OF END-POINTS COORDINATES

CCC OF EACH SECTION.

CCC XP & YP ARE VECTORS OF MID-POINT COORDINATES

CCC OF EACH SECTION.

REAL B(K,1),WKAREA(K),WK(130)

INTEGER M,O,IA,IDGT,IERR

REAL INC,KO

INTEGER IER

CCC INC IS THE SIZE OF THE ELEMENTAL PIPE SECTION

REAL DBLIN

CCC DBLIN IS A DOUBLE INTEGRATION SUBROUTINE FROM IMSL LIBRARY.

EXTERNAL POLY

EXTERNAL FSXPR,FSXQR,FSYPR,FSYQR

CCC THESE ARE THE STRAIN FUNCTIONS UPON WHICH DOUBLE

CCC INTEGRATION IS PERFORMED TO GET DISP. INFLUENCE

CCC FACTORS DUE TO A UNIT NORMAL STRESS.

EXTERNAL FSXPT,FSXQT,FSYPT,FSYQT

CCC THESE ARE THE STRAIN FUNCTIONS UPON WHICH DOUBLE

CCC INTEGRATION IS PERFORMED TO GET DISP. INFLUENCE

CCC FACTORS DUE TO A UNIT TANGENTIAL STRESS.

EXTERNAL AX,BX,AY,BY

CCC INTEGRATION LIMIT FUNCTIONS FOR DBLIN SUBROUTINE.

EXTERNAL FVSPR,FHSPR,FSSPVR,FSSPHR,

\$FVSQR,FHSQR,FSSQVR,FSSQHR,

\$FVSPT,FHSPT,FSSPVT,FSSPHT,

\$FVSQT,FHSQT,FSSQVT,FSSQHT

CCC THESE ARE STRESS FUNCTIONS IN TERMS OF VER. AND

CCC HOR. COMPONENTS OF NORMAL AND TANGENTIAL STRESS.

EXTERNAL XL1,XL2,YL1,YL2


```
DO 90 ,J=1,N/2
A(J,K)=-1*E .
90 CONTINUE
DO 95,J=N/2+1,K
95 A(J,K)=0.0
DO 100,I=1,N/2
A(K,I)=2.*INC*COS(ANG)
A(K,I+L)=2.*INC*SIN(ANG)
100 CONTINUE
DO 105,I=1,K-1
105 B(I,1)=0.0
B(K,1)=W
CCC LEQT1F IS AN IMSL LIBRARY SUBROUTINE TO SOLVE
CCC A SYSTEM OF LINEAR EQUATIONS.
CALL LEQT1F(A,M,O,JA,B,IDGT,WKAREA,IER)
CCC GENERATING STRESS INFLUENCE FACTORS.
DO 40,J=1,N/2
X1=XF(J)
Y1=YF(J)
X2=XF(J+1)+INC
Y2=YF(J+1)
DO 45,I=1,N/2
AN=ANG
T1=SF(I)+EPS
T2=SF(I+1)-EPS
X=X2
Y=Y1
VSP1=DBLIN(FVSPR,T1,T2,YL1,YL2,AERR,ERROR,IER)
$-DBLIN(FSSPVR,T1,T2,XL1,XL2,AERR,ERROR,IER)
$-DBLIN(FVSQR,T1,T2,YL1,YL2,AERR,ERROR,IER)
$+DBLIN(FSSQVR,T1,T2,XL1,XL2,AERR,ERROR,IER)
HSP1=-DBLIN(FHSPR,T1,T2,XL1,XL2,AERR,ERROR,IER)
$+DBLIN(FSSPHR,T1,T2,YL1,YL2,AERR,ERROR,IER)
$+DBLIN(FHSQR,T1,T2,XL1,XL2,AERR,ERROR,IER)
$-DBLIN(FSSQHR,T1,T2,YL1,YL2,AERR,ERROR,IER)
VSQ1=DBLIN(FVSPT,T1,T2,YL1,YL2,AERR,ERROR,IER)
$-DBLIN(FSSPVT,T1,T2,XL1,XL2,AERR,ERROR,IER)
$+DBLIN(FVSQT,T1,T2,YL1,YL2,AERR,ERROR,IER)
$-DBLIN(FSSQVT,T1,T2,XL1,XL2,AERR,ERROR,IER)
HSQ1=-DBLIN(FHSPT,T1,T2,XL1,XL2,AERR,ERROR,IER)
$+DBLIN(FSSPHT,T1,T2,YL1,YL2,AERR,ERROR,IER)
$-DBLIN(FHSQT,T1,T2,XL1,XL2,AERR,ERROR,IER)
$+DBLIN(FSSQHT,T1,T2,YL1,YL2,AERR,ERROR,IER)
X=X2
Y=Y2
VSP1=VSP1+DBLIN(FSSPVR,T1,T2,XL1,XL2,AERR,ERROR,IER)
$-DBLIN(FSSQVR,T1,T2,XL1,XL2,AERR,ERROR,IER)
HSP1=HSP1+DBLIN(FHSPR,T1,T2,XL1,XL2,AERR,ERROR,IER)
$-DBLIN(FHSQR,T1,T2,XL1,XL2,AERR,ERROR,IER)
VSQ1=VSQ1+DBLIN(FSSPVT,T1,T2,XL1,XL2,AERR,ERROR,IER)
$+DBLIN(FSSQVT,T1,T2,XL1,XL2,AERR,ERROR,IER)
HSQ1=HSQ1+DBLIN(FHSPT,T1,T2,XL1,XL2,AERR,ERROR,IER)
$+DBLIN(FHSQT,T1,T2,XL1,XL2,AERR,ERROR,IER)
AN=-1.*ANG
```

T1=-T1
T2=-T2
X=X2
Y=Y1
VSP2=DBLIN(FVSPR,T2,T1,YL1,YL2,AERR,ERROR,IER)
\$-DBLIN(FSSPVR,T2,T1,XL1,XL2,AERR,ERROR,IER)
\$-DBLIN(FVSQR,T2,T1,YL1,YL2,AERR,ERROR,IER)
\$+DBLIN(FSSQVR,T2,T1,XL1,XL2,AERR,ERROR,IER)
HSP2=-DBLIN(FHSPR,T2,T1,XL1,XL2,AERR,ERROR,IER)
\$+DBLIN(FSSPHR,T2,T1,YL1,YL2,AERR,ERROR,IER)
\$+DBLIN(FHSQR,T2,T1,XL1,XL2,AERR,ERROR,IER)
\$-DBLIN(FSSQHR,T2,T1,YL1,YL2,AERR,ERROR,IER)
VSQ2=-DBLIN(FVSPT,T2,T1,YL1,YL2,AERR,ERROR,IER)
\$+DBLIN(FSSPVT,T2,T1,XL1,XL2,AERR,ERROR,IER)
\$-DBLIN(FVSQT,T2,T1,YL1,YL2,AERR,ERROR,IER)
\$+DBLIN(FSSQVT,T2,T1,XL1,XL2,AERR,ERROR,IER)
HSQ2=DBLIN(FHSPT,T2,T1,XL1,XL2,AERR,ERROR,IER)
\$-DBLIN(FSSPHT,T2,T1,YL1,YL2,AERR,ERROR,IER)
\$+DBLIN(FHSQT,T2,T1,XL1,XL2,AERR,ERROR,IER)
\$-DBLIN(FSSQHT,T2,T1,YL1,YL2,AERR,ERROR,IER)
X=X2.
Y=Y2
VSP2=VSP2+DBLIN(FSSPVR,T2,T1,XL1,XL2,AERR,ERROR,IER)
\$-DBLIN(FSSQVR,T2,T1,XL1,XL2,AERR,ERROR,IER)
HSP2=HSP2+DBLIN(FHSPR,T2,T1,XL1,XL2,AERR,ERROR,IER)
\$-DBLIN(FHSQR,T2,T1,XL1,XL2,AERR,ERROR,IER)
VSQ2=VSQ2-DBLIN(FSSPVT,T2,T1,XL1,XL2,AERR,ERROR,IER)
\$-DBLIN(FSSQVT,T2,T1,XL1,XL2,AERR,ERROR,IER)
HSQ2=HSQ2-DBLIN(FHSPT,T2,T1,XL1,XL2,AERR,ERROR,IER)
\$-DBLIN(FHSQT,T2,T1,XL1,XL2,AERR,ERROR,IER)
A(J,I)=VSP1+VSP2
A(J,I+L)=VSQ1+VSQ2
A(J+L,I)=HSP1+HSP2
A(J+L,I+L)=HSQ1+HSQ2
45 CONTINUE
40 CONTINUE
CCC CALCULATING TOTAL VER. & HOR. FORCES
CCC ON BOTH SIDES OF EACH SECTION.
DO 110,J=1,N/2
DO 115,I=1,N/2
A(J,I)=B(I,1)*A(J,I)+B(I+L,1)*A(J,I+L)
A(J+L,I)=B(I,1)*A(J+L,I)+B(I+L,1)*A(J+L,I+L)
115 CONTINUE
110 CONTINUE
DO 120,I=1,N/2
BRS(I)=0.
BTS(I)=0.
120 CONTINUE
DO 125,J=1,N/2
DO 130,I=1,N/2
BRS(J)=BRS(J)+A(J,I)
BTS(J)=BTS(J)+A(J+L,I)
130 CONTINUE
125 CONTINUE

```
AREA=INC
DO 165,I=1,N/2
BRS(I)=BRS(I)/AREA
BTS(I)=BTS(I)/AREA
165 CONTINUE
DO 166,I=1,N/2
URS(I)=BRS(I)-B(I,1)
UTS(I)=B(I+L,1)-BTS(I)
166 CONTINUE
PRINT2050
2050 FORMAT(//1X,'[ RESULTANT STRESS DISTRIBUTION ]')
PRINT3000
PRINT1700
PRINT3000
DO 190,I=1,N/2
PRINT1800,SP(I),B(I,1),B(I+L,1)
190 PRINT3000
PRINT2060
2060 FORMAT(//1X,'[ STRESS DISTRIBUTION ON LOWER SURFACE ]')
PRINT3000
PRINT1700
PRINT3000
DO 191,I=1,N/2
PRINT1800,SP(I),BRS(I),BTS(I)
191 PRINT3000
PRINT2070
2070 FORMAT(//1X,'[ STRESS DISTRIBUTION ON UPPER SURFACE ]')
PRINT3000
PRINT1700
PRINT3000
DO 192,I=1,N/2
PRINT1800,SP(I),URS(I),UTS(I)
192 PRINT3000
1700 FORMAT(1X,'* ','LENGTH',T16,'RAD.',T31,'TAN.',T41,'*')
1800 FORMAT(1X,'*',F5.2,T10,F10.1,T25,F10.1,T41,'*')
PRINT2900,B(K,1)
2900 FORMAT(1X,'* ','VERTICAL DISPLACEMENT IS ','[',F8.6,']',*
$T41,'*')
PRINT3000
3000 FORMAT(1X,'-----*')
STOP
END
```

```
*****  
* PROGRAM "PIPEPLO"  
* "PIPEPLO" PLOTS THE RESULTS OF "PIPE" ON THE  
* CBS MEGATEC GRAPHICS SYSTEM.  
*****  
  
PROGRAM PIPEPLO  
PARAMETER (N=20,L2=10)  
REAL A(N),B1(181),B2(181)  
REAL ORS(181),OTS(181),FRS(181),FTS(181)  
REAL AORS(L2),AOTS(N),AFRS(L2),AFTS(N)  
REAL ANP(N),ANM(L2),ARS(L2),ATS(N)  
INTEGER R1(N)  
REAL DRS(181),DTS(181)  
INTEGER X1,Y1,XT  
REAL INC,DEG,K0  
XT=-1300  
DEG=3.1415927/180.  
DO 1,I=1,N/2  
1 READ(5,*)ARS(I)  
DO 2,I=1,N/2  
2 READ(5,*)ATS(I)  
READ(5,*)RA  
READ(5,*)D  
READ(5,*)DE  
READ(5,*)K0  
R=250  
SC=70./45000.  
PI=3.1415927  
INC=2*PI/N  
DO 10,I=1,L2  
10 ANM(I)=(I*360./N-.5*360./N)/180.  
DO 15,I=1,181  
DRS(I)=0.  
15 DTS(I)=0.  
DO 3000,K=1,181  
V=(K-1)/180.  
DO 2000,I=1,L2  
P=1.  
DO 1000,J=1,L2  
IF(J.NE.I)THEN  
P=P*(V-ANM(J))/(ANM(I)-ANM(J))  
ELSE  
GO TO 1000  
END IF  
1000 CONTINUE  
DRS(K)=DRS(K)+ARS(I)*P  
DTS(K)=DTS(K)+ATS(I)*P  
2000 CONTINUE  
3000 CONTINUE  
DO 40,I=1,N  
40 ANP(I)=I*INC  
CALL MWALDS(1,0)  
CALL MWINIT('SYSP:WORK1.DAT/S')  
CALL MWSLCT(1)
```

```
CALL MWOPEN("SE",1)
ICHECK=0
DO 300,I=1,L2
A(I)=ATS(I)
300 A(I+L2)=ARS(L2+1-I)
    DO 301,I=1,181
    B1(I)=DTS(I)
301 B2(I)=DRS(I)
    GO TO 555
666 DO 303,I=1,N
303 A(I)=AOTS(I)
    DO 304,I=1,181
    B1(I)=OTS(I)
304 B2(I)=ORS(I)
    GO TO 555
999 DO 305,I=1,N
305 A(I)=AFTS(I)
    DO 306,I=1,181
    B1(I)=FTS(I)
306 B2(I)=FRS(I)
555 DO 90,I=1,N
90 A(I)=SC*A(I)
    CALL CIRCLE(XT,0.,R)
    DO 50,I=1,N
    K=(I-1)*360./N
    R1(I)=R+ABS(A(I))
    CALL ARC(R1(I),K,N,XT)
50 CONTINUE
    IF(R1(1).GE.R1(N))THEN
    X1=XT+0
    Y1=R1(1)
    CALL MW2MOV(X1,Y1)
    X1=XT+0
    Y1=R
    CALL MW2DRW(X1,Y1)
    ELSE
    X1=XT+0
    Y1=R1(N)
    CALL MW2MOV(X1,Y1)
    X1=XT+0
    Y1=R
    CALL MW2DRW(X1,Y1)
    ENDIF
    DO 70,I=1,N-1
    IF(ABS(A(I)).GE.ABS(A(I+1)))THEN
    X1=XT+R1(I)*SIN(ANP(I))
    Y1=R1(I)*COS(ANP(I))
    CALL MW2MOV(X1,Y1)
    X1=XT+R*SIN(ANP(I))
    Y1=R*COS(ANP(I))
    CALL MW2DRW(X1,Y1)
    ELSE
    X1=XT+R1(I+1)*SIN(ANP(I))
    Y1=R1(I+1)*COS(ANP(I))
```

```
CALL MW2MOV(X1,Y1)
X1=XT+R*SIN(ANP(I))
Y1=R*COS(ANP(I))
CALL MW2DRW(X1,Y1)
ENDIF
70 CONTINUE
X1=XT+0
Y1=R+SC*ABS(B1(1))
CALL MW2MOV(X1,Y1)
DO 52,I=2,181
X1=XT+(R+SC*ABS(B1(I)))*SIN((I-1)*DEG)
Y1=(R+SC*ABS(B1(I)))*COS((I-1)*DEG)
CALL MW2DRW(X1,Y1)
52 CONTINUE
X1=XT+0
Y1=R+SC*ABS(B2(1))
CALL MW2MOV(X1,Y1)
DO 51,I=2,181
X1=XT+(R+SC*ABS(B2(I)))*SIN((I-1)*DEG)
Y1=(R+SC*ABS(B2(I)))*COS((I-1)*DEG)
CALL MW2DRW(X1,Y1)
51 CONTINUE
333 IF(ICHECK.EQ.0)GO TO 777
IF(ICHECK.EQ.1)GO TO 888
IF(ICHECK.EQ.2)GO TO 444
777 CALL ORFORCE(ORS,OTS,AORS,AQTS,RA,D,DE,K0)
ICHECK=1
XT=0
GO TO 666
888 DO 200,I=1,N/2
AFRS(I)=ARS(I)+AORS(I)
AFTS(I)=ATS(I)+AOTS(I)
200 CONTINUE
KI=0
DO 250,I=L2+1,N
AFTS(I)=AFRS(N/2-KI)
KI=KI+1
250 CONTINUE
DO 260,I=1,181
FRS(I)=DRS(I)+ORS(I)
FTS(I)=DTS(I)+OTS(I)
260 CONTINUE
ICHECK=2
XT=1300
GO TO 999
444 CALL MWCLIN(0)
CALL MWCCSZ(3)
CALL MWCCAN(0)
CALL MW2MOV(-1450,1000)
CALL MWTEXT('DISTURBANCE\')
CALL MWCLIN(0)
CALL MWCCSZ(3)
CALL MWCCAN(0)
CALL MW2MQV(-100,1000)
```

```
CALL MWTEXT('ORIGINAL')
CALL MWCLIN(0)
CALL MWCCSZ(3)
CALL MWCCAN(0)
CALL MW2MOV(1200,1000)
CALL MWTEXT('FINAL')
CALL MWCLIN(0)
CALL MWCCSZ(4)
CALL MWCCAN(0)
CALL MW2MOV(-700,-1400)
CALL MWTEXT('FIG.( ),HOR. PIPE STRESS DISTRIBUTION.')
CALL MWCLIN(0)
CALL MWCCSZ(4)
CALL MWCCAN(0)
CALL MW2MOV(-400,-1500)
CALL MWTEXT('(R=3,D=15,H=30,V=.3)')
CALL MWCLIN(0)
CALL MWCCSZ(4)
CALL MWCCAN(0)
CALL MW2MOV(1200,1000)
CALL MWTEXT('CIRCLE(X,Y,R)')
SUBROUTINE CIRCLE(X,Y,R)
INTEGER X
DEG=3.1415927/180.
XC=X
YC=R
CALL MW2MOV(INT(XC),INT(YC))
DO 55,I=0,360
CALL MW2DRW(INT(SIN(FLOAT(I)*DEG)*R+X),
$INT(COS(FLOAT(I)*DEG)*R))
55 CONTINUE
RETURN
END
SUBROUTINE ANC(R,K,N,XT)
INTEGER XT,R
DEG=3.1415927/180.
XC=XT+INT(R*SIN(K*DEG))
YC=INT(R*COS(K*DEG))
INC=360/N
CALL MW2MOV(INT(XC),INT(YC))
DO 60,I=K,K+INC
CALL MW2DRW(INT(SIN(FLOAT(I)*DEG)*R+XT),
$INT(COS(FLOAT(I)*DEG)*R))
60 CONTINUE
RETURN
END
SUBROUTINE ORFORCE(ORS,OTS,AORS,AOTS,R,D,DE,K0)
PARAMETER (NA=20,L1=10)
REAL ORS(181),OTS(181),AORS(L1),AOTS(NA)
REAL R,D,DE,K0
DEG=3.1415927/180.
DO 1000,I=1,181
X=D-R*COS((I-1)*DEG)
VS=X*DE
HS=K0*VS
```

T=3.1415927/2.- (I-1)*DEG
ORS(I)=(0.5*(VS+HS)+0.5*(HS-VS)*COS(2*T))
OTS(I)=-1*0.5*(HS-VS)*SIN(2*T)
1000 CONTINUE
DO 1200, I=1,L1
K=INT(360/NA*(I-.5)+.5)
AORS(I)=ORS(K)
AOTS(I)=OTS(K)
1200 CONTINUE
KI=0
DO 1400, I=L1+1,NA
AOTS(I)=AORS(NA/2-KI)
KI=KI+1
1400 CONTINUE
RETURN
END

```
*****  
* PROGRAM "CIRPLO"  
* "CIRPLO" PLOTS THE RESULTS OF "CIRFDN" ON THE  
* CBS MEGATEC GRAPHICS SYSTEM.  
*****  
  
PROGRAM CIRPLO  
PARAMETER(N=20,L=10)  
REAL AN(L),AT(L),BN(91),BT(91),ANP(N),ANM(L)  
REAL INC  
INTEGER R,RR,X,Y,XT,ANG  
READ(5,*)BR  
READ(5,*)ANG  
R=500  
SC=500./20000.  
XT=-1000  
PI=3.14160  
INC=ANG*PI/180./N  
DEG=PI/180.  
AANG=ANG/2.  
CALL MWALDS(1,0)  
CALL MWINIT('SYSP:WORK1.DAT/S')  
CALL MWSLCT(1)  
CALL MWOPEN('SE',1)  
DO 5,I=1,L+1  
5 ANP(I)=(I-1)*INC  
DO 40,I=1,L  
40 ANM(I)=(I*ANG/N-.5*ANG/N)/AANG  
RA=BR/SIN(ANG*PI/360.)  
DO 100,JJ=1,2  
DO 30,I=1,N/2  
30 READ(5,*)AN(I)  
DO 35,I=1,N/2  
35 READ(5,*)AT(I)  
DO 3000,K=1,ANG/2+1  
V=(K-1)/AANG  
BN(K)=0.  
BT(K)=0.  
DO 2000,I=1,L  
P=1.  
DO 1000,J=1,L  
IF(J.NE.I)THEN  
P=P*(V-ANM(J))/(ANM(I)-ANM(J))  
ELSE  
GO TO 1000  
END IF  
1000 CQNTINUE  
BN(K)=BN(K)+AN(I)*P  
BT(K)=BT(K)+AT(I)*P  
2000 CQNTINUE  
3000 CQNTINUE  
CALL CIR(XT,R,ANG)  
Z=1.  
DO 700,K=1,2  
X=XT
```

```
Y=R
CALL MW2MOV(X,Y)
DO 300,I=1,N/2
K1=(I-1)*ANG/N
IF(K1.EQ.0)K1=1
K2=I*ANG/N
RR=R+SC*ABS(AT(I))
X=XT+Z*RR*SIN(ANP(I))
Y=RR*COS(ANP(I))
CALL MW2DRW(X,Y)
CALL ARC(RR,K1,K2,XT,Z)
300 CONTINUE
X=XT+Z*R*SIN(ANP(L+1))
Y=R*COS(ANP(L+1))
CALL MW2DRW(X,Y)
X=XT
Y=R
CALL MW2MOV(X,Y)
DO 400,I=1,ANG/2+1
RR=R+SC*ABS(BT(I))
X=XT+Z*RR*SIN((I-1)*DEG)
Y=RR*COS((I-1)*DEG)
CALL MW2DRW(X,Y)
400 CONTINUE
X=XT+Z*R*SIN(ANP(L+1))
Y=R*COS(ANP(L+1))
CALL MW2DRW(X,Y)
333 DO 70,I=1,N/2
70 AT(I)=AN(I)
DO 65,I=1,ANG/2+1
65 BT(I)=BN(I)
Z=-1.
700 CONTINUE
XT=1000
100 CONTINUE
CALL MWCLIN(0)
CALL MWCCSZ(3)
CALL MWCCAN(0)
CALL MW2MOV(-1100,1000)
CALL MWTEXT('*BOTTOM*\')
CALL MWCLIN(0)
CALL MWCCSZ(3)
CALL MWCCAN(0)
CALL MW2MOV(900,1000)
CALL MWTEXT('*TOP*\')
CALL MWCLIN(0)
CALL MWCCSZ(3)
CALL MWCCAN(0)
CALL MW2MOV(-700,-100)
CALL MWTEXT('FIG.( ),CIR. STRIP FOOTING STRESS DIST.\')
CALL MWCLIN(0)
CALL MWCCSZ(3)
CALL MWCCAN(0)
CALL MW2MOV(-400,-200)
```

```
CALL MWTEXT('(BR=1,HT=3,H=10,ANG=120,W=30000)\')  
CALL MWCLOS  
CALL MWTERM  
STOP  
END  
SUBROUTINE ARC(R,K1,K2,XT,Z)  
INTEGER XT,R,X,Y  
DEG=3.14160/180.  
X=XT+Z*R*SIN(K1*DEG)  
Y=R*COS(K1*DEG)  
CALL MW2MOV(X,Y)  
DO 10,I=K1,K2  
X=XT+Z*R*SIN(FLOAT(I)*DEG)  
Y=R*COS(FLOAT(I)*DEG)  
CALL MW2DRW(X,Y)  
10 CONTINUE  
RETURN  
END  
SUBROUTINE CIR(XT,R,ANG)  
INTEGER XT,R,ANG,X,Y  
DEG=3.14160/180.  
X=XT-R*SIN(ANG*DEG/2.)  
Y=R*COS(ANG*DEG/2.)  
CALL MW2MOV(X,Y)  
DO 10,I=1,ANG+1  
X=XT+R*SIN(FLOAT(I-ANG/2)*DEG)  
Y=R*COS(FLOAT(I-ANG/2)*DEG)  
CALL MW2DRW(X,Y)  
10 CONTINUE  
RETURN  
END
```

```
*****  
* PROGRAM "TRIPLO"  
* "TRIPLO" PLOTS THE RESULTS OF "TRIFDN" AND  
* "FLAFDN" ON THE CBS MEGATEC GRAPHICS SYSTEM.  
*-----  
PROGRAM TRIPLO  
PARAMETER(N=20,L=10)  
REAL AN(L),AT(L),BN(91),BT(91),S(N),SI(L)  
REAL INC  
INTEGER W,X,Y,XT  
READ(5,*)BR  
READ(5,*)ANG  
W=500  
SC="3^./20000.  
XT=-1000  
PI=3.14159  
ANG=PI/2.-ANG*PI/360.  
T=W/COS(ANG)/90.  
INC=W/COS(ANG)/L  
DIV=BR/COS(ANG)/90.  
DD=BR/COS(ANG)/L  
SI(1)=DD/2.  
DO 40,I=2,L  
40 SI(I)=SI(I-1)+DD  
CALL MWALDS(1,0)  
CALL MWINIT('SYSP:WORK1.DAT/S')  
CALL MWSLCT(1)  
CALL MWOPEN('SE',1)  
DO 10,I=1,L+1  
10 S(I)=(I-1)*INC  
DO 100,JJ=1,2  
DO 30,I=1,N/2  
30 READ(5,*)AN(I)  
DO 35,I=1,N/2  
35 READ(5,*)AT(I)  
DO 3000,K=1,91  
V=(K-1)*DIV  
BN(K)=0.  
BT(K)=0.  
DO 2000,I=1,L  
P=1.  
DO 1000,J=1,L  
IF(J.NE.I)THEN  
P=P*(V-SI(J))/(SI(I)-SI(J))  
ELSE  
GO TO 1000  
END IF  
1000 CONTINUE  
BN(K)=BN(K)+AN(I)*P  
BT(K)=BT(K)+AT(I)*P  
2000 CONTINUE  
3000 CONTINUE  
CALL TRI(XT,ANG,W)  
Z=1.
```

```
DO 700,K=1,2
X=XT
Y=0
CALL MW2MOV(X,Y)
DO 300,I=1,N/2
X=XT+Z*(S(I)*COS(ANG)+SC*ABS(AT(I)*SIN(ANG)))
Y=-S(I)*SIN(ANG)+SC*ABS(AT(I)*COS(ANG))
CALL MW2DRW(X,Y)
X=XT+Z*(S(I+1)*COS(ANG)+SC*ABS(AT(I)*SIN(ANG)))
Y=-S(I+1)*SIN(ANG)+SC*ABS(AT(I)*COS(ANG))
CALL MW2DRW(X,Y)
300 CONTINUE
X=XT+Z*W
Y=-W*TAN(ANG)
CALL MW2DRW(X,Y)
X=XT
Y=0
CALL MW2MOV(X,Y)
DO 400,I=1,91
X=XT+Z*((I-1)*T*COS(ANG)+SC*ABS(BT(I)*SIN(ANG)))
Y=-(I-1)*T*SIN(ANG)+SC*ABS(BT(I)*COS(ANG))
CALL MW2DRW(X,Y)
400 CONTINUE
X=XT+Z*W
Y=-W*TAN(ANG)
CALL MW2DRW(X,Y)
DO 60,I=1,N/2
60 AT(I)=AN(I)
DO 65,I=1,91
65 BT(I)=BN(I)
Z=-1.
700 CONTINUE
XT=1000
100 CONTINUE
CALL MWCLIN(0)
CALL MWCCSZ(3)
CALL MWCCAN(0)
CALL MW2MOV(-1100,650)
CALL MWTEXT('*BOTTOM*\\" )
CALL MWCLIN(0)
CALL MWCCSZ(3)
CALL MWCCAN(0)
CALL MW2MOV(900,650)
CALL MWTEXT('*TOP*\\" )
CALL MWCLIN(0)
CALL MWCCSZ(3)
CALL MWCCAN(0)
CALL MW2MOV(-700,-700)
CALL MWTEXT('FIG.( ),TRI. STRIP FOOTING STRESS DIST.\\" )
CALL MWCLIN(0)
CALL MWCCSZ(3)
CALL MWCCAN(0)
CALL MW2MOV(-400,-80)
CALL MWTEXT('(BR=1,HT=3,H=10,ANG=120,W=30000)\\" )
```

```
CALL MWCLOS
CALL MWTERM
STOP
END
SUBROUTINE TRI(XT,ANG,W)
INTEGER X,Y,W,XT
X=XT+W
Y=-W*TAN(ANG)
CALL MW2MOV(X,Y)
X=XT
Y=0
CALL MW2DRW(X,Y)
X=XT-W
Y=-W*TAN(ANG)
CALL MW2DRW(X,Y)
RETURN
END
```